OPTIMUM NOISE PERFORMANCE OF MULTITERMINAL AMPLIFIERS

WILLIAM D. RUMMLER

TECHNICAL REPORT 417

FEBRUARY 1, 1964

MASSACHUSETTS INSTITUTE OF TECHNOLOGY
RESEARCH LABORATORY OF ELECTRONICS
CAMBRIDGE, MASSACHUSETTS

The Research Laboratory of Electronics is an interdepartmental laboratory in which faculty members and graduate students from numerous academic departments conduct research.

The research reported in this document was made possible in part by support extended the Massachusetts Institute of Technology, Research Laboratory of Electronics, jointly by the U.S. Army (Electronics Materiel Agency), the U.S. Navy (Office of Naval Research), and the U.S. Air Force (Office of Scientific Research) under Contract DA36-039-AMC-03200(E); and in part by Grant DA-SIG-36-039-61-G14.

MASSACHUSETTS INSTITUTE OF TECHNOLOGY

RESEARCH LABORATORY OF ELECTRONICS

Technical Report 417 February 1, 1964

OPTIMUM NOISE PERFORMANCE OF MULTITERMINAL AMPLIFIERS

William D. Rummler

This report is based on a thesis submitted to the Department of Electrical Engineering, M. I. T., August 19, 1963, in partial fulfillment of the requirements for the degree of Doctor of Science.

(Manuscript received October 1, 1963)

Abstract

A measure is determined of the optimum noise performance of a linear multiterminal-pair amplifier; this optimum performance is achieved with a multiterminal-pair source in a narrow band of frequencies Δf at a single-output terminal pair. The optimum noise performance of such a system is defined as the maximum signal-to-noise ratio achievable at large exchangeable signal power. It is shown that this is a meaningful criterion for any system that is to deliver ultimately an amount of signal power considerably greater than $kT_o\Delta f$, the noise power available from a resistor at a temperature T_o. The techniques described can be used, however, to determine the maximum signal-to-noise ratio achievable at any value of exchangeable (or available) signal power.

The results are presented in a plot with noise-to-signal ratio and the reciprocal of exchangeable signal power as coordinates — the noise-performance plane. The noise figure, exchangeable-power gain, and noise measure are given a geometrical interpretation in this plane.

It is shown that the optimum noise performance, achieved by imbedding a multiterminal-pair source and a multiterminal-pair amplifier in an arbitrary lossless network, can also be achieved by imbedding the source in an arbitrary lossless network to reduce it to a one-terminal-pair source and then using it to drive an arbitrary lossless reduction of the amplifier. Thus the optimization problem can be solved by considering separately the noise performances of the source and amplifier. Accordingly, the problem can be attacked by considering a set of problems of increasing difficulty. First, the noise performance achievable with a noisy (positive or negative) resistance used in conjunction with a one-terminal-pair source is examined. The points in the noise-performance plane achievable at the output of such a system all lie on a straight line through the source point with a slope equal to the exchangeable noise power of the resistance. Subsequently, the problem of the noise performance of a multiterminal-pair amplifier used with a one-terminal-pair source is considered. After the noise performance of a multiterminal-pair source imbedded in an arbitrary lossless network has been examined, the general noise-performance problem can be solved by inspection.

With this work used as a basis, definitions are given for the noise figure, exchangeable-power gain, and noise measure of a multiterminal-pair amplifier used with a multiterminal-pair source.

The optimization procedure is extended to multifrequency networks coupled in an arbitrary manner by a lossless nonlinear device that obeys the Manley-Rowe formulas. In this context, the optimum noise performance of an ideal (lossless) double-sideband parametric amplifier is examined for both the cases in which the noises in the two sidebands are uncorrelated and partially correlated.

TABLE OF CONTENTS

CONTENTS

I. INTRODUCTION

The problem with which we shall be concerned is the noise performance of a multiterminal-pair amplifier used in conjunction with a multiterminal-pair signal source. We shall investigate the values of signal-to-noise ratio and exchangeable signal power that can be obtained at a single-output terminal pair by interconnecting such a source and amplifier. We shall consider these two quantities only as they apply to a narrow band of frequencies (essentially one frequency). We refer to the way in which the amplifier affects these two quantities in a narrow band as the "spot-noise performance" of the amplifier, or simply the noise performance of the amplifier. We address ourselves to this problem exclusively, without intending to intimate that other features of the general noise and information problem are less important.

It is appropriate to begin by describing some of the problems that arise in practice for which such a theory would be useful, and some of the work that has been done on such problems.

A multiterminal-pair noise theory is particularly useful in evaluating the optimum noise performance of parametric amplifiers. Whereas for single-sideband parametric amplifiers the noise performance can be calculated directly, in many cases[1] it is also possible, and desirable, since this is the conceptual basis originally used by Manley and Rowe,[2] to formulate and solve the problem on a multiterminal-pair basis by allowing terminal pairs at each frequency.[3,4] For double-sideband, degenerate, parametric amplifiers (by degenerate we imply that the frequencies of the two sidebands are close but distinguishable), however, the problem becomes more complicated, even though the multiterminal-pair formalism is still applicable, and at present a unique optimization has only been carried out for single-sideband operation of the degenerate amplifier.[5] Double-sideband operation is fundamentally a multiterminal-pair type of operation, and has not been optimized because of the lack of criteria for multiterminal-pair operation.

Another problem to which such a noise theory would be applicable arises in diversity reception. Here we have a set of receiving antennas; each antenna has both signal and noise present at its output terminals, and we would like to know how to amplify and combine the signals to obtain the best signal-to-noise ratio at a single-output terminal pair. This problem has never been solved in a completely general manner.

Actually this problem is complicated by the fact that the signal statistics are not stationary. The signals and noise are usually characterized by their properties as determined over a short time interval; and these properties are assumed to vary slowly in time.[6] The optimum receiving system, therefore, is a network that optimizes the output at every instant of time, and must vary slowly in time in order to accomplish this optimization. Although we do not consider this problem explicitly, we shall give a brief discussion of some of the work that has been done on it.

The optimization that has been performed is that of combining the antenna outputs or doing the equivalent, that is, amplifying the output of each antenna and combining

the outputs of the amplifiers, usually before detection to obtain the maximum signal-to-noise ratio. In the first analytic treatment to be reported,[7] Kahn solves the problem of combining two noisy signal-voltage sources. Brennan extends this optimization to cover n sources for the case in which the signals are completely correlated and the noise voltages are completely uncorrelated.[8] A slightly different approach to the problem has been given by Granlund.[9] He solves the problem of optimizing the available power of an n-terminal-pair source network by imbedding it in an (n+1)-terminal-pair lossless network. He shows that, if the noise sources have a particular form, and if the signal sources are coherent, the lossless network that yields the maximum available power also gives the best (maximum) signal-to-noise ratio that can be obtained with such a lossless network. Although he does not make the observation, the condition on the noise sources for which this situation occurs is that the sources be thermal,[10] or proportional to thermal sources. His results are significant, since it is generally assumed in designing diversity reception systems that these conditions are satisfied. We shall see that if these conditions are not satisfied, none of the optimizations described above is strictly correct.

It is customary to describe the noise performance of a two-terminal-pair amplifier at a given frequency by its spot-noise figure. Since the introduction of spot-noise figure,[11,12] it has been realized that this quantity has certain disadvantages as a criterion of merit. Perhaps the most obvious of these shortcomings is the fact that noise figure does not properly take into account the amount of gain which a device gives. Consequently, if we attempt to minimize the noise figure of an amplifier by external lossless circuit operations such as lossless feedback, we find that the minimum value of noise figure is unity and is the same thing as not using the amplifier at all. Another difficulty with noise figure is that it becomes undefined when the output impedance of the amplifier has a negative real part. In recent years, these problems have been resolved and put into their proper perspective by Haus and Adler. Their work has appeared in a number of journal papers,[13-17] and also in comprehensive form in a research monograph.[18]

The problem of negative output impedances is avoided by formulating the problem in terms of exchangeable power rather than available power. Exchangeable power is just the stationary value of the power supplied by a source to an impedance. If the source impedance has a positive real part, the exchangeable power is identical to the available power. If the source impedance has a negative real part, the exchangeable power is negative; it is equal to the negative of the maximum power that can be pushed back into the source by a (negative resistance) load. By using the exchangeable power concept it is possible to define an extended noise figure that is valid for negative output impedances.

Haus and Adler define a new quantity, which they call noise measure, as a criterion of the noise performance of an amplifier. The noise measure of an amplifier is equal to the minimum noise figure attainable at large exchangeable gain – when allowance is made for lossless imbedding of the amplifier to achieve this minimum. The noise measure has many advantages; the optimum value is an invariant of the amplifier alone and

lossless imbeddings cannot reduce its value.

The invariance of the optimum noise measure is a clue to the deeper significance of noise measure. The optimum noise measure is only one of the n invariants of an n-terminal-pair, noisy network (amplifier). If we imbed an n-terminal-pair noisy network in an arbitrary 2n-terminal-pair lossless network and ask how the exchangeable power at one of the output terminal pairs depends on the imbedding, we find that there are n stationary values of exchangeable power with respect to variations of this imbedding network. These n stationary values are invariant with respect to all of those lossless transformations that preserve the number of terminal pairs.

If the network under consideration contains only noise sources, these n stationary values are the negatives of the eigenvalues of the characteristic noise matrix of the network. The least positive eigenvalue of the characteristic noise matrix divided by $kT_o\Delta f$ (where k is Boltzmann's constant, T_o is standard temperature of 290°K, and Δf is the bandwidth over which the network is characterized) is equal to the optimum value of the noise measure. The optimum value of the noise measure for an n-terminal-pair amplifier is the best noise measure obtainable by using the device as a two-terminal-pair amplifier.

These n invariants are also important in the canonic representation of noisy networks. It can be shown that an n-terminal-pair noisy network can always be put into canonical form by imbedding it in a linear lossless 2n-terminal-pair network. The canonical form consists of n uncoupled and independently noisy resistors. The exchangeable power of each of these resistors is the negative of one of the eigenvalues of the characteristic noise matrix.

Most of the work of Haus and Adler that has been discussed here is presented in considerable detail in Section II.

Our problem, as it now appears, is to determine how these concepts may be extended to apply to the case of a multiterminal-pair amplifier used with a multiterminal-pair source. Since the concepts of noise figure, noise measure, and exchangeable gain are not directly extendable to multiterminal-pair devices, we must use indirect methods that do not involve these quantities explicitly. What we shall do, therefore, is to imbed the amplifier and source in a linear lossless imbedding network and investigate the noise performance (signal-to-noise ratio and exchangeable signal power) that can be obtained at a single output. This is the most general way in which we can use a linear multiterminal-pair amplifier in a linear way with a linear multiterminal-pair source to obtain a single output. Such an imbedding allows for arbitrary lossless feedback, and has the additional advantage that the same performance is achievable, irrespective of the number of independent identical amplifiers that might be chosen for incorporation into our system. Consequently, we need only consider a given amplifier once.

This approach, however, lacks direction. We are not only interested in determining what values of signal-to-noise ratio and exchangeable power can be obtained, we are also interested in determining which of the obtainable values is the most desirable. We can begin by adopting the viewpoint that we are really trying to achieve large positive

exchangeable power. For most systems this is a reasonable assumption and is, in fact, fulfilled; most amplifying systems have a large exchangeable gain. That is, we can obtain much more signal power from the output of the system than we could by using the signal-source network alone.

But this is still not sufficient, for a system might have a negative value of exchangeable signal power at the output. For such a system we may (in principle) extract infinite amounts of signal power from the output by loading the output with a positive resistance equal in magnitude to the negative resistance of the output and tuning out any reactance. We show in Section II that the actual noise performance of such a system (in terms of the ratio of signal power delivered to the load-to-noise power delivered to the load) can be no better than the best signal-to-noise ratio that can be achieved with the system at infinite exchangeable power.

For this reason, we shall define the optimum noise performance of a system as the largest value of signal-to-noise ratio that can be achieved with the elements of the system, at large exchangeable power. When we carry out these calculations we shall not be concerned with the way in which this result may be realized. That is, we shall not worry about the stability or reliability of a given configuration. We are only interested in the fact that the optimum limit exists and may be attained through some realizable network configuration. Because of the complexity of the algebra involved in carrying out the calculations, we shall rely extensively on matrix techniques so as not to become hopelessly buried in algebraic detail. (For those who are not familiar with matrix algebra, a reasonably good background in elementary matrix algebra such as that given by Hildebrand,[19] or Perlis,[20] is sufficient for understanding this material.)

As we have mentioned, the two quantities of interest in evaluating the noise performance of a system are the exchangeable signal power and the signal-to-noise ratio, that is, the ratio of exchangeable signal power to exchangeable noise power. Consequently, we would like to display our results on a plot with these two quantities as coordinates. It turns out, however, that the most convenient plot to use is one with noise-to-signal ratio and the reciprocal of exchangeable signal power as coordinates. As we shall show, there are many advantages in using these particular coordinates for our plots; only incidental among these is the fact that large values of signal-to-noise ratio and large values of exchangeable signal power are centrally located. Since the characteristics of the amplifier and source networks are easily displayed upon this plot, we shall refer to it as the noise-performance plane.

Due to the fact that it is conceptually simple to base our thinking upon operation in the noise-performance plane, we shall begin, in Section III, by examining some simple problems in this plane in order to become familiar with its use. We begin by examining the performance of a cascade of identical two-terminal-pair amplifiers, each having a fixed noise figure (or noise measure) and a fixed exchangeable gain (positive and greater than unity). In terms of the geometric relationship between the point prescribed by the amplifier input (the source) and the point determined by the amplifier output,we show

how the quantities exchangeable gain, noise figure, and noise measure may be defined. We show that for a cascade of two-terminal-pair amplifiers, each having the same noise measure M, the points determined by the outputs of successive stages all lie upon a straight line of slope $-MkT_o\Delta f$.

We subsequently generalize this problem by considering the arbitrary interconnection of a noisy impedance (positive or negative) and a given one-terminal-pair source. We find that the values of the noise-to-signal ratio and the reciprocal of the exchangeable power that may be achieved lie on a straight line. This line has a slope of $-MkT_o\Delta f$, where in view of our discussion of the work of Haus and Adler, this quantity is just the exchangeable noise power of the impedance. Actually, we can only realize points on the half of the line lying above the noise-to-signal ratio of the source network. With the use of these facts it is a simple matter to find the values of noise-to-signal ratio and reciprocal exchangeable signal power which can be obtained by interconnecting a multiterminal-pair amplifier and a one-terminal-pair source. We solve this problem by considering the interconnection of the source with the canonical form of the amplifier network.

Before we apply these techniques to the case of a multiterminal-pair amplifier used with a multiterminal-pair source, we must have an appreciation of the properties of a multiterminal-pair source. As we have mentioned, a one-terminal-pair source determines a point in the noise-performance plane; a multiterminal-pair source, on the other hand, is not so easily described. Since we are interested in devices with a single-output terminal pair we investigate the values of noise-to-signal ratio and the reciprocal exchangeable signal power that can be obtained at a single-output terminal pair by imbedding the source in a lossless network. For a multiterminal-pair source network we find that a whole region of values of these two parameters is achievable. We refer to this region as the source region. In Section IV we show how one can determine the limits of the source region. We do this by solving an optimization problem that leads to a simple eigenvalue equation. We use this equation to derive several of the important properties of this region such as the fact that the region is always (semi) convex.

With this knowledge as a basis we proceed to analyze the performance of a multiterminal-pair amplifier used in the most general way with a multiterminal-pair source. The most general way to use such an amplifier with such a source is to imbed both in a single lossless imbedding network. We show in Section V that we can always achieve the same results by imbedding the amplifier and source independently, reducing both networks to one-terminal-pair networks, and subsequently by combining these two one-terminal-pair networks. It is for this reason that so much attention is devoted to the determination of the source region. For, by losslessly reducing the source to a one-terminal-pair source network we can obtain a one-terminal-pair source whose parameters (noise-to-signal ratio and the reciprocal of exchangeable signal power) are given by the coordinates of any point in the source region. Thus the problem of the optimum performance of a multiterminal-pair amplifier with a multiterminal-pair source can

be handled in much the same way as the optimum performance of a multiterminal-pair amplifier with a one-terminal-pair source; this problem is considered in Section III. These methods are used in Section V to solve the simple illustrative problem of the optimum performance of a two-terminal-pair source used with a multiterminal-pair amplifier.

In Section VI we shift our viewpoint. We apply the knowledge obtained thus far to the problem of evaluating the noise performance of a given system with a specified source driving a specified amplifier with one output port. We can do this by making one assumption with respect to the performance criteria: We must not charge against the amplifier the way in which it combines the voltages (signal and noise) of the source. While this might appear to be an overly restrictive assumption, it is merely a generalization of the fact that we do not usually charge the noise temperature of the source, or the size of the exchangeable signal power of the source, against the performance (exchangeable gain and noise figure) of a two-terminal-pair amplifier driven by a one-terminal-pair source. What we are really doing when we make this assumption is to compare the performance of the amplifier with the performance of a lossless reduction network that combines the source voltages in the same way. On this basis we present definitions of noise figure, noise measure, and exchangeable gain for a multiterminal-pair amplifier used with a multiterminal-pair source. A simple method of measuring these parameters is also given.

Up to this point we have been discussing single-frequency linear devices, however, many of the ideas that are relevant to single-frequency devices may also be applied to some classes of multifrequency devices. In particular, consider the case of a source network that contains signal and noise generators at a number of frequencies, and of an amplifier (an independently noisy device) that has noise generators at a number of frequencies. If both of these networks have a linear relation between the components of their terminal voltages and currents at these frequencies, and if it is possible to pump a lossless device that obeys the Manley-Rowe relations in such a way that the device couples power at each of these frequencies, we can consider the noise performance (signal-to-noise ratio and exchangeable signal power) that can be achieved at a given output terminal pair (hence at a given frequency) by interconnecting this source and amplifier through an arbitrary lossless device that obeys the Manley-Rowe relations. This problem is considered in Section VII. We show that if we represent the terminal relations of the source and amplifier in terms of currents and voltages normalized to the square root (positive or negative depending on the particular frequency) of their respective frequencies, the problem is completely analogous to the single-frequency problem already considered. We illustrate these techniques by considering the interesting problem of the optimum noise performance of a two-frequency, two-terminal-pair source. Such a source, for instance, might consist of the two sidebands of a modulated carrier. We determine the minimum noise-to-signal ratio that can be achieved at large exchangeable signal power, both with and without independent amplifiers, for the case in which the

signals are completely correlated and the noises are uncorrelated. Subsequently we compare the optimum results obtained when the noises are partially correlated with the uncorrelated case.

II. FUNDAMENTAL CONCEPTS

We shall now discuss some of the basic ideas upon which we shall rely extensively. In section 2.1 we shall describe the fundamental circuit representation that we shall use. Sections 2.2-2.6 give essentially a review of those parts of the work of Haus and Adler[18] that are particularly relevant to the theory presented here. These discussions are carried out in considerable detail. The amount of detail is justifiable because a thorough knowledge of the topics discussed is essential for the understanding of the work to follow. In section 2.7 we consider the effects of load noise on the specified output parameters (signal-to-noise ratio) of an amplifying system. These considerations lead us to a unique way of specifying the quality of an amplifying system. The important results of the work of Haus and Adler to which we shall have recourse are summarized in a set of theorems appearing at the ends of appropriate sections. For convenience, we number them H&A-1 through H&A-4.

2.1 IMPEDANCE-MATRIX REPRESENTATION OF A MULTITERMINAL NETWORK

We shall be concerned for the most part with multiterminal-pair networks such as the n-terminal-pair network shown in Fig. 1. For such a network the voltages and

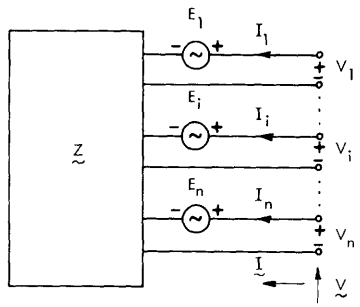

Fig. 1. Linear n-terminal-pair network.

currents in a small band Δf about some given frequency are related by a set of linear equations. We can summarize this set of equations in matrix form by the relation

$$\underset{\sim}{V} = \underset{\sim}{Z}\,\underset{\sim}{I} + \underset{\sim}{E}. \tag{1}$$

Here $\underset{\sim}{V}$ is a column matrix (or vector) of the complex Fourier amplitudes of the terminal voltages

$$\underset{\sim}{V} = \begin{bmatrix} V_1 \\ \vdots \\ V_i \\ \vdots \\ V_n \end{bmatrix}$$

and $\underset{\sim}{I}$ is a column matrix of the complex Fourier amplitudes of the terminal currents

$$\underset{\sim}{I} = \begin{bmatrix} I_1 \\ \vdots \\ I_i \\ \vdots \\ I_n \end{bmatrix}.$$

The network relates these two sets of variables through its impedance matrix

$$\underset{\sim}{Z} = \begin{bmatrix} Z_{11} & \cdots & Z_{1i} & \cdots & Z_{1n} \\ \vdots & & \vdots & & \vdots \\ Z_{i1} & \cdots & Z_{ii} & \cdots & Z_{in} \\ \vdots & & \vdots & & \vdots \\ Z_{n1} & \cdots & Z_{ni} & \cdots & Z_{nn} \end{bmatrix}$$

and the column matrix of the complex Fourier amplitudes of its open-circuit terminal voltages

$$\underset{\sim}{E} = \begin{bmatrix} E_1 \\ \vdots \\ E_i \\ \vdots \\ E_n \end{bmatrix}. \tag{2}$$

Since the network of Fig. 1 may contain both signal and/or noise-voltage generators, the open-circuit voltage amplitudes may be noise voltages and/or signal voltages. If the internal generators are all random-noise sources, the voltages $E_1 \ldots E_n$ are complex random variables. The physical significance of these variables usually appears in their self- and cross-power spectral densities, $\overline{E_i E_k^*}$.[21,22] The bar indicates an average over an ensemble of processes with identical statistical properties. If the only internal generators are signal generators, we can also define similar self- and cross-power spectral densities, but whether an ensemble average might or might not be necessary depends on whether the internal generators are defined explicitly or on a statistical basis. In order to preserve the form of the expressions of power of random and nonrandom voltage variables, we shall depart from convention and use rms values for all complex signal amplitudes.

The power expressions, which we shall derive later, involve the power spectral-density matrix

$$\overline{\underset{\sim}{E}\underset{\sim}{E}^{\dagger}} = \begin{bmatrix} \overline{E_1 E_1^*} & \cdots & \overline{E_1 E_i^*} & \cdots & \overline{E_1 E_n^*} \\ \vdots & & \vdots & & \vdots \\ \overline{E_i E_1^*} & & \overline{E_i E_i^*} & & \overline{E_i E_n^*} \\ \vdots & & \vdots & & \vdots \\ \overline{E_n E_1^*} & \cdots & \overline{E_n E_i^*} & \cdots & \overline{E_n E_n^*} \end{bmatrix} \tag{3}$$

in which the matrix $\underset{\sim}{E}^{\dagger}$ is defined as the complex conjugate of the transpose of the matrix $\underset{\sim}{E}$. In general, a matrix $\underset{\sim}{A}^{\dagger}$ is said to be the Hermitian conjugate or Hermitian transpose of a matrix $\underset{\sim}{A}$. Any matrix that is equal to its Hermitian conjugate is said to be a Hermitian matrix. The matrix in Eq. 3 is such a matrix.

By examining the quadratic form associated with the matrix $\overline{\underset{\sim}{E}\underset{\sim}{E}^{\dagger}}$, it can be shown that the matrix $\overline{\underset{\sim}{E}\underset{\sim}{E}^{\dagger}}$ is a positive definite or positive semidefinite matrix.[18] In general, if the voltages of $\overline{\underset{\sim}{E}\underset{\sim}{E}^{\dagger}}$ are noise voltages it can usually be argued from physical grounds (barring trivial degeneracies and noiseless positive or negative resistances) that the matrix is positive definite. On the other hand, if the voltages of $\overline{\underset{\sim}{E}\underset{\sim}{E}^{\dagger}}$ are signal voltages, the matrix will frequently be positive semidefinite.

2.2 EXCHANGEABLE POWER

In describing the performance of multiterminal devices we shall necessarily be concerned with the power that a network can exchange with a load. For this purpose we shall use the concept of exchangeable power. The exchangeable power of a one-terminal-pair source is the stationary value of the power output from the source obtained by arbitrary variation of the terminal current or voltage.

Thus for the Thévenin equivalent representation of the source of Fig. 2, which has a complex open-circuit voltage E and an impedance Z, we are interested in the stationary

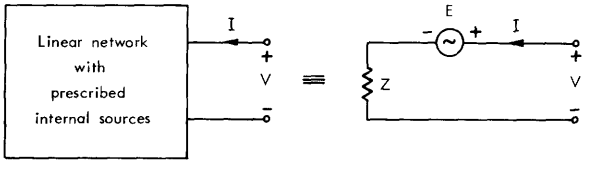

Fig. 2. Thévenin equivalent of a one-terminal-pair linear network.

value of the power out

$$P = -\frac{1}{2}[VI^* + IV^*]. \tag{4}$$

The terminal current and voltage of this network are related by

$$V = ZI + E. \tag{5}$$

If we use Eq. 5 in (4) to eliminate V and V^*, we find that

$$P = -\frac{1}{2}[II^*(Z+Z^*)+IE^*+I^*E]. \tag{6}$$

The exchangeable power of the network is then just that value of P in Eq. 6 for which the partial derivative of P with respect to either I or I^* is zero. The exchangeable power is, then,

$$P = \frac{EE^*}{2(Z+Z^*)}. \tag{7}$$

If the source is random, a bar over EE^* is needed in Eq. 7. No other change is necessary, inasmuch as we are using rms amplitudes for signal voltages.

If the real part of the source impedance is positive ($Z+Z^* > 0$), the exchangeable power of the source is the same as the available power. In this case the exchangeable power will be delivered to a load whose impedance is Z^*. On the other hand, if the real part of the source impedance is negative, the exchangeable power is negative. Consequently, the source receives an amount of power equal to the magnitude of the exchangeable power when a nonpassive impedance Z^* is connected to its terminals. This is the largest amount of power that can be pushed into the source network.

2.3 LOSSLESS IMBEDDINGS

In this report we shall use extensively the concept of lossless imbedding networks. In order to make these later discussions as simple as possible, we shall give a rather complete review of the concept of lossless imbeddings now. A network is said to be imbedded in a lossless network if it can only be excited through that lossless network. If we were to imbed the network of Fig. 2 in a 2n-terminal-pair lossless network, we would obtain the new n-terminal-pair network shown in Fig. 3.

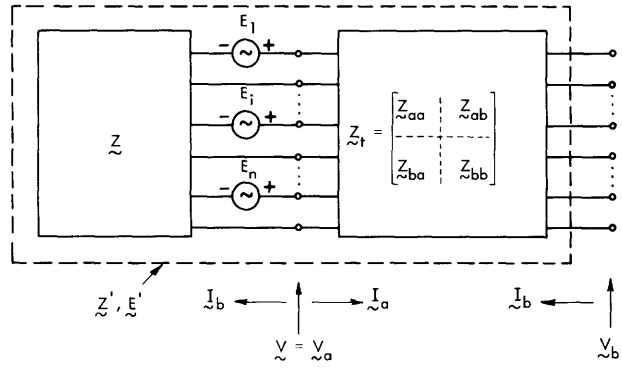

Fig. 3. Lossless imbedding of an n-terminal-pair network.

We would like to know in general terms how the parameters of the new network are related to those of the original network. The imbedding network alone

satisfies the terminal relations

$$\begin{bmatrix} \underset{\sim}{V}_a \\ \cdots \\ \underset{\sim}{V}_b \end{bmatrix} = \left[\begin{array}{c:c} \underset{\sim}{Z}_{aa} & \underset{\sim}{Z}_{ab} \\ \hdashline \underset{\sim}{Z}_{ba} & \underset{\sim}{Z}_{bb} \end{array}\right] \begin{bmatrix} \underset{\sim}{I}_a \\ \cdots \\ \underset{\sim}{I}_b \end{bmatrix} = \underset{\sim}{Z}_t \begin{bmatrix} \underset{\sim}{I}_a \\ \cdots \\ \underset{\sim}{I}_b \end{bmatrix} \tag{8}$$

or

$$\underset{\sim}{V}_a = \underset{\sim}{Z}_{aa}\underset{\sim}{I}_a + \underset{\sim}{Z}_{ab}\underset{\sim}{I}_b \tag{9a}$$

$$\underset{\sim}{V}_b = \underset{\sim}{Z}_{ba}\underset{\sim}{I}_a - \underset{\sim}{Z}_{bb}\underset{\sim}{I}_b. \tag{9b}$$

Since this network is lossless, the time average power delivered to it must be zero. Then

$$P = \frac{1}{2}\begin{bmatrix} \underset{\sim}{V}_a \\ \cdots \\ \underset{\sim}{V}_b \end{bmatrix}^{\dagger} \begin{bmatrix} \underset{\sim}{I}_a \\ \cdots \\ \underset{\sim}{I}_b \end{bmatrix} + \frac{1}{2}\begin{bmatrix} \underset{\sim}{I}_a \\ \cdots \\ \underset{\sim}{I}_b \end{bmatrix}^{\dagger} \begin{bmatrix} \underset{\sim}{V}_a \\ \cdots \\ \underset{\sim}{V}_b \end{bmatrix} = 0 , \tag{10}$$

Using Eq. 8 in Eq. 10, we find that

$$\frac{1}{2}\begin{bmatrix} \underset{\sim}{I}_a \\ \cdots \\ \underset{\sim}{I}_b \end{bmatrix}^{\dagger} \left[\underset{\sim}{Z}_t + \underset{\sim}{Z}_t^{\dagger}\right] \begin{bmatrix} \underset{\sim}{I}_a \\ \cdots \\ \underset{\sim}{I}_b \end{bmatrix} = 0. \tag{11}$$

Equation 11 can be satisfied under all loadings, that is, for any set of currents $\underset{\sim}{I}_a$ and $\underset{\sim}{I}_b$, if and only if

$$\underset{\sim}{Z}_t + \underset{\sim}{Z}_t^{\dagger} = 0 \tag{12}$$

or

$$\underset{\sim}{Z}_{aa} = -\underset{\sim}{Z}_{aa}^{\dagger} \qquad \underset{\sim}{Z}_{ab} = \underset{\sim}{Z}_{ba}^{\dagger} \qquad \underset{\sim}{Z}_{bb} = -\underset{\sim}{Z}_{bb}^{\dagger}. \tag{13}$$

The relation between the terminal voltages and currents of the original network are given by Eq. 1. From Fig. 3 we see that the voltages $\underset{\sim}{V}$ are equal to the voltages $\underset{\sim}{V}_a$, and the currents $\underset{\sim}{I}$ are equal to the negatives of the currents $\underset{\sim}{I}_a$ into one side of the imbedding network. Thus

$$\underset{\sim}{V} = \underset{\sim}{V}_a \quad \text{and} \quad \underset{\sim}{I} = -\underset{\sim}{I}_a. \tag{14}$$

By using Eqs. 14 in Eq. 5 and eliminating the voltages $\underset{\sim}{V}_a$ between the resulting equation and Eq. 9a, we obtain

$$\underset{\sim}{I}_a = (\underset{\sim}{Z} + \underset{\sim}{Z}_{aa})^{-1}\,\underset{\sim}{E} - (\underset{\sim}{Z}+\underset{\sim}{Z}_{aa})^{-1}\,\underset{\sim}{Z}_{ab}\underset{\sim}{I}_b. \tag{15}$$

When this equation is substituted in Eq. 9b we obtain the relations between the new terminal variables $\underset{\sim}{V}_b$ and $\underset{\sim}{I}_b$.

$$\underset{\sim}{V}_b = \underset{\sim}{Z}' \underset{\sim}{I}_b + \underset{\sim}{E}', \tag{16}$$

where

$$\underset{\sim}{Z}' = -\underset{\sim}{Z}_{ba}(\underset{\sim}{Z}+\underset{\sim}{Z}_{aa})^{-1}\,\underset{\sim}{Z}_{ab} + \underset{\sim}{Z}_{bb} \tag{17}$$

$$\underset{\sim}{E}' = \underset{\sim}{Z}_{ba}(\underset{\sim}{Z}+\underset{\sim}{Z}_{aa})^{-1}\,\underset{\sim}{E}. \tag{18}$$

Here $\underset{\sim}{Z}'$ and $\underset{\sim}{E}'$ are the impedance matrix and the open-circuit voltage matrix of the transformed network, respectively.

2.4 EXCHANGEABLE POWER OF AN IMBEDDED NETWORK

Now we shall determine the exchangeable power at the i^{th} terminal pair of the new network when all other terminal pairs are open-circuited. From Eq. 7 we see that it must be

$$P_{e,i} = \frac{\overline{E'_i E'^{*}_i}}{2\left(Z'_{ii}+Z'^{*}_{ii}\right)}, \tag{19}$$

where E'_i is the open-circuit voltage at this terminal pair, the i^{th} component of $\underset{\sim}{E}'$ of Eq. 18, and Z'_{ii} is the impedance at this terminal pair, the i^{th} element in the i^{th} column of $\underset{\sim}{Z}'$ of Eq. 17. We may also write Eq. 19 as

$$P_{e,i} = \frac{\underset{\sim}{\xi}^{\dagger}\,\overline{\underset{\sim}{E}'\,\underset{\sim}{E}'^{\dagger}}\,\underset{\sim}{\xi}}{2\underset{\sim}{\xi}^{\dagger}\left(\underset{\sim}{Z}'+\underset{\sim}{Z}'^{\dagger}\right)\underset{\sim}{\xi}}, \tag{20}$$

where $\underset{\sim}{\xi}$ is a real column vector with all elements zero except the i^{th} which is unity.

$$\underset{\sim}{\xi} = \begin{bmatrix} \xi_1 \\ \vdots \\ \xi_i \\ \vdots \\ \xi_n \end{bmatrix} = \begin{bmatrix} 0 \\ \vdots \\ 1 \\ \vdots \\ 0 \end{bmatrix} \qquad \begin{cases} \xi_j = 0 & j \neq i \\ \xi_i = 1 \end{cases} \tag{21}$$

The matrix $\underset{\sim}{\xi}$ may be visualized as a double-pole n-throw selector switch that connects one of the terminal pairs of the transformed network to an output terminal pair.

If we define the matrix $\underset{\sim}{\tau}^{\dagger}$ as

$$\underset{\sim}{\tau}^{\dagger} = \underset{\sim}{Z}_{ba}(\underset{\sim}{Z}+\underset{\sim}{Z}_{aa})^{-1}, \tag{22}$$

we see from Eq. 18 that

$$\overline{\underset{\sim}{E}'\,\underset{\sim}{E}'^{\dagger}} = \underset{\sim}{\tau}^{\dagger}\,\overline{\underset{\sim}{E}\,\underset{\sim}{E}^{\dagger}}\,\underset{\sim}{\tau}. \tag{23}$$

From (13) and (17) we find that

$$\underset{\sim}{Z}' + \underset{\sim}{Z}'^{\dagger} = \underset{\sim}{Z}_{ba}(\underset{\sim}{Z}+\underset{\sim}{Z}_{aa})^{-1}\,\underset{\sim}{Z}_{ba}^{\dagger} + \underset{\sim}{Z}_{ba}(\underset{\sim}{Z}+\underset{\sim}{Z}_{aa})^{\dagger-1}\,\underset{\sim}{Z}_{ba}^{\dagger}$$

$$= \underset{\sim}{\tau}^{\dagger}(\underset{\sim}{Z}+\underset{\sim}{Z}_{aa})^{\dagger}\,(\underset{\sim}{Z}+\underset{\sim}{Z}_{aa})^{\dagger-1}\,\underset{\sim}{Z}_{ba}^{\dagger} + \underset{\sim}{Z}_{ba}(\underset{\sim}{Z}+\underset{\sim}{Z}_{aa})^{-1}\,(\underset{\sim}{Z}+\underset{\sim}{Z}_{aa})\,\underset{\sim}{\tau}$$

$$= \underset{\sim}{\tau}^{\dagger}(\underset{\sim}{Z}+\underset{\sim}{Z}^{\dagger})\,\underset{\sim}{\tau}. \tag{24}$$

Using (23) and (24) in Eq. 20, we obtain

$$P_{e,i} = \frac{\underset{\sim}{\xi}^{\dagger}\underset{\sim}{\tau}^{\dagger}\overline{\underset{\sim}{E}\underset{\sim}{E}^{\dagger}}\,\underset{\sim}{\tau}\,\underset{\sim}{\xi}}{2\underset{\sim}{\xi}^{\dagger}\underset{\sim}{\tau}^{\dagger}(\underset{\sim}{Z}+\underset{\sim}{Z}^{\dagger})\,\underset{\sim}{\tau}\,\underset{\sim}{\xi}} \tag{25}$$

or

$$P_{e,i} = \frac{\underset{\sim}{x}^{\dagger}\overline{\underset{\sim}{E}\underset{\sim}{E}^{\dagger}}\,\underset{\sim}{x}}{2\underset{\sim}{x}^{\dagger}(\underset{\sim}{Z}+\underset{\sim}{Z}^{\dagger})\,\underset{\sim}{x}}, \tag{26}$$

where

$$\underset{\sim}{x} = \underset{\sim}{\tau}\,\underset{\sim}{\xi}. \tag{27}$$

The components of the column vector $\underset{\sim}{x}$ defined in Eq. 27 have a simple physical interpretation. From Eq. 26 it may be seen that they are complex voltage ratios. For instance, if all voltage sources in the network are short-circuited except E_1, which is the open-circuit voltage at the first terminal pair of the original network, the open-circuit voltage at the i^{th} output terminal pair is $x_1\,E_1$, where x_1 is the first component of the column matrix $\underset{\sim}{x}$. Similarly, the other components of $\underset{\sim}{x}$ relate the open-circuit voltages at the other terminal pairs of the original network to the open-circuit voltage at the output.

We would now like to determine the range of values that the exchangeable power of Eq. 26 may take on as the imbedding network is varied arbitrarily. As we vary the imbedding network in an arbitrary fashion we see that $\underset{\sim}{\tau}$ as defined in Eq. 22 is completely unrestricted, since $\underset{\sim}{Z}_{ba}$ in Eq. 13 is unrestricted. Thus we conclude that $\underset{\sim}{\tau}$ may be any square matrix of order n. It follows that the column vector $\underset{\sim}{x}$ defined by Eq. 27 is likewise unrestricted – its elements take on all possible values as the lossless network is varied through all forms consistent with the constraint of Eq. 12. Consequently, we shall look for the extrema of $P_{e,i}$ with respect to variations in the imbedding network.

2.5 STATIONARY VALUE PROBLEM

Rather than look for the stationary values of $P_{e,i}$ of Eq. 26, we shall follow Haus and Adler and look for stationary values of p_z.

$$p_z = -P_{e,i} = -\frac{\underset{\sim}{x}^{\dagger}\overline{\underset{\sim}{E}\underset{\sim}{E}^{\dagger}}\,\underset{\sim}{x}}{2\underset{\sim}{x}^{\dagger}(\underset{\sim}{Z}+\underset{\sim}{Z}^{\dagger})\,\underset{\sim}{x}}. \tag{28}$$

Looking for stationary values of p_z expressed as a function of the variables x_i is, however, equivalent to the problem of looking for the stationary values of $\underset{\sim}{x}^\dagger \overline{\underset{\sim}{E}\underset{\sim}{E}^\dagger}\, \underset{\sim}{x}$, subject to the constraint that $-2\underset{\sim}{x}^\dagger(\underset{\sim}{Z}+\underset{\sim}{Z}^\dagger)\,\underset{\sim}{x}$ = constant. Thus introducing the Lagrange multiplier, λ, we may look for the stationary values of $\underset{\sim}{x}^\dagger \overline{\underset{\sim}{E}\underset{\sim}{E}^\dagger}\, \underset{\sim}{x} + 2\,\lambda \underset{\sim}{x}^\dagger(\underset{\sim}{Z}+\underset{\sim}{Z}^\dagger)\,\underset{\sim}{x}$. This quantity may be regarded as a function of either the variables x_i or the variables x_i^*. Regarding it as a function of the set of variables x_i^*, we require that the set of conditions

$$\frac{\partial}{\partial x_i^*}\left[\underset{\sim}{x}^\dagger \overline{\underset{\sim}{E}\underset{\sim}{E}^\dagger}\, \underset{\sim}{x} + 2\,\lambda \underset{\sim}{x}^\dagger(\underset{\sim}{Z}+\underset{\sim}{Z}^\dagger)\,\underset{\sim}{x}\right] = 0 \qquad i = 1,\ 2,\ 3,\ \ldots,\ n \tag{29}$$

be satisfied. This leads to the eigenvalue equation

$$\overline{\underset{\sim}{E}\underset{\sim}{E}^\dagger}\, \underset{\sim}{x} + 2\lambda(\underset{\sim}{Z}+\underset{\sim}{Z}^\dagger)\,\underset{\sim}{x} = 0. \tag{30}$$

Note that if we had performed the differentiation with respect to the variables x_i rather than x_i^*, we would have obtained the Hermitian transpose of Eq. 30. Since both of the matrices involved explicitly in Eq. 30 are Hermitian, the eigenvalues of Eq. 30 are all real.[19] Therefore the eigenvalues of the equation that is the Hermitian transpose of Eq. 30 are the same as the eigenvalues of (30).

If we multiply Eq. 30 by $-\frac{1}{2}(\underset{\sim}{Z}+\underset{\sim}{Z}^\dagger)^{-1}$, we obtain the equivalent eigenvalue equation

$$\underset{\sim}{N}\underset{\sim}{x} - \lambda \underset{\sim}{x} = 0, \tag{31}$$

where

$$\underset{\sim}{N} = -\tfrac{1}{2}(\underset{\sim}{Z}+\underset{\sim}{Z}^\dagger)^{-1}\, \overline{\underset{\sim}{E}\underset{\sim}{E}^\dagger}.$$

The matrix N is defined as the characteristic noise matrix of the network. The cases for which $\underset{\sim}{Z} + \underset{\sim}{Z}^\dagger$ does not have a formal inverse can always be handled by introducing a suitable perturbation such as a small perturbing loss into the network. Comparing (30) and (31), we see that the eigenvalues of the characteristic noise matrix are also the eigenvalues of Eq. 30. Also it may be seen from Eqs. 23 and 24 that the characteristic noise matrix of a network that has been derived from another network by a lossless imbedding that preserves the number of terminal pairs (see Fig. 3) is related to the characteristic noise matrix of the original network by a similarity transformation, $\underset{\sim}{N}' = \underset{\sim}{T}^{-1}\, \underset{\sim}{N}\underset{\sim}{T}$. Thus the eigenvalues of the characteristic noise matrix are invariant with respect to lossless imbeddings that preserve the number of terminal pairs.

The range of p_z may now be determined from Eq. 30. Let λ_1 be an eigenvalue of Eq. 30, and $\underset{\sim}{x}^{(1)}$ be the corresponding eigenvector. If we premultiply (30) by $\underset{\sim}{x}^{(1)}$ and solve for λ_1, we find

$$\lambda_1 = -\frac{\underset{\sim}{x}^{(1)\dagger} \overline{\underset{\sim}{E}\underset{\sim}{E}^\dagger}\, \underset{\sim}{x}^{(1)}}{2\underset{\sim}{x}^{(1)\dagger}(\underset{\sim}{Z}+\underset{\sim}{Z}^\dagger)\,\underset{\sim}{x}^{(1)}} = p_{z,\ \mathrm{stat}} \tag{32}$$

Then λ_1 is real and a stationary value of p_z. It follows that the stationary values of

$P_{e,i}$ are the negatives of the eigenvalues of the characteristic noise matrix.

From Eq. 32 we see that the range of p_z is the same as the range of its eigenvalues. To determine this range we must consider three cases: (a) $\underset{\sim}{Z} + \underset{\sim}{Z}^\dagger$ positive definite; (b) $\underset{\sim}{Z} + \underset{\sim}{Z}^\dagger$ negative definite; and (c) $\underset{\sim}{Z} + \underset{\sim}{Z}^\dagger$ indefinite. Since we are considering only noise sources in $\underset{\sim}{E}$, we expect $\underset{\sim}{E}\underset{\sim}{E}^\dagger$ to be positive definite. If $\underset{\sim}{Z} + \underset{\sim}{Z}^\dagger$ is positive definite, we see from Eq. 32 that all of the eigenvalues are negative as shown in Fig. 4a. One of the

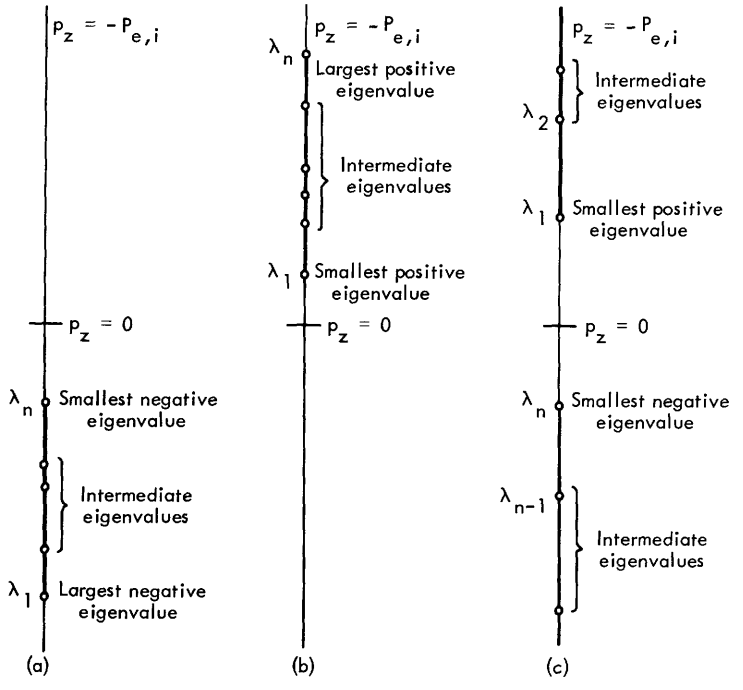

Fig. 4. Permitted ranges of p_z.

eigenvalues, λ_1, will be the largest negative eigenvalue; another, λ_n, will be the smallest negative eigenvalue. Since p_z is a continuous function of the variables x_i, the range of p_z must be between these two extreme eigenvalues as shown in Fig. 4a. The second case, in which $\underset{\sim}{Z} + \underset{\sim}{Z}^\dagger$ is negative definite, is handled by a similar argument; the range of p_z for this case is shown in Fig. 4b.

The third case, in which $\underset{\sim}{Z} + \underset{\sim}{Z}^\dagger$ is indefinite, is likewise handled quite easily. We see that for this case $\underset{\sim}{x}^\dagger(\underset{\sim}{Z}+\underset{\sim}{Z}^\dagger)\,\underset{\sim}{x}$ may be either positive or negative. Thus there will be both positive and negative eigenvalues for which solutions to Eq. 30 exist. The numerator of the expression in Eq. 32 is always greater than zero, and the denominator is always finite. Thus we conclude that p_z may be infinite, but it will have a smallest positive value equal to the smallest positive eigenvalue and a smallest negative value equal to the smallest negative eigenvalue. The indefinite case is illustrated in Fig. 4c.

For convenience, we shall adopt the convention of always numbering the eigenvalues of Eq. 30 in accordance with the range of the associated quadratic function p_z. Thus

we shall label the eigenvalues consecutively along the range of p_z from the smallest positive eigenvalue (or the largest negative eigenvalue if there are no positive eigenvalues) which we label λ_1, to the smallest negative eigenvalue (or largest positive eigenvalue if there are no negative eigenvalues) which we label λ_n. This numbering is illustrated in Fig. 4.

The principal results of this section may be summarized in two theorems.

THEOREM H&A-1. The stationary values of the exchangeable power, $P_{e,i}$, of a noisy network are the negatives of the (real) eigenvalues of the characteristic noise matrix, $\underset{\sim}{N}$.

THEOREM H&A-2. The eigenvalues of the characteristic noise matrix, $\underset{\sim}{N}$, are invariant with respect to lossless imbeddings which preserve the number of terminal pairs.

2.6 CANONICAL FORM OF A NOISY NETWORK

Additional insight into the meaning of the eigenvalues of the characteristic noise matrix of a network may be obtained from the canonical form of the network. The canonical form of a network may be derived from the original network by imbedding it in a lossless network that preserves the number of terminal pairs. This procedure, as shown in Fig. 3, led to a new network with an impedance matrix $\underset{\sim}{Z}'$, with

$$\underset{\sim}{Z}' = -\underset{\sim}{Z}_{ba}(\underset{\sim}{Z}+\underset{\sim}{Z}_{aa})^{-1}\underset{\sim}{Z}_{ab} + \underset{\sim}{Z}_{bb}.$$

Using Eq. 22 and Eq. 13, we can write

$$\underset{\sim}{Z}' = \underset{\sim}{\tau}^{\dagger}\left(\underset{\sim}{Z}^{\dagger}+\underset{\sim}{Z}_{aa}^{\dagger}\right)\underset{\sim}{\tau} + \underset{\sim}{Z}_{bb}$$

or

$$\underset{\sim}{Z}' = \frac{1}{2}\underset{\sim}{\tau}^{\dagger}(\underset{\sim}{Z}+\underset{\sim}{Z}^{\dagger})\underset{\sim}{\tau} + \frac{1}{2}\underset{\sim}{\tau}^{\dagger}(\underset{\sim}{Z}^{\dagger}-\underset{\sim}{Z})\underset{\sim}{\tau} + \underset{\sim}{\tau}^{\dagger}\underset{\sim}{Z}_{aa}^{\dagger}\underset{\sim}{\tau} + \underset{\sim}{Z}_{bb}. \tag{33}$$

From Eq. 22 we see that $\underset{\sim}{\tau}$ is independent of $\underset{\sim}{Z}_{bb}$ and from Eq. 13 we see that the only constraint on $\underset{\sim}{Z}_{bb}$ is that it be skew-Hermitian. One possible choice for the matrix $\underset{\sim}{Z}_{bb}$, then, is

$$\underset{\sim}{Z}_{bb} = \frac{1}{2}\underset{\sim}{\tau}^{\dagger}(\underset{\sim}{Z}-\underset{\sim}{Z}^{\dagger})\underset{\sim}{\tau} - \underset{\sim}{\tau}^{\dagger}\underset{\sim}{Z}_{aa}^{\dagger}\underset{\sim}{\tau}. \tag{34}$$

This choice satisfies the skew-Hermitian constraint, since the Hermitian transpose of this matrix is the negative of the matrix. Introducing Eq. 34 into Eq. 33, we find that this choice for $\underset{\sim}{Z}_{bb}$ gives

$$\underset{\sim}{Z}' = \frac{1}{2}\underset{\sim}{\tau}^{\dagger}(\underset{\sim}{Z}+\underset{\sim}{Z}^{\dagger})\underset{\sim}{\tau}. \tag{35}$$

Then using Eq. 22 in Eq. 18, we may write the relations between the terminal variables of the imbedded network of Fig. 3 as

$$\underset{\sim}{V}_b = \frac{1}{2}\,\underset{\sim}{\tau}^{\dagger}(\underset{\sim}{Z}+\underset{\sim}{Z}^{\dagger})\,\underset{\sim}{\tau}\,\underset{\sim}{I}_b + \underset{\sim}{\tau}^{\dagger}\,\underset{\sim}{E}. \tag{36}$$

Let us for the moment consider the power spectral-density matrix of this imbedded network which is written as

$$\overline{\underset{\sim}{E}'\,\underset{\sim}{E}'^{\dagger}} = \underset{\sim}{\tau}^{\dagger}\,\overline{\underset{\sim}{E}\,\underset{\sim}{E}^{\dagger}}\,\underset{\sim}{\tau}. \tag{37}$$

It is always possible to simultaneously diagonalize two Hermitian matrices one of which is positive definite by the same conjunctive transformation. Since $\underset{\sim}{E}'\,\underset{\sim}{E}'^{\dagger}$ is related to the positive definite matrix $\underset{\sim}{E}\,\underset{\sim}{E}^{\dagger}$ by a conjunctive transformation and $\underset{\sim}{Z}'$ in Eq. 35 is related to $\underset{\sim}{Z} + \underset{\sim}{Z}^{\dagger}$ by the same conjunctive transformation, it is always possible to find a lossless network that will simultaneously diagonalize $\underset{\sim}{Z}'$ and $\underset{\sim}{E}'\,\underset{\sim}{E}'^{\dagger}$. The network obtained through this network transformation is the canonical network shown in Fig. 5.

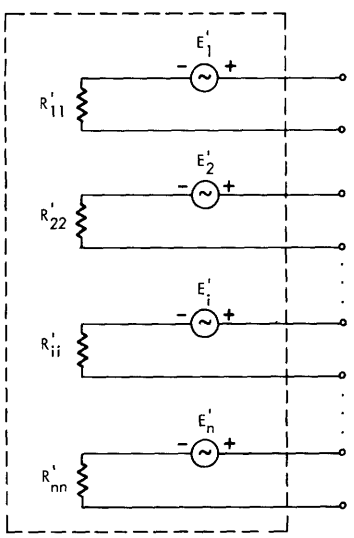

Fig. 5. Canonical form of a noisy network.

Since $\overline{E'\,E'^{\dagger}}$ is diagonal, none of the voltages is correlated with any other voltage, and the canonical form consists of a set of independently noisy resistors. The characteristic noise matrix of the canonical network is diagonal with elements along the diagonal which are the negatives of the exchangeable powers of each of these resistors

$$\underset{\sim}{N}' = \mathrm{Diag}\left(-\overline{E'_1 E'^{*}_1}/4R'_{11}, -\overline{E'_2 E'^{*}_2}/4R'_{22}, \ldots, -\overline{E'_n E'^{*}_n}/4R'_{nn}\right). \tag{38}$$

Since the eigenvalues of the characteristic noise matrix are invariant under such a lossless imbedding, we see that the elements of $\underset{\sim}{N}'$ are the eigenvalues of the characteristic noise matrix of the original network. We conclude that the exchangeable powers of the n independently noisy resistors that constitute the canonical form of a network are the negatives of the eigenvalues of the characteristic noise matrix of the original network.

We have also proved the two following theorems.

THEOREM H&A-3. At any particular frequency, every n-terminal-pair noisy network can be reduced by lossless imbedding to a canonical form consisting of n separate (possibly negative) resistances each in series with an uncorrelated noise voltage generator.

THEOREM H&A-4. The exchangeable powers of the n independent sources of the canonical form of any n-terminal-pair noisy network are equal and opposite in sign to the n eigenvalues of the characteristic noise matrix, $\underset{\sim}{N}$, of the original network.

2.7 LOAD NOISE

In order to set up meaningful performance criteria for linear amplifying systems we must determine the effects that load noise has on the specification of the noise performance of such a system. Let us, then, consider a system consisting of a multiterminal noisy signal source connected in some fashion with a noisy multiterminal amplifier to produce an output at a single terminal pair. At this single-output terminal pair the system may be represented by its Thévenin equivalent source which consists of an open-circuit noise-voltage source, E_n, an open-circuit signal-voltage source, E_s, and an impedance, Z_o, as shown in Fig. 6. Generally we specify the quality of the output of

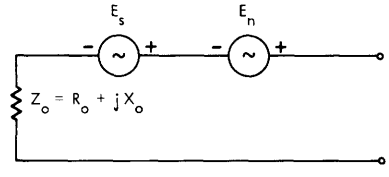

Fig. 6. Thévenin equivalent of a linear amplifying system.

such a system by specifying the exchangeable signal power at the output and the ratio of exchangeable signal power to exchangeable noise power. The signal-to-noise ratio defined in this way, which we shall refer to as the exchangeable signal-to-noise ratio, may be realized as the ratio of signal power delivered to a noiseless load resistor to the noise power delivered to the same noiseless resistor. But in building amplifying systems we must take the viewpoint that ultimately we shall connect the output to a real (noisy) load resistor. The question that must necessarily be resolved is, Under what conditions is the ratio of exchangeable signal power to exchangeable noise power at the output a good measure of the quality of the signal received by the load?

This problem is usually circumvented by stating that the exchangeable signal-to-noise ratio is a valid measure of the quality of the signal received if the temperature of the load resistor is "sufficiently low." Such a viewpoint, however, merely avoids the issue. We must still determine what temperature is sufficiently low. For some systems even liquid-helium temperatures might not be sufficiently low,[23,24] while for others room temperature is sufficiently low – as in an ordinary commercial phonograph amplifier. This difficulty is compounded by the fact that it is not generally convenient

to keep our loads at low temperatures. We shall attack this problem by setting up several criteria for specifying the signal-to-noise ratio at the output for the case in which the load is noisy. We shall then compare these criteria with the exchangeable signal-to-noise ratio.

The situation that we are considering is shown in Fig. 7. We have connected a noisy load resistor at temperature T_1 to the output of a linear system through an ideal transformer with a turns ratio of n:1. Rather than show the transformer, we have merely

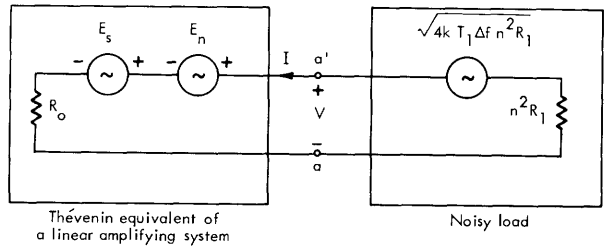

Fig. 7. Noisy loading of the output of a linear system.

indicated the values of the load resistor and its noise voltage as they would appear when referred to the input side of the transformer. The transformer has been included to enable us to vary the load resistance by varying the transformer ratio, n. We have dropped all reactive elements from the circuit, since they contribute nothing to the results and, in any event, can always be tuned out.

We must now set up several signal-to-noise ratio criteria for the circuit shown. One possible criterion is the ratio of the mean-square signal voltage appearing across the terminals a and a' to the mean-square noise voltage between these two terminal pairs. We shall refer to this quantity as the signal-to-noise voltage ratio. Another criterion is the ratio of the mean-square signal current flowing in the circuit of Fig. 7 to the mean-square noise voltage flowing in this circuit. We shall refer to this quantity as the signal-to-noise current ratio. It has been pointed out elsewhere[18] that if we were interested only in signal-to-noise voltage or current ratios we would never use amplifiers in any system because we may always obtain as much voltage or current gain as we want, without adding any noise by using ideal lossless transformers. The fact that we are considering the use of amplifiers in a system implies that we are basically interested in obtaining a certain amount of signal power from the output of the device shown in Fig. 7. (Also, presumably this amount of power is larger than that which would have been obtained if amplifiers had not been used. Thus it is assumed that the system whose output is represented in Fig. 7 has gain.) The third criterion that we choose, then, should be one that is based on power considerations. The most obvious criterion to choose is one that can be measured most easily. This is the ratio of the signal power delivered to the load network (both noise sources short-circuited) to the net noise power delivered to the load network by both noise sources. Physically, we can measure these powers by

calorimetric methods. If we place the load network in a calorimeter, we can measure the power delivered to the load when the circuit is as shown in Fig. 7; we can perform a similar measurement with the signal source shut off. The second measurement is the relevant noise power; the difference of the first minus the second is the relevant signal power.

Let us now calculate these quantities for the circuit shown in Fig. 7. The exchangeable signal power at the output of the linear system is

$$p_o = \frac{\overline{|E_s|^2}}{4R_o}, \tag{39}$$

and the ratio of exchangeable signal power to exchangeable noise power is

$$s_s = \frac{\overline{|E_s|^2}}{\overline{|E_n|^2}}. \tag{40}$$

The powers delivered to the load may each be calculated independently, since the three voltage sources shown in Fig. 7 are statistically independent. The signal power delivered to the load is given by the product $\overline{|I_s|^2}\, n^2R_1$, where I_s is the current when E_n and T_1 are zero.

$$p_1 = \frac{\overline{|E_s|^2}\, n^2R_1}{\left(R_o+n^2R_1\right)^2} = p_o \frac{4n^2R_1R_o}{\left(R_o+n^2R_1\right)^2}. \tag{41a}$$

We may also write this as

$$p_1 = p_o \frac{4}{2 + \frac{R_o}{n^2R_1} + \frac{n^2R_1}{R_o}}. \tag{41b}$$

Similarly, the power delivered to the load when all voltages except E_n are short-circuited is

$$p_{n1} = \frac{\overline{|E_n|^2}\, n^2R_1}{\left(R_o+n^2R_1\right)^2} = \frac{p_o}{s_o} \frac{4n^2R_1R_o}{\left(R_o+n^2R_1\right)^2}. \tag{42}$$

The power, p_{n2}, delivered to the load by the load noise is just the negative of the power delivered to the resistance R_o of the amplifying system by the thermal generator of the load.

$$p_{n2} = -\frac{\left(4kT_1\Delta f n^2R_1\right) R_o}{\left(R_o+n^2R_1\right)^2} = -kT_1\Delta f \frac{4n^2R_1R_o}{\left(R_o+n^2R_1\right)^2}. \tag{43}$$

The total noise power, p_n, delivered to the load network is just the algebraic

sum of p_{n1} and p_{n2}.

$$p_n = \left[\frac{p_o}{s_o} - kT_1\Delta f\right] \frac{4n^2R_1R_o}{\left(R_o+n^2R_1\right)^2} . \tag{44}$$

The ratio of the signal power delivered to the load to the noise power delivered to the load, which we shall designate as s_1, is obtained by dividing p_s by p_n. This yields

$$s_1 = \frac{1}{\frac{1}{s_o} - \frac{kT_1\Delta f}{p_o}} . \tag{45}$$

The noise-to-signal current ratio may be calculated by noting that the mean-square current flowing in the circuit of Fig. 9 is just

$$\overline{|I|^2} = \frac{\overline{|E_s|^2} + \overline{|E_n|^2} + 4kT_1\Delta fn^2R_1}{\left(R_o+n^2R_1\right)^2}$$

The noise-to-signal current ratio is, therefore, given by

$$\frac{\overline{|I_n|^2}}{\overline{|I_s|^2}} = \frac{\overline{|E_n|^2} + 4kT_1\Delta fn^2R_1}{\overline{|E_s|^2}} = \frac{1}{s_o} + \frac{kT_1\Delta f}{p_o}\frac{n^2R_1}{R_o} \tag{46}$$

The noise-to-signal voltage ratio may be calculated by noting that the mean-square voltage across the terminal pair a - a' is just

$$\overline{|V|^2} = \left[\overline{|E_s|^2} + \overline{|E_n|^2}\right]\left[\frac{n^2R_1}{R_o + n^2R_1}\right]^2 + 4kT_1\Delta fn^2R_1\left[\frac{R_o}{R_o + n^2R_1}\right]^2 .$$

The noise-to-signal voltage ratio is, therefore, given by

$$\frac{\overline{|V_n|^2}}{\overline{|V_s|^2}} = \frac{\overline{|E_n|^2}}{\overline{|E_s|^2}} + \frac{kT_1\Delta f4R_o^2}{\overline{|E_s|^2}n^2R_1} = \frac{1}{s_o} + \frac{kT_1\Delta f}{p_o}\frac{R_o}{n^2R_1}. \tag{47}$$

The relations between the quantities of interest can best be shown by plotting the various noise-to-signal ratios against $1/p_1$, the reciprocal of the signal power delivered to the load. The output of the linear system determines a point (the source point) on this plane as shown in Fig. 8 for the case in which p_o is positive (positive output resistance). If a line of slope $kT_1\Delta f$ is drawn through this point, it intersects the noise-to-signal ratio axis at a distance $1/s_1$ from the origin. Since s_1 is independent of the transformer ratio, n, and $1/p_1$ varies from $1/p_o$ to infinity as n is varied, a plot of $1/s_1$ as a function

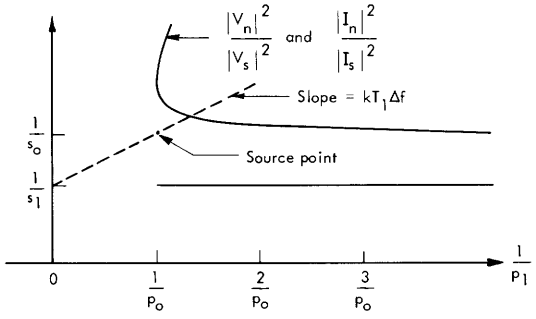

Fig. 8. Noise performance of a positive resistance source.

of $1/p_1$ appears as a half-line, as shown in Fig. 8. Thus, we see that the signal-to-noise ratio defined on a power-flow basis, s_1, is independent of the amount of power that is extracted from the output of the linear device.

The ratio of exchangeable signal power to exchangeable noise power characterizes the signal-to-noise ratio at the output under loaded conditions only if the fractional difference between s_1 and s_o is small, for instance, much less than unity. This procedure gives

$$\frac{s_1 - s_o}{s_1} = \frac{\frac{1}{s_o} - \frac{1}{s_1}}{1/s_o} = \frac{s_o}{p_o} kT_1\Delta f \ll 1 \tag{48}$$

or

$$\frac{p_o}{s_o} \gg kT_1\Delta f. \tag{49}$$

Referring back to the definitions of p_o and s_o, we see that p_o/s_o is the exchangeable noise power at the output of the linear system. If this condition is satisfied, there is no difficulty; the two criteria of performance are essentially in agreement. Let us consider for the moment the situations that can arise if the condition (49) is not satisfied.

From Fig. 8 we see that if the temperature of the load, T_1, is large enough, s_1 becomes large or possibly negative. Referring back to the equations from which this plot was derived, we see from Eq. 44 that negative s_1 implies that p_n is negative which means that the net noise-power flow is from the load to the system. It appears then that under these conditions neither s_1 or s_o characterizes the signal-to-noise ratio at the output. The paradox has occurred because we are trying to observe our signal and its concomitant noise in an extremely noisy environment. The primary reason, however, for using amplifying systems in the first place is to enable us to observe the signal above the background noise of the environment into which it is to be delivered. For this reason, we must conclude that any system that does not satisfy the conditions of (49) is not a satisfactory amplifying system at all. (If a system has a large exchangeable signal power, but also has such a large exchangeable signal-to-noise ratio that the inequality (49)

is not satisfied, we can only conclude that noise is unimportant in such a system.)

Using Eqs. 47 and 48 with Eq. 41a we can plot the noise-to-signal current ratio and the noise-to-signal voltage ratio as a function of $1/p_1$. These two curves fall on top of each other (see Fig. 8). We see from these curves that the noise-to-signal voltage ratio (or current ratio) is always greater than $1/s_o$ for any degree of mismatch. Moreover, it is apparent that if the inequality of Eq. 49 is satisfied and the mismatch at the output is not too great, the noise-to-signal voltage ratio and current ratio are both essentially equal to $1/s_o$.

Now let us consider the case in which the output resistance of the amplifying system is negative. Equations 39-47 are still valid; the only difference is that p_o changes sign. Thus a plot of $1/s_1$ as a function of $1/p_1$ gives the straight line shown in Fig. 9.

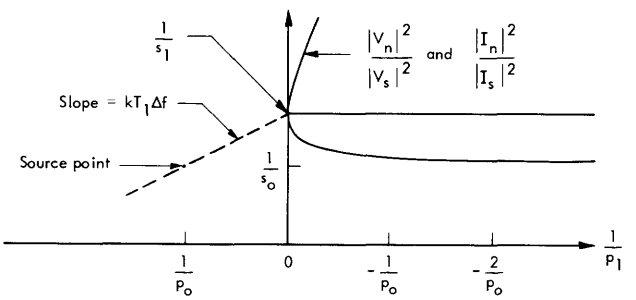

Fig. 9. Noise performance of a negative resistance source.

In this case the question of whether the device is indeed an amplifier never arises. The fact that $1/s_1$ is always greater than $1/s_o$ is due to the fact that the negative resistance at the output of the system is amplifying the noise generated by the load resistance; the net flow of this noise, then, is always into the load. It is apparent for this case that the signal-to-noise ratio s_1 is a better measure of noise performance than s_o. These two quantities agree only if $(1/s_1 - 1/s_o)/(1/s_o)$ is much less than unity. This condition is satisfied only if

$$\frac{|p_o|}{s_o} \ll kT_1\Delta f. \tag{50}$$

Comparing (50) with (49), we see that (50) is valid for positive or negative output resistances.

Now let us also examine the noise-to-signal current ratio and voltage ratio. These curves are also shown in Fig. 9. We see that if the inequality (50) is satisfied, the better segment of the curve of the noise-to-signal voltage ratio or current ratio comes arbitrarily close to the noise-to-signal ratio $1/s_o$ for any degree of mismatch. Let us consider, however, what happens when the inequality (50) is not satisfied. We note that for most systems the exchangeable signal-to-noise ratio at the output is unity within a factor

of several orders of magnitude. Thus, if p_o/s_o is of the order of $kT_1\Delta f$, p_o is within several orders of magnitude of $kT_1\Delta f$. But since we are considering the ultimate output of an amplifying system, we are, in general, interested in extracting an amount of signal power that is many orders of magnitude greater than the exchangeable noise power of the load resistor. Hence we shall be extracting an amount of power, p_1, that is orders of magnitude greater than p_o. From Fig. 9 we see that the signal-to-noise current or voltage ratio obtained is essentially that obtained at $1/p_1 = 0$, which is the same as the signal-to-noise power ratio, s_1. Moreover, we shall show in section 3.2 that if we incorporate into our system a resistor of temperature T_1, the best signal-to-noise ratio that can be obtained when this system is adjusted to give infinite exchangeable signal power at the output, is at least as large as s_1.

The obvious conclusion to draw from these discussions is that the quantity that characterizes the quality of a given amplifying system uniquely is the ratio of exchangeable signal power to exchangeable noise power when the system is adjusted for infinite exchangeable signal power. For, under these conditions, the inequality (48) is satisfied for any load temperature; thus such a signal-to-noise ratio characterizes the quality of the output of the system independently of the conditions of loading. Therefore, we shall define the optimum noise performance of a system as the best exchangeable signal-to-noise ratio that can be achieved at a single output by combining the elements of the system in such a way as to simultaneously obtain infinite exchangeable power.

This viewpoint does not preclude the use of specifications of exchangeable signal-to-noise ratios at finite exchangeable signal power; it merely shows us in what sense they are meaningful as output quantities. Thus if we have a system which does not satisfy the inequality (50) at its "output," we should regard the specification of exchangeable signal power and exchangeable signal-to-noise ratio at this "output" only as a meaningful way of specifying the characteristics of this device as an input source for some amplifying system to follow. In this sense, then, it is still meaningful to compare the exchangeable signal-to-noise ratio of two systems that have the same exchangeable signal power. In Section III we shall show how the noise measure and noise figure of an amplifier may be interpreted from this viewpoint.

III. NOISE-PERFORMANCE PLANE

We shall study three examples in accordance with the viewpoint described in section 2.6. We shall first consider the problem of a linear two-terminal-pair amplifier driven by a one-terminal-pair noisy signal source. Then we shall consider what we can accomplish by imbedding a one-terminal-pair noisy signal source and a noisy resistor in an arbitrary three-terminal-pair network. Finally, we shall consider the imbedding of a one-terminal-pair noisy signal source and an n-terminal-pair noisy network in an (n+2)-terminal-pair lossless network. We shall present the results of these three examples in a plot with exchangeable noise-to-signal ratio and the reciprocal of exchangeable signal power as coordinates. We shall refer to this plot as the noise-performance plane. By means of this plot we can give a simple geometric interpretation of noise measure and noise figure and bring out the relationships between the eigenvalues of the characteristic noise matrix of a noisy network and its optimal performance as an amplifier.

3.1 NOISE MEASURE OF A TWO-TERMINAL-PAIR AMPLIFIER

We shall now consider the situation shown in Fig. 10 where we have a noisy signal source driving a noisy two-terminal-pair amplifier. The noise performance of such an

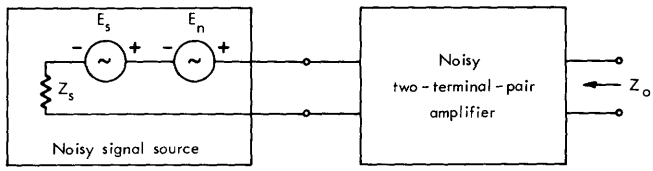

Fig. 10. Operation of a two-terminal-pair amplifier.

amplifier with a specified source is described in terms of its noise figure and exchangeable gain. The exchangeable gain of an amplifier is defined as the ratio of the exchangeable signal power at the output to the exchangeable signal power of the source. We denote the exchangeable signal power at the output as p_o.

$$p_o = \frac{\overline{|E_o|^2}}{4R_o}, \tag{51}$$

where E_o is the rms open-circuit signal voltage at the output, and R_o is the real part of the output impedance, Z_o, of the amplifier. We denote the exchangeable signal power of the source as p_s.

$$p_s = \frac{\overline{|E_s|^2}}{4R_s}, \tag{52}$$

where E_s is the rms open-circuit signal voltage of the source, and R_s is the real part of the source impedance Z_s. The exchangeable gain of the amplifier in Fig. 10 is

$$G_e = \frac{\text{Exchangeable Signal Power at the Output}}{\text{Exchangeable Signal Power of the Source}} = \frac{p_o}{p_s}. \tag{53}$$

The exchangeable noise figure, F_e, of the amplifier is defined by the relation

$$F_e = 1 + \frac{N_{e,i}}{kT_o \Delta f\, G_e}. \tag{54}$$

Here, $N_{e,i}$ is the exchangeable noise power at the output when the only sources present are the internal noise sources of the amplifier. The power $kT_o\Delta f$ is the exchangeable power of the source impedance when it is held in thermal equilibrium at temperature T_o. Thus $kT_o\Delta f\, G_e$ is the exchangeable noise power at the output when the only source present in the network is the thermal noise of the source when it is at temperature T_o. If the source has a negative resistance, we use the same definition (Eq. 54) for noise figure, but we must interpret $kT_o\Delta f$ merely as a convenient weighting factor for this case.

Let us now compute the ratio of exchangeable noise power to exchangeable signal power at the output of the device of Fig. 10 and see how the noise figure enters this expression. This ratio is given by

$$\frac{1}{s_o} = \frac{\left[\overline{\frac{|E_n|^2}{4R_o}}\right] G_e + N_{e,i}}{\overline{\frac{|E_s|^2}{4R_s}}\, G_e}. \tag{55}$$

By using Eqs. 52 and 54 in Eq. 55, we write this ratio as

$$\frac{1}{s_o} = \frac{1}{s_s} + \frac{kT_o\Delta f(F_e - 1)}{p_s}, \tag{56}$$

where s_s is the ratio of the exchangeable signal power of the source to the exchangeable noise power of the source. If we solve (56) for $F_e - 1$, the excess noise figure, we obtain an expression for this quantity in terms of the input and output parameters.

$$F_e - 1 = \frac{\frac{1}{s_o} - \frac{1}{s_s}}{1/p_s} \frac{1}{kT_o\Delta f}. \tag{57}$$

Before discussing (57) let us derive a similar expression for the noise measure of the amplifier. The noise measure, M_e, is defined in terms of the noise figure and exchangeable gain of the amplifier.

$$M_e = \frac{F_e - 1}{1 - 1/G_e}. \tag{58}$$

Using Eqs. 58 and 57, we rewrite this noise measure as

$$M_e = -\frac{\frac{1}{s_o} - \frac{1}{s_s}}{\frac{1}{p_o} - \frac{1}{p_s}} \frac{1}{kT_o \Delta f}. \tag{59}$$

Equations 57 and 59 suggest that we examine these results in a plot with exchangeable noise-to-signal ratio, $\frac{1}{s}$, and the reciprocal of exchangeable signal power, $1/p$, as coordinates. These coordinates define a plane to which we shall refer as the noise-performance plane. On such a plot, as shown in Fig. 11, the attributes of the source, $1/s_s$ and $1/p_s$ determine a point (the source point), and the attributes of the output terminal pair, $1/s_o$ and $1/p_o$ determine a second point (the point labeled first-stage output). Figure 11 has been drawn to illustrate the case in which the real part of the source impedance is positive and the real part of the output impedance of the amplifier is positive. Thus, for the purposes of this example, we do not really need the exchangeable power concept. We could carry out the discussion by using available power and available gain rather than exchangeable power and exchangeable gain. But Eqs. 51-59 are valid in any case, and we shall refer to them in connection with more general problems that are to be considered. The limited application of these concepts here is justifiable only because we are allowing ourselves no control over the parameters of the amplifier.

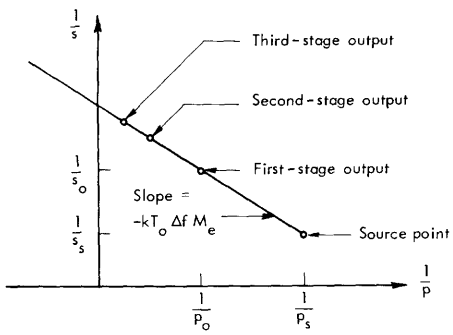

Fig. 11. Noise-performance plane.

Let us now use the plot in Fig. 11 to discuss the noise figure and noise measure of the amplifier shown in Fig. 10. The noise figure of the amplifier (see Eq. 57) is proportional to the increase in noise-to-signal ratio from input to output divided by the reciprocal of the exchangeable signal power of the source. On the other hand, the noise measure of the amplifier (see Eq. 59) is proportional to the negative of the increase in noise-to-signal ratio divided by the increase in the reciprocal of the exchangeable signal power. Therefore the line connecting the source point and the output point in the noise-performance plane has a slope $-kT_o \Delta f M_e$. Thus we see that noise measure is, in general, a much better measure of the quality of the noise performance of the amplifier, since it essentially tells us how much noise we are adding for a given increase in exchangeable signal power. There is another advantage in using noise measure. If we cascade a set of amplifiers each having the same noise measure, the noise measure

of the over-all amplifier so derived is the same as the noise measure of each of these component amplifiers.

To prove this last statement, we take the device shown in Fig. 10 and attach a transformer and reactance to the output. In this way we can make the output impedance of the amplifier equal to the impedance of the source ($Z_o=Z_s$). If we then connect another identical amplifier to this modified output, the second amplifier will have the same noise measure and exchangeable gain as the first. (Recall that both the exchangeable gain and the noise figure of an amplifier are dependent on the source impedance.) The exchangeable signal-to-noise ratio and exchangeable signal power at the output terminal pair of this second amplifier determine a point on the noise-performance plane. This point, labeled "second-stage output," is shown in Fig. 11. If we add more identical stages by following the same procedure we obtain additional points as shown. The case illustrated in Fig. 11 is for an exchangeable gain of 2 per stage.

If we cascade a large number of stages each having the same noise measure and a positive exchangeable gain greater than unity, we ultimately approach the limit of infinite exchangeable signal power. The noise-to-signal ratio that is obtained in the limit of infinite exchangeable signal power, $1/s_\infty$, may be written by inspection from Fig. 11.

$$\frac{1}{s_\infty} = \frac{1}{s_s} + \frac{kT_o \Delta f M_e}{p_s}. \tag{60}$$

Comparing Eq. 57 with Eq. 60, we see that the excess noise figure of the over-all chain of amplifiers with high gain is the same as the noise measure.

3.2 IMBEDDING OF A ONE-TERMINAL-PAIR SOURCE AND A ONE-TERMINAL-PAIR AMPLIFIER

We shall now investigate the values of exchangeable signal-to-noise ratio and exchangeable signal power that can be achieved at an output terminal pair by imbedding a noisy resistor (possibly negative) and a one-terminal-pair signal source in a lossless network. The circuit that we are considering is shown in Fig. 12.

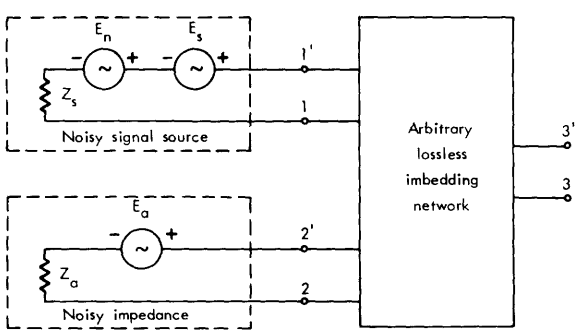

Fig. 12. Imbedding of a one-terminal-pair amplifier and a one-terminal-pair source.

Alternatively, we may regard the device with input terminals 1 - 1' and output terminals 3 - 3' as a two-terminal-pair device constructed from a one-terminal-pair device – the noisy resistor Z_a. We are then investigating the noise performance of the two-terminal-pair devices that can be constructed from one-terminal-pair devices through lossless imbeddings. From a theoretical standpoint it is simpler to regard the problem as an imbedding of the two terminal-pair network consisting of the source and resistor. The network that is being imbedded has an impedance matrix $\underset{\sim}{Z}$, and a cross spectral-density matrix $\underset{\sim}{E}\underset{\sim}{E}^{\dagger}$, with

$$\underset{\sim}{Z} = \begin{bmatrix} Z_s & \vdots & 0 \\ \cdots & \vdots & \cdots \\ 0 & \vdots & Z_a \end{bmatrix} \tag{61}$$

and

$$\overline{\underset{\sim}{E}\underset{\sim}{E}^{\dagger}} = \begin{bmatrix} \overline{|E_s|^2} + \overline{|E_n|^2} & \vdots & 0 \\ \cdots & \vdots & \cdots \\ 0 & \vdots & \overline{|E_a|^2} \end{bmatrix}. \tag{62}$$

Here, Z_s is the source impedance, and Z_a is the impedance of the resistor. The mean-square voltage $\overline{|E_s|^2}$ is the mean-square signal voltage of the source, $\overline{|E_n|^2}$ is the mean-square noise voltage of the source, and $\overline{|E_a|^2}$ is the mean-square noise voltage of the impedance Z_a. The matrix $\underset{\sim}{E}\underset{\sim}{E}^{\dagger}$ is diagonal, since the three voltages are assumed to be statistically independent. In accordance with Eq. 26, the exchangeable power at the output terminal pair is given by

$$P_{e,i} = \frac{\underset{\sim}{x}^{\dagger}\overline{\underset{\sim}{E}\underset{\sim}{E}^{\dagger}}\,\underset{\sim}{x}}{2\underset{\sim}{x}^{\dagger}(\underset{\sim}{Z}+\underset{\sim}{Z}^{\dagger})\,\underset{\sim}{x}}, \tag{63}$$

where $\underset{\sim}{x}$ is an arbitrary two-dimensional vector with components x_1 and x_2. Using (61) and (62) in (63) and expanding the expression, we obtain

$$P_{e,i} = \frac{|x_1|^2\,\overline{|E_s|^2} + |x_1|^2\,\overline{|E_n|^2} + |x_2|^2\,\overline{|E_a|^2}}{4|x_1|^2 R_s + 4|x_2|^2 R_a}. \tag{64}$$

From Eq. 64 we see that we may express the exchangeable signal power at the output as

$$p_o = \frac{|x_1|^2\,\overline{|E_s|^2}}{4|x_1|^2 R_s + 4|x_2|^2 R_a}, \tag{65}$$

and the ratio of exchangeable signal power to exchangeable noise power at the output as

$$s_o = \frac{|x_1|^2\,\overline{|E_s|^2}}{|x_1|^2\,\overline{|E_n|^2} + |x_2|^2\,\overline{|E_a|^2}}. \tag{66}$$

Again using p_s (see Eq. 52) for the exchangeable signal power of the source and defining

$$s_s = \frac{\overline{|E_s|^2}}{\overline{|E_n|^2}} \tag{67}$$

as the exchangeable signal-to-noise ratio of the source, we may rewrite (65) and (66) as

$$\frac{1}{s_o} = \frac{1}{s_s} + \frac{\overline{|E_a|^2}}{\overline{|E_s|^2}} \left|\frac{x_2}{x_1}\right|^2 \tag{68}$$

and

$$\frac{1}{p_o} = \frac{1}{p_s} + \frac{4R_a}{\overline{|E_s|^2}} \left|\frac{x_2}{x_1}\right|^2. \tag{69}$$

Equations 68 and 69 are a pair of linear parametric equations for $1/s_o$ and $1/p_o$, with $|x_2|/|x_1|\ \overline{|E_s|^2}$ as the parameter. Eliminating this parameter between the two equations, we obtain the relation

$$\frac{1}{s_o} = \frac{1}{s_s} + \frac{\overline{|E_a|^2}}{4R_o}\left[\frac{1}{p_o} - \frac{1}{p_s}\right]. \tag{70}$$

Comparing (70) with (59), we see that we may define a noise measure for the resistor equal to the negative of its exchangeable noise power divided by $kT_o\Delta f$.

$$M_e = -\frac{\overline{|E_a|^2}}{4R_a}\frac{1}{kT_o\Delta f}. \tag{71}$$

From Eq. 70 we also conclude that the noise measure of a single resistor used as an amplifier is invariant; varying the imbedding network in Fig. 12 varies only the exchangeable gain at constant noise measure.

Although Eq. 70, regarded as an equation for $1/s_o$ as a function of $1/p_o$, is the equation of a straight line, we can only realize half of this line. From Eq. 68 we see that the noise-to-signal ratio at the output is always equal to or greater than the noise-to-signal ratio of the source:

$$\frac{1}{s_o} \geqslant \frac{1}{s_s}. \tag{72}$$

Hence we can only realize points on the line determined by (70) that lie above the point $1/s_s$. Consequently, plots of (70) in the noise-performance plane appear as shown in Fig. 13. We show four distinct cases. Figure 13a illustrates the results obtained when the source resistance is positive and the amplifier resistance R_a is negative. Figure 13b

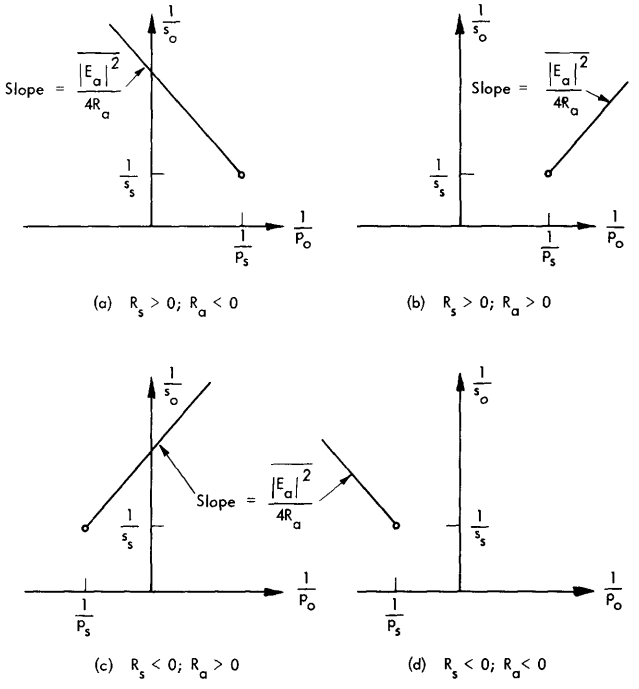

Fig. 13. Noise performance of noisy resistances.

applies when the source has a positive resistance and R_a is positive. Similarly, Fig. 13c and 13d are drawn for the case in which the source has negative exchangeable signal power: Fig. 13c is drawn for R_a positive; Fig. 13d for R_a negative.

Only two of the cases considered in Fig. 13 may be regarded as amplifying systems – these are cases a and c. Consider the case (Fig. 13a) of a positive resistance source combined with a noisy negative resistance. Such a device is usually referred to as a negative-resistance amplifier. By varying the coupling to the negative resistance, we can achieve arbitrarily large positive or negative exchangeable signal power at the output. The negative resistance used with a positive-resistance source may also be classified as an amplifier on the basis of its exchangeable gain; its exchangeable gain is positive and greater than unity, or it is negative. We would never, from noise considerations alone, use such a device to obtain negative exchangeable gain (negative exchangeable power at the output) because the noise-to-signal ratio is always larger for negative exchangeable gain than for positive or infinite exchangeable gain.

The situation shown in Fig. 13b does not in any sense correspond to amplification. By combining a noisy positive resistance with a positive-resistance source, we only increase the noise-to-signal ratio and decrease the exchangeable (available) signal power at the output. Correspondingly, the exchangeable gain for this case is positive and less than unity. On the other hand, if a positive noisy resistance is connected to a negative-resistance source, we have the situation shown in Fig. 13c. By varying the imbedding network, we can obtain infinite exchangeable signal power at the output; hence this

positive resistance is operating as an amplifier in the sense discussed in section 2.6. On an exchangeable gain basis, we can achieve exchangeable gain positive and greater than unity, or negative, by varying the imbedding network. Actually we would not use such a device to obtain negative exchangeable gain because the exchangeable signal-to-noise ratio at the output decreases as the exchangeable gain is decreased from minus infinity through smaller finite negative values.

For a positive resistance to be useful with a negative-resistance source its noise temperature must be lower than the temperature of any load under consideration. Otherwise one could use part of such a low-temperature load as an "amplifier" to achieve a lower noise-to-signal ratio at all exchangeable powers than one could obtain by using the noisy resistance. Applying similar arguments to the case of a negative noisy resistance combined with a negative-resistance source (Fig. 13d), we conclude that for this case the noisy negative resistance does not perform as an amplifier.

From these discussions we see that we could define an amplifier as a device which when driven by a particular source has a positive exchangeable gain greater than unity, but, in connection with Fig. 13, we have shown that under appropriate conditions both positive resistances and negative resistances may act as amplifiers. Therefore we may conclude that any linear noisy network may perform as an amplifier if it is used with an appropriate source. For this reason we shall use the term amplifier very loosely. We shall refer to any linear noisy network as an amplifier if we are investigating the problem of what ranges of performance in the noise-performance plane may be obtained by using the network in conjunction with a specified signal-source network. Subsequently, we shall determine whether or not the amplifier does indeed amplify when used in a given way with the prescribed source network.

We summarize the results presented in this section with two theorems.

THEOREM 1. The noise measure of a noisy impedance (having either a positive or negative real part) used as an amplifier with a one-terminal-pair (signal) source network is equal to the negative of the exchangeable noise power of this impedance divided by $kT_o\Delta f$.

THEOREM 2. For an amplifier used with a one-terminal-pair source, varying the exchangeable gain at constant noise measure, M, defines a continuum of output points in the noise-performance plane. These points lie on half of the line of slope $-MkT_o\Delta f$ passing through the point defined by the source; they lie on the half of this line lying above the source point.

3.3 IMBEDDING OF AN n-TERMINAL-PAIR AMPLIFIER AND A ONE-TERMINAL-PAIR SOURCE

The problem that we shall consider now is a generalization of the problem considered above. We are going to imbed a one-terminal-pair signal source and an n-terminal-pair amplifier in an arbitrary (n+2)-terminal-pair lossless network as shown in Fig. 14.

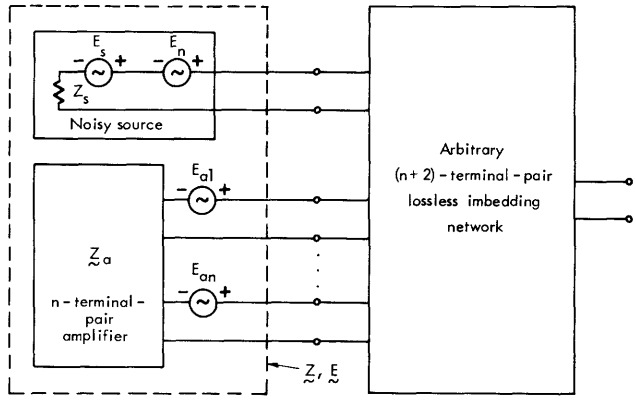

Fig. 14. Imbedding of an n-terminal-pair amplifier and a one-terminal-pair source.

The impedance matrix of the network that we are imbedding is $\underset{\sim}{Z}$, and the open-circuit cross spectral-density matrix is $\overline{\underset{\sim}{E}\,\underset{\sim}{E}^{\dagger}}$. From Fig. 14 we see that these matrices may be written

$$\underset{\sim}{Z} = \left[\begin{array}{c:c} Z_s & \underset{\sim}{0} \\ \hdashline \underset{\sim}{0} & \underset{\sim}{Z}_a \end{array}\right] \tag{73}$$

and

$$\overline{\underset{\sim}{E}\,\underset{\sim}{E}^{\dagger}} = \left[\begin{array}{c:c} \overline{|E_s|^2} + \overline{|E_n|^2} & \underset{\sim}{0} \\ \hdashline \underset{\sim}{0} & \overline{\underset{\sim}{E}_a\,\underset{\sim}{E}_a^{\dagger}} \end{array}\right]. \tag{74}$$

Here, $\underset{\sim}{Z}_a$ is the impedance matrix of the amplifier, and $\underset{\sim}{E}_a$ is the open-circuit voltage matrix of the amplifier. The exchangeable power at the output terminal pair in Fig. 14 is given by Eq. 26.

$$P_{e,i} = \frac{\underset{\sim}{x}^{\dagger}\,\overline{\underset{\sim}{E}\,\underset{\sim}{E}^{\dagger}}\,\underset{\sim}{x}}{2\underset{\sim}{x}^{\dagger}(\underset{\sim}{Z}+\underset{\sim}{Z}^{\dagger})\,\underset{\sim}{x}}. \tag{75}$$

Here, $\underset{\sim}{x}$ is an arbitrary (n+1)-dimensional vector to conform to $\underset{\sim}{E}$ and $\underset{\sim}{Z}$. For convenience, we shall partition the column vector $\underset{\sim}{x}$.

$$\underset{\sim}{x} = \left[\begin{array}{c} x_1 \\ \hdashline \underset{\sim}{x}_2 \end{array}\right] = \left[\begin{array}{c} x_1 \\ \vdots \\ x_{21} \\ x_{22} \\ \vdots \\ x_{2n} \end{array}\right] \tag{76}$$

Substituting (73), (74), and (76) in Eq. 75, we obtain

$$P_{e,i} = \frac{|x_1|^2 \overline{|E_s|^2} + |x_1|^2 \overline{|E_n|^2} + \underset{\sim}{x}_2^\dagger \overline{\underset{\sim}{E}_a \underset{\sim}{E}_a^\dagger} \underset{\sim}{x}_2}{2|x_1|^2 \left(Z_s + Z_s^*\right) + 2\underset{\sim}{x}_2^\dagger \left(\underset{\sim}{Z}_a + \underset{\sim}{Z}_a^\dagger\right) \underset{\sim}{x}_2}. \tag{77}$$

From Eq. 77 we see that the output exchangeable signal power is given by

$$p_o = \frac{|x_1|^2 \overline{|E_s|^2}}{4|x_1|^2 R_s + 2\underset{\sim}{x}_2^\dagger \left(\underset{\sim}{Z}_a + \underset{\sim}{Z}_a^\dagger\right) \underset{\sim}{x}_2}, \tag{78}$$

and the ratio of exchangeable signal power to exchangeable noise power at the output is given by

$$s_o = \frac{|x_1|^2 \overline{|E_s|^2}}{|x_1|^2 \overline{|E_n|^2} + \underset{\sim}{x}_2^\dagger \overline{\underset{\sim}{E}_a \underset{\sim}{E}_a^\dagger} \underset{\sim}{x}_2}. \tag{79}$$

In terms of the exchangeable signal power of the source, p_s, and the exchangeable signal-to-noise ratio of the source, s_s, we rewrite Eqs. 78 and 79.

$$\frac{1}{p_o} = \frac{1}{p_s} = \frac{2\underset{\sim}{x}_2^\dagger \left(\underset{\sim}{Z}_a + \underset{\sim}{Z}_a^\dagger\right) \underset{\sim}{x}_2}{|x_1|^2 \overline{|E_s|^2}} \tag{80}$$

and

$$\frac{1}{s_o} = \frac{1}{s_s} + \frac{\underset{\sim}{x}_2^\dagger \overline{\underset{\sim}{E}_a \underset{\sim}{E}_a^\dagger} \underset{\sim}{x}_2}{|x_1|^2 \overline{|E_s|^2}}. \tag{81}$$

Recall that the vector $\underset{\sim}{x}$ is completely arbitrary. That is, by varying the imbedding network in Fig. 14 we may vary independently each of the components of the vector $\underset{\sim}{x}$. Let us assume that we have adjusted the imbedding network for some specified vector $\underset{\sim}{x}_2$. We can now vary the imbedding network in such a way that $\underset{\sim}{x}_2$ is held constant and only x_1, the first component of $\underset{\sim}{x}$ (see Eq. 75), is varied. In this sense we may consider Eqs. 80 and 81 to be a pair of parametric equations relating $1/p_o$ and $1/s_o$ through the parameter x_1. Eliminating x_1 between these two equations, we find that $1/s_o$ and $1/p_o$ are related by

$$\frac{1}{s_o} = \frac{1}{s_s} + \frac{\underset{\sim}{x}_2^\dagger \overline{\underset{\sim}{E}_a \underset{\sim}{E}_a^\dagger} \underset{\sim}{x}_2}{2\underset{\sim}{x}_2^\dagger \left(\underset{\sim}{Z}_a + \underset{\sim}{Z}_a^\dagger\right) \underset{\sim}{x}_2} \left(\frac{1}{p_o} - \frac{1}{p_s}\right). \tag{82}$$

Defining the function λ as

$$\lambda = -\frac{\underset{\sim}{x}_2^\dagger \overline{\underset{\sim}{E}_a \underset{\sim}{E}_a^\dagger}\, \underset{\sim}{x}_2}{2\underset{\sim}{x}_2^\dagger \left(\underset{\sim}{Z}_a + \underset{\sim}{Z}_a^\dagger\right) \underset{\sim}{x}_2}, \tag{83}$$

we write Eq. 82 as

$$\frac{1}{s_o} = \frac{1}{s_s} - \lambda\left[\frac{1}{p_o} - \frac{1}{p_s}\right]. \tag{84}$$

Comparing Eq. 84 with Eq. 59, we see that by fixing the elements of the vector $\underset{\sim}{x}_2$ we have defined a noise measure for the amplifier:

$$M_e = \frac{\lambda}{kT_o\Delta f}. \tag{85}$$

Having fixed $\underset{\sim}{x}_2$, we vary the exchangeable gain of the amplifier at constant noise measure when we vary $\underset{\sim}{x}_1$. This is the kind of situation that was shown in Fig. 13.

But now we must ask what can be accomplished by varying the vector $\underset{\sim}{x}_2$. By varying $\underset{\sim}{x}_2$, we merely vary λ, and hence vary the slope of the line of output points that can be obtained in the noise-performance plane by subsequently varying x_1. Thus comparing (85) with (81), we see that the range of slopes that can be obtained is the same as the negative of the range of λ. The function λ is the same as the function p_z defined in section 2.5; hence the range of λ can be determined from its stationary values. The stationary values of λ are the eigenvalues of the equation

$$\overline{\underset{\sim}{E}_a \underset{\sim}{E}_a^\dagger}\, \underset{\sim}{x}_2 + 2\lambda\left(\underset{\sim}{Z}_a + \underset{\sim}{Z}_a^\dagger\right) \underset{\sim}{x}_2 = 0. \tag{86}$$

The stationary values of λ are also the eigenvalues of the characteristic noise matrix, $\underset{\sim}{N}$, of the amplifier, where $\underset{\sim}{N} = -\frac{1}{2}\left(\underset{\sim}{Z}_a + \underset{\sim}{Z}_a^\dagger\right)^{-1} \overline{\underset{\sim}{E}_a \underset{\sim}{E}_a^\dagger}$. Let us assume that we are considering an amplifier that has a characteristic noise matrix with both positive and negative eigenvalues; we number them as shown in Fig. 4c. If we plot Eq. 84 for the stationary values of λ, we obtain the set of curves shown in Fig. 15a for a positive resistance source, and the set of curves shown in Fig. 15b for a negative-resistance source.

From Fig. 4c we see that the range of λ is from $\lambda_1 (\lambda_1 > 0)$ to plus infinity and from $\lambda_n (\lambda_n < 0)$ to minus infinity. Thus, by varying the vector $\underset{\sim}{x}_2$, we can choose any slope between $-\lambda_1$ and $-\lambda_n$. Thus, by adjusting both $\underset{\sim}{x}_2$ and $\underset{\sim}{x}_1$, we can make the characteristics of the output terminal pair in Fig. 14 correspond to the coordinates of any point on the noise-performance plane included in the infinite sector bounded by the curves with slopes $-\lambda_1$ and $-\lambda_n$ in Fig. 15. The curves in Fig. 15 with slopes $-\lambda_1$ and $-\lambda_n$, therefore, may be considered as a plot of the minimum noise-to-signal ratio of the system as a function of the reciprocal of the exchangeable signal power at the output.

We may interpret the plots in Fig. 15a and 15b in terms of the canonical form of the amplifier network. We imbed the amplifier network in the lossless network; this puts

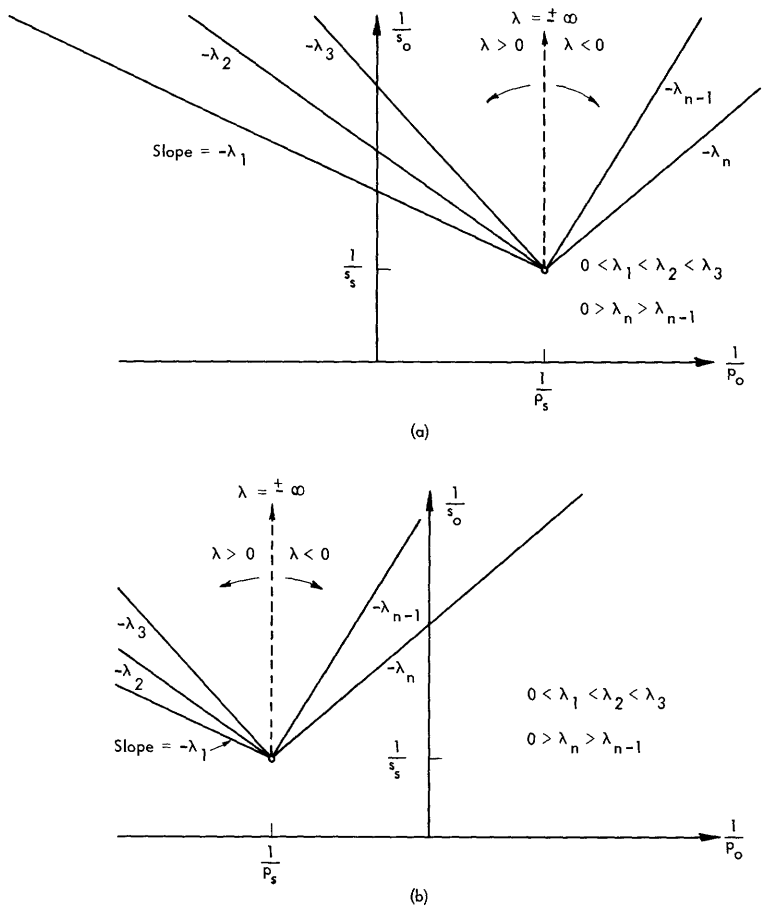

Fig. 15. (a) Plot of Eq. 84 for stationary values of λ with a positive-resistance source.
(b) Plot of Eq. 84 for stationary values of λ with a negative-resistance source.

it into canonical form. We order the terminals for convenience so that the exchangeable noise power at the first terminal pair is $-\lambda_1$, the exchangeable noise power at the second terminal pair is $-\lambda_2$, etc. If then we imbed the first element of the canonical form and the source network in a three-terminal-pair imbedding network as shown in Fig. 12, we may obtain the points on the straight line of slope $-\lambda_1$, in Fig. 15a or 15b by varying this second imbedding network. Varying this second network is equivalent to varying x_1 in Eqs. 80 and 81. If we imbed only the second element of the canonical form with the source, we obtain the line with slope $-\lambda_2$ in Fig. 15. Thus we obtain any one of the lines in Fig. 15a or 15b by interconnecting the source in an arbitrary way with the appropriate element of the canonical form of the amplifier network.

This reasoning may be extended. By imbedding both the first and second terminal pairs of the canonical form of the amplifier with the source in a four-terminal-pair lossless network, we can obtain any point in the region between the curves with slope $-\lambda_1$ and $-\lambda_2$ in Fig. 15a or 15b by varying the four-terminal-pair imbedding network. Hence we conclude that we could obtain any point in the region between the lines λ_1 and λ_n by losslessly interconnecting the source with only the first and n^{th} terminal pairs of the

canonical form of the amplifier.

From Fig. 15 we see that the optimal performance of the linear noisy network as an amplifier is determined by the smallest positive eigenvalue, λ_1, of its characteristic noise matrix, if the source has a positive resistance (Fig. 15a); or by the smallest negative eigenvalue, λ_n, of its characteristic noise matrix if the source has a negative resistance. We shall discuss these two cases briefly.

Let us first consider the case shown in Fig. 15a for which the real part of the source impedance is positive. We see that the best noise-to-signal ratio that can be achieved at infinite exchangeable signal power is given by

$$\frac{1}{s_{\infty, \text{opt}}} = \frac{1}{s_s} + \frac{\lambda_1}{p_s}. \tag{87}$$

Thus the best signal-to-noise ratio at infinite exchangeable power depends on the amplifier only through λ_1, the smallest positive eigenvalue of the characteristic noise matrix of the amplifier. The output point $s_{\infty, \text{opt}}$, in accordance with Eq. 59, determines a noise measure

$$M_{e, \text{opt}} = \frac{\lambda_1}{kT_o \Delta f}. \tag{88}$$

Equation 88 could also have been predicted from Eq. 87. We may regard the imbedding network of Fig. 14 as an imbedding that reduces the n-terminal-pair amplifier to a two-terminal-pair amplifier. Therefore, the optimum noise performance of the n-terminal-pair network used with a positive-resistance source is governed by the least positive noise measure that can be achieved by any two-terminal-pair amplifier derived from this amplifier through a lossless imbedding.

The optimum performance for the case in which the source impedance has a negative real part can be determined by referring to Fig. 15b. The minimum noise-to-signal ratio at infinite exchangeable power for this case is given by

$$\frac{1}{s_{\infty, \text{opt}}} = \frac{1}{s_s} + \frac{\lambda_n}{p_s}. \tag{89}$$

Here the smallest negative eigenvalue, λ_n, of the characteristic noise matrix of the amplifier determines the optimum signal-to-noise ratio that can be obtained at infinite exchangeable power with a specified negative-resistance source. This result may also be stated in terms of noise measure, as in the case of the positive-resistance source. It is more instructive, however, to consider the realization of this point in terms of an interconnection of the source with the canonical form.

We can use the n^{th} element of the canonical form of the amplifier, which has a positive exchangeable noise power $-\lambda_n$, as an amplifier (as in Fig. 12) to obtain infinite exchangeable gain. If instead we had merely used this resistor as a load resistor for the one-terminal-pair source as shown in Fig. 7, the ratio of the noise power delivered

to this resistor to the signal power delivered to this resistor would be given by Eq. 45 as

$$\frac{1}{s_1} = \frac{1}{s_s} + \frac{\lambda_n}{p_s}. \tag{90}$$

Comparing (89) and (90), we see that the ratio of signal power to noise power delivered to this resistance as a load, s_1, is equal to the signal-to-noise ratio $s_{\infty, opt}$ that can be delivered to any load if this resistor is used as an amplifier with infinite exchangeable gain. This fact reinforces the statement made previously that the maximum signal-to-noise ratio that can be achieved with a given amplifying system at infinite exchangeable power is the best way of specifying the quality of the system. The obvious conclusion to draw from this discussion is that we should include any low-temperature resistor that is available as an independent part of the amplifier. That is, we should introduce this resistor as an additional, independent terminal pair for the amplifier. Subsequently, we can determine whether or not it should be used and, if it should be used, what can be accomplished with it.

We summarize these results in two theorems.

THEOREM 3. Consider the set of lossless transformations that carry an n-terminal-pair noisy network into a two-terminal-pair network. When driven by a one-terminal-pair (signal) source the transformed network may have any noise measure that is greater than $\lambda_1/kT_o\Delta f$ or less than $\lambda_n/kT_o\Delta f$, where λ_1 is the smallest positive eigenvalue of the characteristic noise matrix $\underset{\sim}{N}$ of the original network, and λ_n is the smallest negative eigenvalue of $\underset{\sim}{N}$.

THEOREM 4. The optimum noise performance (in terms of the maximum signal-to-noise ratio at large exchangeable power) of an n-terminal-pair network (amplifier) used with a one-terminal-pair source is limited by λ_1 if the source has an impedance with a positive real part, and by λ_n if the source has an impedance with a negative real part. (These optimum noise-to-signal ratios are given by Eqs. 86 and 88, respectively.)

IV. MULTITERMINAL-PAIR SOURCE

We have examined the ranges of performance that can be obtained by using a multiterminal-pair amplifier in the most general way with a one-terminal-pair source. This is a rather narrow view; presumably the principal reason for using a multiterminal-pair amplifier in the first place is to take advantage of a multiplicity of sources of the signal. That is, we want to use the multiterminal-pair amplifier with a multiterminal-pair signal-source network. But before we consider this general problem we should have a complete understanding of multiterminal-pair source networks. Therefore we shall now describe the properties of multiterminal-pair signal-source networks.

We shall begin by describing the model of the source that we shall use. We shall then imbed the source network in a lossless imbedding network and investigate the values of exchangeable signal power and exchangeable signal-to-noise ratio that can be obtained at a single-output terminal pair by varying the imbedding. When we describe the results of this operation on the noise-performance plane by plotting the values of exchangeable noise-to-signal ratio that can be achieved as a function of the reciprocal of the exchangeable signal power, we shall find that we have access to a region of this plane. We shall show that the boundary of this region can be obtained from an eigenvalue equation derived by a simple optimization procedure. We shall derive a number of the properties of the boundary of this region and investigate the effects of some of the more common types of degeneracies that can occur. We conclude this section by working out an illustrative example.

4.1 IMBEDDING OF A MULTITERMINAL-PAIR SOURCE

A typical multiterminal-pair source is shown in Fig. 16. The source network has an impedance matrix $\underset{\sim}{Z}_s$, and an open-circuit voltage column matrix $\underset{\sim}{E}$. The open-circuit voltage matrix, $\underset{\sim}{E}$, is composed of the open-circuit noise-voltage column matrix $\underset{\sim}{E}_n$ and the open-circuit signal-voltage column matrix $\underset{\sim}{E}_s$.

$$\underset{\sim}{E} = \underset{\sim}{E}_n + \underset{\sim}{E}_s. \tag{91}$$

We assume that the noise voltages are not correlated with the signal voltages. This assures us that every element of the matrix $\underset{\sim}{E}_s \underset{\sim}{E}_n^\dagger$ is zero. This is a necessary assumption, since we recognize only two classes of power – signal power and noise power. Any power involving a mean-square voltage that appears in the matrix $\underset{\sim}{E}_s \underset{\sim}{E}_n^\dagger$ would not be classifiable on this basis. In any practical situation it is always possible to define the signal and noise voltages to satisfy the condition

$$\overline{\underset{\sim}{E}_s \underset{\sim}{E}_n^\dagger} = 0. \tag{92}$$

If we imbed the source shown in Fig. 16 in an (m+1)-terminal-pair lossless network as shown in Fig. 17, we find that the exchangeable power at the output terminal pair is

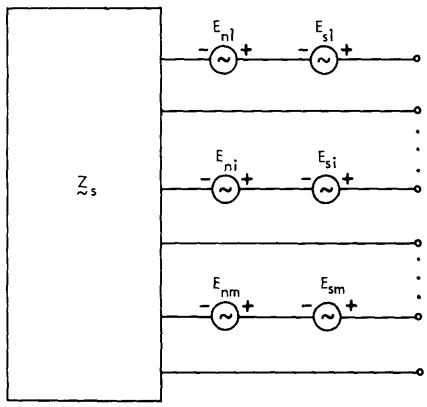

Fig. 16. Typical multiterminal source network.

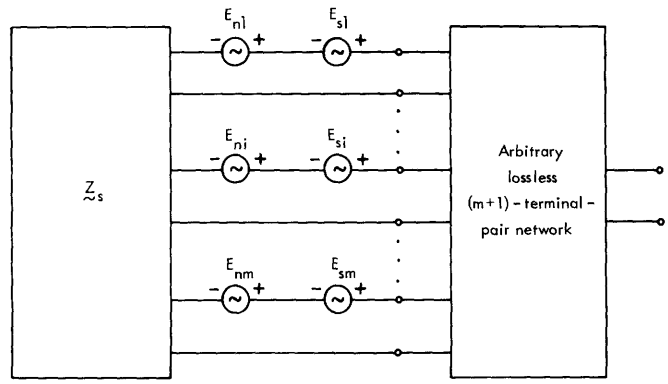

Fig. 17. Imbedding of an m-terminal-pair source.

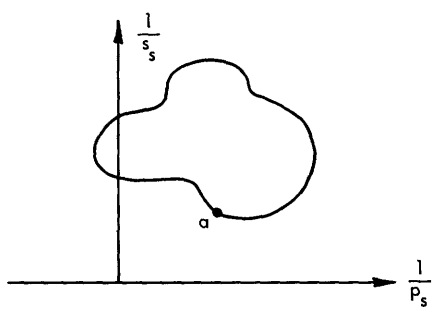

Fig. 18. Hypothetical source region.

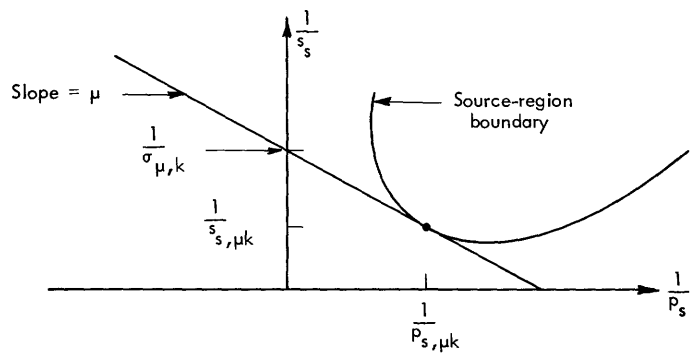

Fig. 19. Geometric interpretation of $\sigma_{\mu k}$.

given by Eq. 26 as

$$P_{e,i} = \frac{\underset{\sim}{x}^{\dagger}\,\overline{\underset{\sim}{E}\underset{\sim}{E}^{\dagger}}\,\underset{\sim}{x}}{2\underset{\sim}{x}^{\dagger}\left(\underset{\sim}{Z}_s+\underset{\sim}{Z}_s^{\dagger}\right)\underset{\sim}{x}},$$

where the components of the vector $\underset{\sim}{x}$ are the open-circuit voltage transfer ratios for the particular lossless imbedding network. Using (91) and (93), we see that we may rewrite Eq. 26 as

$$P_{e,i} = \frac{\underset{\sim}{x}^{\dagger}\,\overline{\underset{\sim}{E}_s\underset{\sim}{E}_s^{\dagger}}\,\underset{\sim}{x} + \underset{\sim}{x}^{\dagger}\,\overline{\underset{\sim}{E}_n\underset{\sim}{E}_n^{\dagger}}\,\underset{\sim}{x}}{2\underset{\sim}{x}^{\dagger}\left(\underset{\sim}{Z}_s+\underset{\sim}{Z}_s^{\dagger}\right)\underset{\sim}{x}}. \tag{93}$$

From Eq. 93 we see that the exchangeable signal power, p_s, at the output of the network in Fig. 18 is given by

$$p_s = \frac{\underset{\sim}{x}^{\dagger}\,\overline{\underset{\sim}{E}_s\underset{\sim}{E}_s^{\dagger}}\,\underset{\sim}{x}}{2\underset{\sim}{x}^{\dagger}\left(\underset{\sim}{Z}_s+\underset{\sim}{Z}_s^{\dagger}\right)\underset{\sim}{x}}. \tag{94}$$

The ratio of exchangeable signal power to exchangeable noise power, s_s, is given by

$$s_s = \frac{\underset{\sim}{x}^{\dagger}\,\overline{\underset{\sim}{E}_s\underset{\sim}{E}_s^{\dagger}}\,\underset{\sim}{x}}{\underset{\sim}{x}^{\dagger}\,\overline{\underset{\sim}{E}_n\underset{\sim}{E}_n^{\dagger}}\,\underset{\sim}{x}}. \tag{95}$$

Here, as before, we shall work principally with the reciprocals of these two quantities. The reciprocal quantities are

$$\frac{1}{p_s} = \frac{2\underset{\sim}{x}^{\dagger}\left(\underset{\sim}{Z}_s+\underset{\sim}{Z}_s^{\dagger}\right)\underset{\sim}{x}}{\underset{\sim}{x}^{\dagger}\,\overline{\underset{\sim}{E}_s\underset{\sim}{E}_s^{\dagger}}\,\underset{\sim}{x}} \tag{96}$$

and

$$\frac{1}{s_s} = \frac{\underset{\sim}{x}^{\dagger}\,\overline{\underset{\sim}{E}_n\underset{\sim}{E}_n^{\dagger}}\,\underset{\sim}{x}}{\underset{\sim}{x}^{\dagger}\,\overline{\underset{\sim}{E}_s\underset{\sim}{E}_s^{\dagger}}\,\underset{\sim}{x}}. \tag{97}$$

Our principal interest here is to determine what values of $1/s_s$ and $1/p_s$ can be achieved by varying the lossless imbedding network of Fig. 17. Recall that taking arbitrary variations of this network is equivalent to taking arbitrary variations of the vector $\underset{\sim}{x}$ in (96) and (97). We shall describe the results of performing this variation on a plot with exchangeable noise-to-signal ratio and the reciprocal of exchangeable signal power as coordinates – the noise-performance plane. For any particular lossless

imbedding network, corresponding to a particular vector $\underset{\sim}{x}$, we may represent the values of $1/p_s$ and $1/s_s$ by a point in the noise-performance plane. It is apparent that as we vary the lossless network this point will move in the noise-performance plane. But even under arbitrary variations of the imbedding network the coordinates of this point will be confined to some region of the noise-performance plane; we shall refer to this region as the source region. We shall show how the boundary of the source region may be obtained.

4.2 DETERMINATION OF THE SOURCE REGION

In this section and in sections 4.3 and 4.4 we shall consider only cases for which $\underset{\sim}{E}_s \underset{\sim}{E}_s^\dagger$ is positive definite. This assumption simplifies the mathematics because the positive definiteness of $\underset{\sim}{E}_s \underset{\sim}{E}_s^\dagger$ insures that both the noise-to-signal ratio, $1/s_s$, and the reciprocal of exchangeable signal power, $1/p_s$, will be bounded. This, in turn, guarantees that the source region in the noise-performance plane will be a bounded region. Since this condition is not usually satisfied in practical systems, we must ultimately consider the case for which $\underset{\sim}{E}_s \underset{\sim}{E}_s^\dagger$ is positive semidefinite. This case is considered in section 4.5, and it is shown that allowing $\underset{\sim}{E}_s \underset{\sim}{E}_s^\dagger$ to be positive semidefinite does not materially affect the more important results derived for the positive definite case. From a physical standpoint one need only consider sources from which a limited amount of power may be extracted; that is, sources that have a $\underset{\sim}{Z}_s + \underset{\sim}{Z}_s^\dagger$ matrix that is positive definite. We shall find, however, that the source regions for multifrequency sources used in conjunction with lossless Manley-Rowe devices are, in general, indefinite (see Section VII). For this reason, we shall give considerable attention in the present section to sources that have $\underset{\sim}{Z}_s + \underset{\sim}{Z}_s^\dagger$ matrices that are indefinite.

Let us assume that we have an m-terminal-pair source network such as that shown in Fig. 16 which satisfies the condition that the matrix $\underset{\sim}{E}_s \underset{\sim}{E}_s^\dagger$ is positive definite. Let us also assume that we have imbedded this network in an (m+1)-terminal-pair lossless network as shown in Fig. 17. For the sake of argument we shall hypothesize that the region of values of $1/s_s$ and $1/p_s$ that can be obtained at the output is as shown in Fig. 18.

We are interested in finding the boundary of the region shown in Fig. 18. We could find this boundary by varying $\underset{\sim}{x}$ to find the extrema of $1/s_s$ under the constraint that $1/p_s$ be constant; but this is a difficult constraint to apply. A more direct approach may be derived by noting that the boundary of the source region is an extremum in another sense. Let us assume that we have adjusted the imbedding network of Fig. 17 so that the noise-to-signal ratio and exchangeable signal power at the output correspond to the point "a" (a source point) on the boundary of the source region in Fig. 18. The network determines these coordinates by specifying a particular vector, $\underset{\sim}{x}^{(a)}$, in Eqs. 96 and 97. Any small variation of this network from this configuration produces a small change in the vector $\underset{\sim}{x}^{(a)}$. We designate this vector change $\Delta\underset{\sim}{x}^{(a)}$. This small network variation also varies the position of the source point "a". To first order, that is, linear in the $\Delta\underset{\sim}{x}^{(a)}$, however, the source point cannot move away from the boundary. Since we can achieve

any vector $\underset{\sim}{x}$, we could vary the network to produce a variation of $\underset{\sim}{x}$ about $\underset{\sim}{x}^{(a)}$ of $-\Delta\underset{\sim}{x}^{(a)}$, that is, the negative of the first variation. If the first variation, $\Delta\underset{\sim}{x}^{(a)}$, moved us inside the region, this second variation, $-\Delta\underset{\sim}{x}^{(a)}$, would move us outside the region in violation of the assumption that we are already on the outer boundary of the region. Consequently, any first-order change in the position of the point "a" because of small variation in the vector $\underset{\sim}{x}^{(a)}$ must be along the source-region boundary.

It is apparent that if the point "a" were a general point within the source region, a small variation of the imbedding network corresponding to $\Delta\underset{\sim}{x}_a$ would move us in one direction, while a variation $-\Delta\underset{\sim}{x}_a$ would move us in the other. For that matter, the direction in which we could move by varying the imbedding would be dependent on exactly how we varied the network. By taking the appropriate variation, we could move in any desired direction. It is only for points on the boundary that arbitrary variations always move us in a single direction. Note, however, that there may be internal points for which this condition is valid. These internal points would be on internal boundaries of the source region.

From the discussion above we see that we can find points on the boundary of the source region by picking the slope of the boundary curve. Then, if we want the points on the boundary of the source region, where the slope is μ, we see that at these points $1/s_s$ and $1/p_s$ must satisfy the condition that the variation of $1/s_s$ with respect to small variations of the vector $\underset{\sim}{x}$ is equal to μ times the variation of $1/p_s$ with respect to small variations in $\underset{\sim}{x}$.

$$\delta\left(\frac{1}{s_s}\right) = \mu\,\delta\left(\frac{1}{p_s}\right). \tag{98}$$

With the aid of (96) and (97) we may rewrite Eq. 98 as

$$\delta\left[\frac{1}{s_s} - \frac{\mu}{p_s}\right] = \delta\left\{\frac{\underset{\sim}{x}^{\dagger}\left[\overline{\underset{\sim}{E}_n\underset{\sim}{E}_n^{\dagger}} - 2\mu\left(\underset{\sim}{Z}_s + \underset{\sim}{Z}_s^{\dagger}\right)\right]\underset{\sim}{x}}{\underset{\sim}{x}^{\dagger}\,\overline{\underset{\sim}{E}_s\underset{\sim}{E}_s^{\dagger}}\,\underset{\sim}{x}}\right\} = 0. \tag{99}$$

This equation is handled by the same procedure that we employed in solving the stationary value problem in section 2.5. Requiring the variation of the quantity in (99) to be zero is equivalent to requiring the variation of $\underset{\sim}{x}^{\dagger}\left[\overline{\underset{\sim}{E}_n\underset{\sim}{E}_n^{\dagger}} - 2\mu\left(\underset{\sim}{Z}_s + \underset{\sim}{Z}_s^{\dagger}\right)\right]\underset{\sim}{x}$ to be zero, subject to the constraint that $\underset{\sim}{x}^{\dagger}\,\overline{\underset{\sim}{E}_s\underset{\sim}{E}_s^{\dagger}}\,\underset{\sim}{x}$ is constant. Introducing the Lagrangian multiplier $1/\sigma$, we express this condition mathematically (see the discussion in connection with Eq. 29) as

$$\frac{\partial}{\partial x_i^*}\left\{\underset{\sim}{x}^{\dagger}\left[\overline{\underset{\sim}{E}_n\underset{\sim}{E}_n^{\dagger}} - 2\mu\left(\underset{\sim}{Z}_s + \underset{\sim}{Z}_s^{\dagger}\right)\right]\underset{\sim}{x} - \frac{1}{\sigma}\underset{\sim}{x}^{\dagger}\,\overline{\underset{\sim}{E}_s\underset{\sim}{E}_s^{\dagger}}\,\underset{\sim}{x}\right\} = 0 \qquad i = 1, 2, \ldots, m. \tag{100}$$

This leads to the eigenvalue equation

$$\overline{\underset{\sim}{E}_s\underset{\sim}{E}_s^{\dagger}}\,\underset{\sim}{x} - \sigma\left[\overline{\underset{\sim}{E}_n\underset{\sim}{E}_n^{\dagger}}\,\underset{\sim}{x} - 2\mu\left(\underset{\sim}{Z}_s + \underset{\sim}{Z}_s^{\dagger}\right)\underset{\sim}{x}\right] = 0. \tag{101}$$

The eigenvectors of (101) for a given value of μ specify the coordinates of points on the boundary of the source region, where the slope is μ, when these eigenvectors are applied to the expressions for $1/p_s$ and $1/s_s$ in Eqs. 96 and 97. We shall show later that for the most part (barring degeneracies) two of the eigenvectors determine points on the outer boundary of the source region. The remaining eigenvectors determine points on internal boundaries of the source region where the slope is μ.

4.3 INTERPRETATION OF THE EIGENVALUES OF THE SOURCE EQUATION

We shall give a geometric interpretation of the eigenvalues of Eq. 101 in the noise-performance plane, and we shall discuss the ranges of these eigenvalues. Assume that for some value of μ the k^{th} eigenvalue of Eq. 101 is $\sigma_{\mu k}$, and the eigenvector corresponding to this eigenvalue is $\underset{\sim}{x}^{(\mu k)}$. (Note that we need a double subscript notation here, since all eigenvalues and eigenvectors of (101) depend on the value of μ.) If we premultiply Eq. 101 by $\underset{\sim}{x}^{(\mu k)}$, we obtain the relation

$$\underset{\sim}{x}^{(\mu k)\dagger}\,\overline{\underset{\sim}{E}_s\underset{\sim}{E}_s^{\dagger}}\,\underset{\sim}{x}^{(\mu k)} - \sigma_{\mu k}\left[\underset{\sim}{x}^{(\mu k)\dagger}\,\overline{\underset{\sim}{E}_n\underset{\sim}{E}_n^{\dagger}}\,\underset{\sim}{x}^{(\mu k)} - 2\mu\,\underset{\sim}{x}^{(\mu k)\dagger}\left(\underset{\sim}{Z}_s+\underset{\sim}{Z}_s^{\dagger}\right)\underset{\sim}{x}^{(\mu k)}\right] = 0. \tag{102}$$

Solving (102) for $1/\sigma_{\mu k}$, we obtain

$$\frac{1}{\sigma_{\mu k}} = \left[\frac{\underset{\sim}{x}^{(\mu k)\dagger}\,\overline{\underset{\sim}{E}_n\underset{\sim}{E}_n^{\dagger}}\,\underset{\sim}{x}^{(\mu k)}}{\underset{\sim}{x}^{(\mu k)\dagger}\,\overline{\underset{\sim}{E}_s\underset{\sim}{E}_s^{\dagger}}\,\underset{\sim}{x}^{(\mu k)}}\right] - \mu\left[\frac{2\underset{\sim}{x}^{(\mu k)\dagger}\left(\underset{\sim}{Z}_s+\underset{\sim}{Z}_s^{\dagger}\right)\underset{\sim}{x}^{(\mu k)}}{\underset{\sim}{x}^{(\mu k)\dagger}\,\overline{\underset{\sim}{E}_s\underset{\sim}{E}_s^{\dagger}}\,\underset{\sim}{x}^{(\mu k)}}\right] \tag{103}$$

or

$$\frac{1}{\sigma_{\mu k}} = \frac{1}{s_{s,\mu k}} - \frac{\mu}{p_{s,\mu k}}, \tag{104}$$

where $1/s_{s,\mu k}$ and $1/p_{s,\mu k}$ are the exchangeable noise-to-signal ratio and the reciprocal of the exchangeable signal power at the output of the imbedding network when this network is adjusted to give the k^{th} point on the source-region boundary, where the slope is μ. In Fig. 19 the quantities in Eq. 104 are plotted on the noise-performance plane. From this plot we see that $1/\sigma_{\mu k}$ is the intercept with the $1/s_s$ axis of the line drawn through the corresponding source point with a slope μ (this is the slope of the source-region boundary at this point). This fact may be stated as a theorem.

THEOREM 5. For a given value of μ the reciprocals of the eigenvalues of the source equation (Eq. 101) are the intercepts with the 1/s axis in the noise-performance plane of those tangents to the source-region boundaries that have a slope μ.

It is advantageous to have a system for numbering the eigenvalues of Eq. 101. For this purpose, we define the function

$$\frac{1}{\sigma_\mu} = \frac{\underset{\sim}{x}^{\dagger}\,\overline{\underset{\sim}{E}_n\underset{\sim}{E}_n^{\dagger}}\,\underset{\sim}{x} - 2\mu\,\underset{\sim}{x}^{\dagger}\left(\underset{\sim}{Z}_s+\underset{\sim}{Z}_s^{\dagger}\right)\underset{\sim}{x}}{\underset{\sim}{x}^{\dagger}\,\overline{\underset{\sim}{E}_s\underset{\sim}{E}_s^{\dagger}}\,\underset{\sim}{x}}. \tag{105}$$

This may also be written with the aid of (96) and (97)

$$\frac{1}{\sigma_\mu} = \frac{1}{s_s} - \frac{\mu}{p_s}. \tag{106}$$

Comparing Eqs. 105 and 101 with Eqs. 28 and 30, we see that the reciprocals of the eigenvalues of (101) (such as $1/\sigma_{\mu k}$) are the stationary values of the function $1/\sigma_\mu$. The range of the function $1/\sigma_\mu$ is the same as the range of the reciprocals of the eigenvalues of Eq. 101.

For $\underset{\sim}{E}_s \underset{\sim}{E}_s^\dagger$ positive definite and for μ fixed, the function $1/\sigma_\mu$ is bounded; it has a maximum value and a minimum value. Thus the range of $1/\sigma_\mu$ must be as shown in Fig. 20a, 20b or 20c, determined by the particular value of μ and the character of the

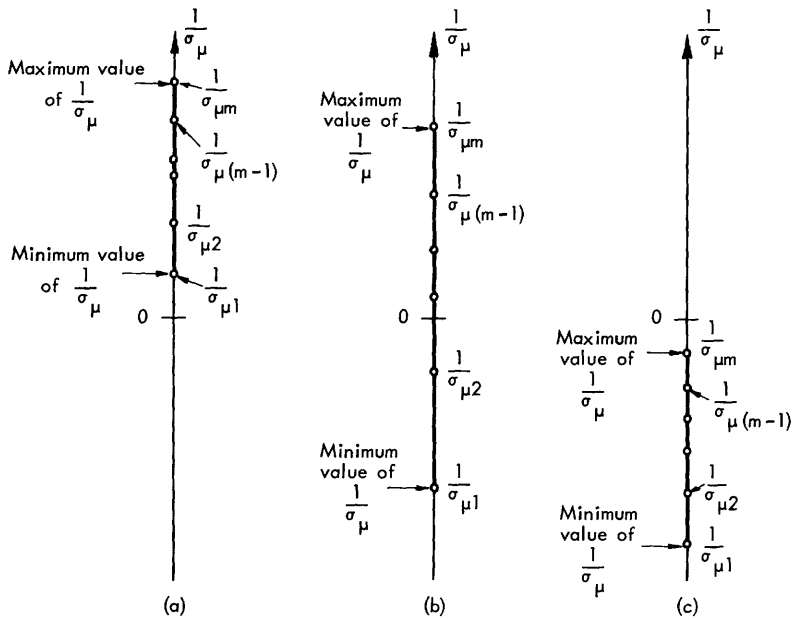

Fig. 20. Range of $1/\sigma_\mu$ for an m-terminal-pair source with $\underset{\sim}{E}_s \underset{\sim}{E}_s^\dagger$ positive definite.

matrix $\underset{\sim}{Z}_s + \underset{\sim}{Z}_s^\dagger$ of the source under consideration. If μ is negative and $\underset{\sim}{Z}_s + \underset{\sim}{Z}_s^\dagger$ is positive definite, or if μ is positive and $\underset{\sim}{Z}_s + \underset{\sim}{Z}_s^\dagger$ is negative definite, the range of $1/\sigma_\mu$ must be as shown in Fig. 20a, since all three terms $\underset{\sim}{x}^\dagger \underset{\sim}{E}_s \underset{\sim}{E}_s^\dagger \underset{\sim}{x}$, $\underset{\sim}{x}^\dagger \underset{\sim}{E}_n \underset{\sim}{E}_n^\dagger \underset{\sim}{x}$ and $2\mu \underset{\sim}{x}^\dagger \left(\underset{\sim}{Z}_s + \underset{\sim}{Z}_s^\dagger\right) \underset{\sim}{x}$ in Eq. 105 are always positive. If $\underset{\sim}{Z}_s + \underset{\sim}{Z}_s^\dagger$ is indefinite, either Fig. 20a or 20b may apply. The range of Fig. 20c is not applicable to this case, since some vector always exists for which $\mu \underset{\sim}{x}^\dagger \left(\underset{\sim}{Z}_s + \underset{\sim}{Z}_s^\dagger\right) \underset{\sim}{x}$ is positive. If $\underset{\sim}{Z}_s + \underset{\sim}{Z}_s^\dagger$ is positive definite and μ is positive, or if $\underset{\sim}{Z}_s + \underset{\sim}{Z}_s^\dagger$ is negative definite and μ is negative, any of the three cases shown in Fig. 20 may apply, the choice depending on the value of μ.

The numbering system that we shall use for the eigenvalues of (101) is also shown

in Fig. 20. We shall number these eigenvalues in accordance with their order along the range of $1/\sigma_\mu$. Thus for a given μ the eigenvalue corresponding to the minimum value of $1/\sigma_\mu$ is $1/\sigma_{\mu 1}$; the eigenvalue corresponding to the maximum value of $1/\sigma_\mu$ is $1/\sigma_{\mu m}$ (for an m-terminal-pair source), etc.

4.4 PROPERTIES OF THE SOURCE-REGION BOUNDARY

We have just constructed the function $1/\sigma_\mu$. For a given imbedding of the source network, the quantities $1/p_s$ and $1/s_s$ at the output are specified through the vector $\underset{\sim}{x}$. These two quantities, $1/s_s$ and $1/p_s$, determine a point in the noise-performance plane. For a specified value of μ, the quantity $1/\sigma_\mu$ is the value of the intercept with the $1/s_s$ axis of the line of slope μ through this point. If we look for stationary values of this intercept for a given μ by varying the imbedding network, we obtain the eigenvalue equation, Eq. 101. For an m-terminal-pair source we get, in general, m stationary values of $1/\sigma_\mu$ for each value of μ. We shall show that only two of these solutions for a given value of μ correspond to points on the outer boundary of the source region. These two solutions are the extremal ones, corresponding to the maximum and minimum values of $1/\sigma_\mu$; the remaining solutions correspond to points on internal "boundaries" of the source region, where these internal "boundaries" have a slope μ. These internal "boundaries" do not separate accessible regions from inaccessible regions as the outer boundary does; they are more aptly described as branch lines or folds. The source region is a manifold region consisting of a number of sheets; the internal "boundaries" denote folds that appear in some of these sheets. In this context it has been shown elsewhere[25] that any point within the outer boundary of the source region may be achieved through the use of at least one lossless imbedding network.

To show that only the extrema of $1/\sigma_\mu$ lead to points on the boundary of the source region, we shall demonstrate that the source region must be (semi) convex. A convex region is one that has a boundary that is convex outward; a semiconvex region is also convex outward, but it may also have straight-line segments as part of its boundary. We shall establish the fact that the outer boundary of the source region is semiconvex by showing that it cannot have any concave segments.

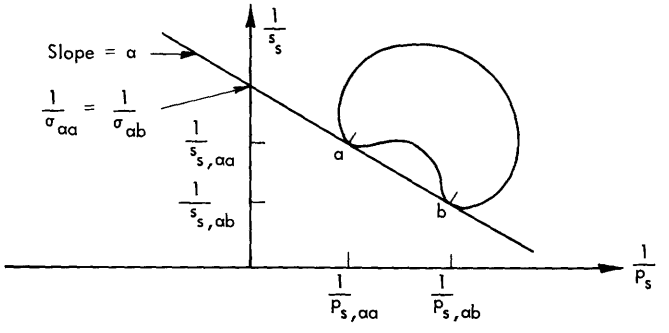

Fig. 21. Hypothetical nonconvex source region.

Assume that we have a source with a nonconvex region such as that shown in Fig. 21. For such a region there is always a line that is tangent to this boundary at two points. This is the line a-b in Fig. 21; it has a slope α. We see that for this source region both of the points a and b correspond to the minimum value of $1/\sigma_\alpha$. The coordinates of the point a are $1/s_{s,\alpha a}$ and $1/p_{s,\alpha a}$. These are the values of $1/s_s$ and $1/p_s$ of Eqs. 96 and 97 when the lossless reduction network is such that it is characterized by a vector $\underset{\sim}{x}^{(\alpha a)}$. The coordinates of the point b are the values of $1/s_s$ and $1/p_s$ when the lossless reduction network is such that it is characterized by a vector $\underset{\sim}{x}^{(\alpha b)}$. In accordance with the discussion presented above, we see from Fig. 21 that $1/\sigma_{\alpha a}$ and $1/\sigma_{\alpha b}$ are equal. Consequently, if we look for solutions to Eq. 101 for this source, we find that for $\mu = \alpha$ both the vector $\underset{\sim}{x}^{(\alpha a)}$ and the vector $\underset{\sim}{x}^{(\alpha b)}$ satisfy the equation for the same eigenvalue, $\sigma_{\alpha a} = \sigma_{\alpha b}$. Thus the vectors $\underset{\sim}{x}^{(\alpha a)}$ and $\underset{\sim}{x}^{(\alpha b)}$ are degenerate solutions to (101).

Consider now an imbedding of this source in a different lossless reduction network characterized by a vector $\underset{\sim}{x}^{(\alpha\gamma)}$. The noise-to-signal ratio and the reciprocal of the exchangeable signal power at the output of this reduction network are given by $1/s_{s,\alpha\gamma}$ and $1/p_{s,\alpha\gamma}$, respectively. Assume that this network is such that the vector $\underset{\sim}{x}^{(\alpha\gamma)}$ is an arbitrary linear combination of the vectors $\underset{\sim}{x}^{(\alpha a)}$ and $\underset{\sim}{x}^{(\alpha b)}$. That is,

$$\underset{\sim}{x}^{(\alpha\gamma)} = \gamma_a \underset{\sim}{x}^{(\alpha a)} + \gamma_b \underset{\sim}{x}^{(\alpha b)}, \tag{107}$$

and we have constructed the imbedding network in such a manner as to enable the scalar parameters γ_a and γ_b to be varied arbitrarily. As the lossless network is varied in this fashion it can be shown (see Appendix A) that the output point in the noise-performance plane moves between the points a and b in Fig. 21 along the straight line a-b.

We may therefore state the two following theorems.

THEOREM 6. Only the reciprocals of the extremal eigenvalues of the source equation (101) are intercepts with the noise-to-signal ratio axis of tangents to the outer boundary of the source region in the noise-performance plane. The reciprocals of extremal eigenvalues correspond to extrema of $1/\sigma_\mu$ of Eq. 105.

THEOREM 7. The outer boundary of the source region in the noise-performance plane must be a (semi) convex curve.

It follows from Theorems 6 and 7, for the restricted case under consideration, that there are only two tangents to the outer boundary of the source region with a given slope. The intercepts of these two tangents with the $1/s$ axis are the maximum and minimum values of the function $1/\sigma_\mu$ of (105) for this particular slope. In section 4.5 we shall show that these two theorems are also valid when $\underset{\sim}{E}_s \underset{\sim}{E}_s^\dagger$ is only semidefinite.

We should also consider another type of degeneracy that can occur. This second type of degeneracy causes the boundary curve to have a break in it as shown in Fig. 22. The coordinates of the point c are the values of $1/s_s$ and $1/p_s$ obtained at the output of the lossless reduction network when this network is characterized by the vector $\underset{\sim}{x}^{(c)}$. The

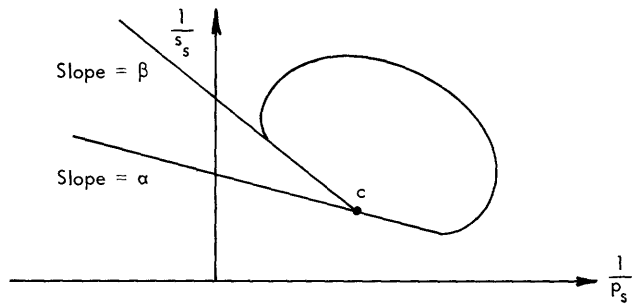

Fig. 22. Degeneracy in a semiconvex source region.

point c in Fig. 22 is clearly degenerate. For any value of μ greater than α and less than β the coordinates of this point minimize the function $1/\sigma_\mu$. Let us see what this implies in Eq. 101. We see that the vector $\underset{\sim}{x}^{(c)}$ must be an eigenvector of (101) for any value of μ between α and β, $\alpha < \mu < \beta$. ($1/\sigma_{\mu c}$ is still a function of μ.) This is possible if and only if $\overline{\underset{\sim}{E}_s \underset{\sim}{E}_s^\dagger}\, \underset{\sim}{x}^{(c)}$, $\overline{\underset{\sim}{E}_n \underset{\sim}{E}_n^\dagger}\, \underset{\sim}{x}^{(c)}$, and $\left(\underset{\sim}{Z}_s + \underset{\sim}{Z}_s^\dagger\right) \underset{\sim}{x}^{(c)}$ are colinear vectors. If this is true, we can always find a value of σ to satisfy (101) for any value of μ when $\underset{\sim}{x}$ is equal to $\underset{\sim}{x}^{(c)}$. For Fig. 22 to be applicable, the value of $1/\sigma$ obtained, $1/\sigma_c$, will only be the minimum value of $1/\sigma_\mu$ if μ is in the range $\alpha < \mu < \beta$.

A simple example can be given to illustrate both of the degeneracies described here. Consider a passive source network with $\underset{\sim}{Z}_s + \underset{\sim}{Z}_s^\dagger$ positive definite in thermal equilibrium at a temperature T. If the only noise present in the source network is the thermal noise, it can be shown[10,18] that $\overline{\underset{\sim}{E}_n \underset{\sim}{E}_n^\dagger} = 2kT\Delta f \left(\underset{\sim}{Z}_s + \underset{\sim}{Z}_s^\dagger\right)$. From definitions of $1/p_s$ and $1/s_s$ in Eqs. 96 and 97, it follows that

$$\frac{1}{s_s} = kT\Delta f \left(\frac{1}{p_s}\right). \tag{108}$$

Consequently, in the noise-performance plane all points in the source region for this case must lie on the straight line through the origin with a slope $kT\Delta f$ as shown in Fig. 23. Since $1/s_s$ (or $1/p_s$) is a bounded positive function for such a thermal source network

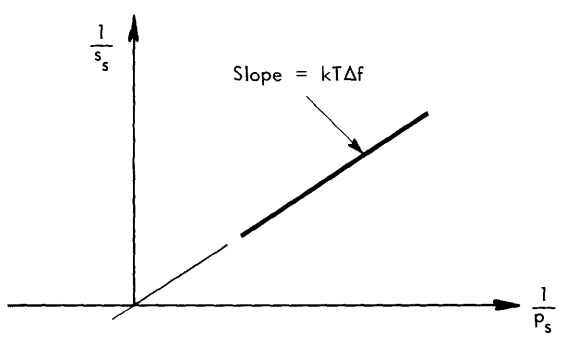

Fig. 23. Source region for a thermal source.

(we are still assuming that $\overline{\underset{\sim}{E}_s \underset{\sim}{E}_s^\dagger}$ is positive definite), we only have access to points along a finite segment of this line as shown.

Under these conditions, we see that the function $1/\sigma_\mu$ of Eq. 106 is stationary at zero for any vector $\underset{\sim}{x}$ if $\mu = kT\Delta f$. Also, since we may write Eq. 101

$$\overline{\underset{\sim}{E}_s \underset{\sim}{E}_s^\dagger}\, \underset{\sim}{x} - 2\sigma(kT\Delta f - \mu)\left(\underset{\sim}{Z}_s + \underset{\sim}{Z}_s^\dagger\right) \underset{\sim}{x} = 0, \tag{109}$$

we see that the eigenvectors are independent of the value of μ even though the eigenvalues of σ are not.

4.5 EFFECTS OF SEMIDEFINITE SIGNAL-VOLTAGE SPECTRAL-DENSITY MATRIX

We would now like to show that Theorems 6 and 7 are valid when $\overline{\underset{\sim}{E}_s \underset{\sim}{E}_s^\dagger}$ is positive semidefinite. Theorem 7 may be extended directly, since the proof given in Appendix A does not depend upon the definiteness of this matrix. It is not quite as simple to extend Theorem 6 to cover the case for which $\overline{\underset{\sim}{E}_s \underset{\sim}{E}_s^\dagger}$ is semidefinite. The problem that arises, when we allow $\overline{\underset{\sim}{E}_s \underset{\sim}{E}_s^\dagger}$ to be semidefinite, is that the function $1/\sigma_\mu$ of Eq. 105 becomes unbounded. Thus, any of the ranges of $1/\sigma_\mu$ shown in Fig. 20 may extend to infinity in either or both directions. We note that $1/s_s$ is a ratio of two positive quantities and, consequently, is always positive. Hence, for any value of $1/p_s$ that can be realized by a lossless reduction of the source there must be a minimum value of $1/s_s$ that is achievable. This minimum corresponds to a point on the outer boundary of the source region. We can conclude that the source region has a well-defined (semi) convex outer boundary.

Let us consider briefly an m-terminal-pair source that has a signal-voltage spectral-density matrix, $\overline{\underset{\sim}{E}_s \underset{\sim}{E}_s^\dagger}$, that is positive semidefinite of rank r ($r < m$). We show in Appendix B that for each value of μ Eq. 101 yields r finite eigenvalues and an (m-r)-fold degenerate set of eigenvalues, $\sigma = 0$. The nature of these m-r zero eigenvalues is very important, since each of the m-r independent eigenvectors associated with this degenerate set of eigenvalues makes $1/\sigma_\mu$ infinite. If $1/\sigma_\mu$ always approaches positive infinity as the vector $\underset{\sim}{x}$ approaches any one of these independent eigenvectors, $1/\sigma_\mu$ must have a minimum value. This minimum value will be an eigenvalue of Eq. 101 for the given value of μ; and will correspond to the intercept of a tangent to the outer boundary of the source region. Similarly, if, for another value of μ, $1/\sigma_\mu$ always approaches negative infinity as the vector $\underset{\sim}{x}$ approaches any one of the independent eigenvectors corresponding to the eigenvalue zero, $1/\sigma_\mu$ must have a maximum value. This appears as an eigenvalue of (101) for this value of μ, and corresponds to the intercept of a tangent to the outer boundary of the source region. But, if $1/\sigma_\mu$ approaches negative infinity as $\underset{\sim}{x}$ approaches any one of 1 of these degenerate eigenvalues and approaches positive infinity as $\underset{\sim}{x}$ approaches any one of the m-r-1 remaining vectors of the set, $1/\sigma_\mu$ may take on any value. We conclude for this case that none of the r finite eigenvalues of (101) corresponds to an extremum of $1/\sigma_\mu$.

We see that Theorem 6 is still satisfied when $\overline{\underset{\sim}{E}_s \underset{\sim}{E}_s^\dagger}$ is positive semidefinite. The

difficulty is in determining whether a given eigenvalue corresponds to an extremum of $1/\sigma_\mu$. For this reason, we shall describe a procedure for determining the outer boundary of the source region. We shall describe this procedure in conjunction with several typical source regions.

Figure 24 shows four possible source regions corresponding to sources with $\underset{\sim}{E}_S \underset{\sim}{E}_S^\dagger$ positive semidefinite. The source corresponding to Fig. 24a has a positive definite impedance matrix $\underset{\sim}{Z}_S + \underset{\sim}{Z}_S^\dagger$. This may be seen by noting that the range of $1/p_s$ in this plot is positive. The other three regions shown in Fig. 24 correspond to sources having a $\underset{\sim}{Z}_S + \underset{\sim}{Z}_S^\dagger$ matrix that is indefinite.

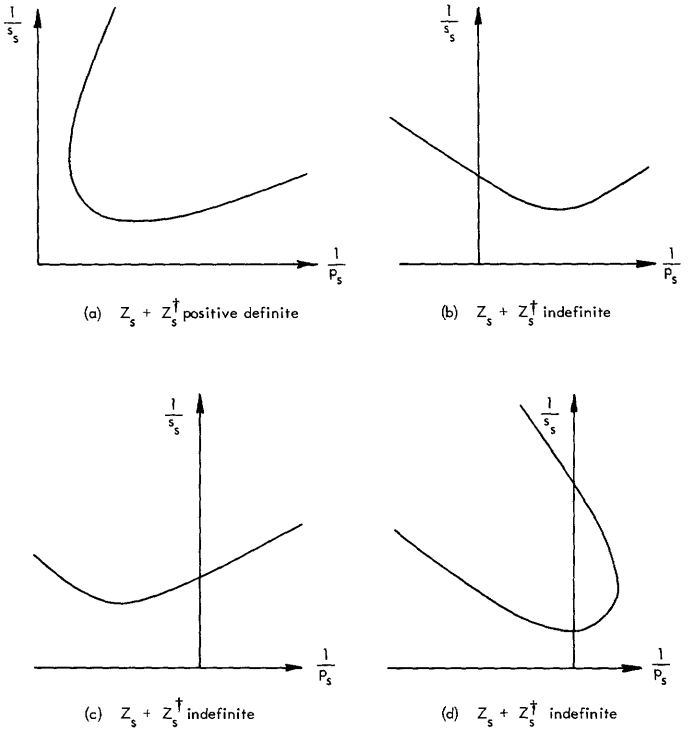

Fig. 24. Examples of typical source regions for sources with $\underset{\sim}{E}_S \underset{\sim}{E}_S^\dagger$ positive definite.

We shall show that we never really have to investigate the nature of the solutions of Eq. 101 that correspond to a zero eigenvalue for σ. An alternative procedure is to solve (101) for $\mu = 0$. We know that there is always an extremal eigenvalue for this case; this is the eigenvalue $1/\sigma_{01}$, the minimum value of $1/\sigma_\mu$ for $\mu = 0$. (It is also the minimum value of $1/s_s$ which is always positive.) From the eigenvector corresponding to this solution we may determine the coordinates of the point on the source boundary corresponding to the eigenvalue $1/\sigma_{01}$. We may now introduce μ as a parameter and investigate in what way the source point corresponding to the eigenvalue $1/\sigma_\mu$ moves as μ is increased from zero. As μ is increased through positive values, this point may move off to infinity for some value of μ, as in Fig. 24a, 24b or 24c. (It may also remain on

the finite plane even for μ approaching infinity as in Fig. 24d.) We have determined a segment of the boundary when the source point moves off to infinity; we therefore need go no farther in this direction for μ. We again go back and follow the source point as μ is decreased from zero through negative values until we reach that negative value of μ for which the point goes off to infinity as it would for the sources shown in Fig. 24b, 24c or 24d. (The point may remain in the finite plane even as μ becomes a large negative quantity. This situation would occur for the source shown in Fig. 24a.) Using this procedure, we can determine the entire source-region boundary for a source such as that shown in Fig. 24b or 24c; but, for a source such as that shown in Fig. 24a or 24d, we have determined only two of three branches of this outer boundary. To obtain the remainder of the source region in Fig. 24a, we follow the source point corresponding to $1/\sigma_{\mu m}$, the maximum value of $1/\sigma_{\mu}$, as μ is decreased from positive infinity through positive values, until the source point moves off to infinity. Similarly, for the source region of Fig. 24d we obtain the remaining segment of the source region by following the source point corresponding to $1/\sigma_{\mu m}$, the maximum value of $1/\sigma_{\mu}$ as μ is increased from minus infinity through finite negative values. We again follow this point until it moves off to infinity. The source-region outer boundary is then completely determined.

In carrying out the above-mentioned procedure it is not really necessary to determine the source point from the eigenvector. It is not even necessary to compute the eigenvector. Every time we pick a value of μ and find the extremal eigenvalue $1/\sigma_{\mu 1}$ (or $1/\sigma_{\mu m}$) we determine a line that is tangent to the outer boundary of the source region. In the $1/p_s$-$1/s_s$ plane (the noise-performance plane) the equation of this tangent is

$$\frac{1}{s_s} = \mu \frac{1}{p_s} + \frac{1}{\sigma_{\mu 1}}. \tag{110}$$

We can obtain a curve given by Eq. 110 for every value of μ for which an extremal eigenvalue exists. Furthermore, every one of the curves in this set is tangent to the outer boundary of the source region. The outer boundary of the source region is, therefore, the envelope of this set of curves. The envelope of a set of curves is defined as the curve tangent to all curves of the set, the individual curves of the set being distinguished from each other by the value of a parameter occurring in the equation of each individual curve. (Since $1/\sigma_{\mu 1}$ for a given source is only a function of μ, the curves described by Eq. 108 are distinguished only by the parameter μ.)

It follows immediately from this (see Goursat[26]) that the value of the reciprocal of exchangeable signal power, $1/p_{s,\mu 1}$, on the source-region boundary at the point, where the slope is μ, is given by

$$\frac{1}{p_{s,\mu 1}} = -\frac{\partial}{\partial \mu}\left(\frac{1}{\sigma_{\mu 1}}\right). \tag{111}$$

A complete derivation of (111) is given in Appendix C. The value of the noise-to-signal ratio at this point on the source-region boundary may be obtained from Eq. 110:

$$\frac{1}{s_{s,\mu 1}} = \frac{1}{\sigma_{\mu 1}} + \frac{\mu}{p_{s,\mu 1}}. \tag{112}$$

Frequently it is simpler to determine the coordinates of the points on the source-region boundary from Eqs. 111 and 112 than to compute the eigenvectors and then use them to determine $1/p_{s,\mu 1}$ and $1/s_{s,\mu 1}$. This will be apparent in the numerical example.

4.6 EXAMPLE OF A TWO-TERMINAL-PAIR SOURCE

We shall now examine the noise performance of the source network shown in Fig. 25.

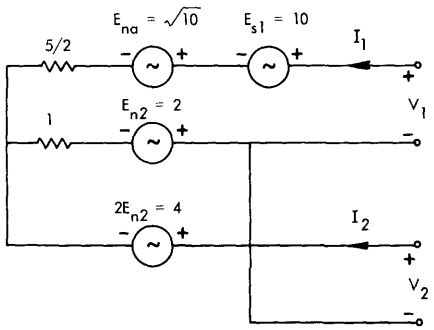

Fig. 25. Two-terminal-pair source network.

The two noise voltages E_{na} and E_2 are uncorrelated. For this network the signal-voltage matrix is

$$\overline{\underset{\sim}{E}_s \underset{\sim}{E}_s^\dagger} = \begin{bmatrix} 100 & 0 \\ 0 & 0 \end{bmatrix}, \tag{113}$$

the noise-voltage matrix is

$$\overline{\underset{\sim}{E}_n \underset{\sim}{E}_n^\dagger} = \begin{bmatrix} 14 & -4 \\ -4 & 4 \end{bmatrix}, \tag{114}$$

and the impedance matrix is

$$\underset{\sim}{Z} = \begin{bmatrix} 7/2 & 1 \\ 1 & 1 \end{bmatrix}. \tag{115}$$

Equation 101 is then written

$$\begin{bmatrix} 100 & 0 \\ 0 & 0 \end{bmatrix}\begin{bmatrix} x_1 \\ x_2 \end{bmatrix} - \sigma\left\{\begin{bmatrix} 14 & -4 \\ -4 & 4 \end{bmatrix} - \mu\begin{bmatrix} 14 & 4 \\ 4 & 4 \end{bmatrix}\right\}\begin{bmatrix} x_1 \\ x_2 \end{bmatrix} = 0 \tag{116}$$

$$\begin{bmatrix} 100 - 14\sigma(1-\mu) & 4\sigma(1+\mu) \\ 4\sigma(1-\mu) & -4\sigma(1-\mu) \end{bmatrix}\begin{bmatrix} x_1 \\ x_2 \end{bmatrix} = 0 \tag{117}$$

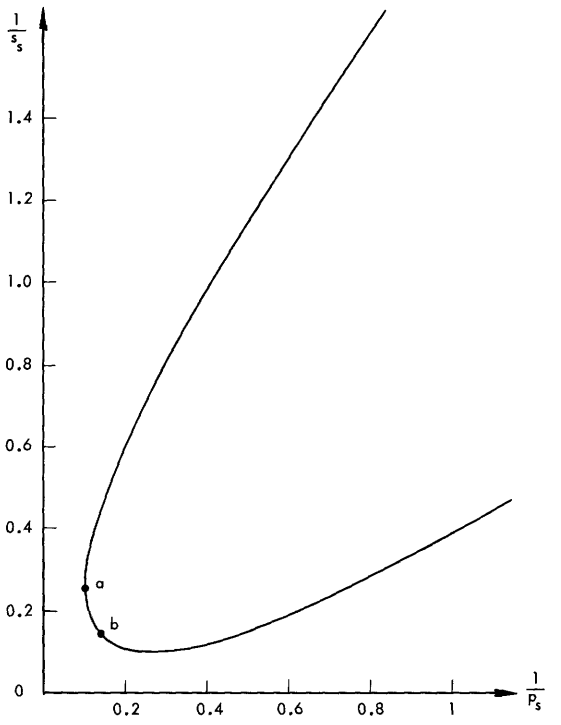

Fig. 26. Source-region boundary for the source of Fig. 25.

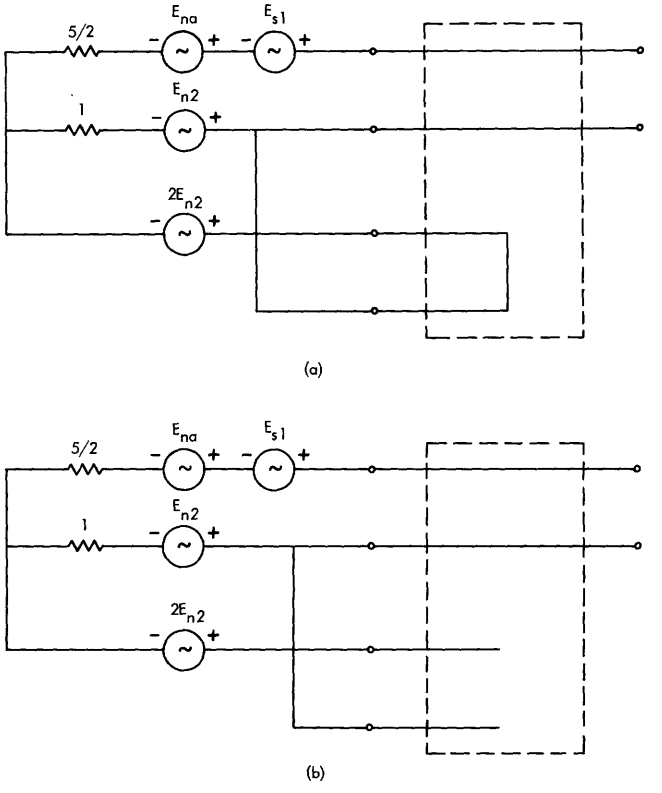

Fig. 27. (a) Source reduction corresponding to point a in Fig. 26.
(b) Source reduction corresponding to point b in Fig. 26.

This equation has a solution only if the determinant of the coefficient matrix vanishes. Setting this determinant equal to zero yields

$$400\sigma(1-\mu) - 56\sigma^2(1-\mu)^2 + 16\sigma^2(1+\mu)^2 = 0. \tag{118}$$

Equation 118 has two solutions $\sigma = 0$ and

$$\frac{1}{\sigma_{\mu 1}} = \frac{7(1-\mu)^2 - 2(1+\mu)^2}{50(1-\mu)} = \frac{5\mu^2 - 18\mu + 5}{50(1-\mu)}. \tag{119}$$

From (117) we see that the components of the eigenvector $x^{(\mu 1)}$ are related by

$$\frac{x_2^{(\mu 1)}}{x_1^{(\mu 1)}} = \frac{1+\mu}{1-\mu}. \tag{120}$$

Since there is only one finite eigenvalue and one zero eigenvalue, every source point determined from (117) is a point on the outer boundary of the source region. The value of the coordinate $1/p_{s,\mu 1}$ as a function of the slope μ is given as

$$\frac{1}{p_{s,\mu 1}} = \frac{2\underset{\sim}{x}^{(\mu 1)\dagger}\left(\underset{\sim}{Z}_s + \underset{\sim}{Z}_s^\dagger\right)\underset{\sim}{x}^{(\mu 1)}}{\underset{\sim}{x}^{(\mu 1)\dagger}\,\overline{\underset{\sim}{E}_s\underset{\sim}{E}_s^\dagger}\,\underset{\sim}{x}^{(\mu 1)}}. \tag{121}$$

Using Eqs. 113-115, we may write (121) as

$$\frac{1}{p_{s,\mu 1}} = \frac{7 + 4\dfrac{1+\mu}{1-\mu} + 2\dfrac{(1+\mu)^2}{(1-\mu)^2}}{50} = \frac{13 - 10\mu + 5\mu^2}{50(1-\mu)^2}. \tag{122}$$

Similarly, we find the noise-to-signal ratio, $1/s_{s,\mu 1}$, to be

$$\frac{1}{s_{s,\mu 1}} = \frac{\underset{\sim}{x}^{(\mu 1)\dagger}\,\overline{\underset{\sim}{E}_n\underset{\sim}{E}_n^\dagger}\,\underset{\sim}{x}^{(\mu 1)}}{\underset{\sim}{x}^{(\mu 1)\dagger}\,\overline{\underset{\sim}{E}_s\underset{\sim}{E}_s^\dagger}\,\underset{\sim}{x}^{(\mu 1)}} = \frac{13\mu^2 - 10\mu + 5}{50(1-\mu)^2}. \tag{123}$$

These relations could have also been derived by taking the derivative of $1/\sigma_{\mu 1}$ in Eq. 119 and using Eqs. 111 and 112. Plotting $1/p_{s,\mu 1}$ and $1/s_{s,\mu 1}$ for a number of values of μ, we obtain the source-region boundary shown in Fig. 26. This curve is a parabola rotated through 45°. By eliminating μ between (122) and (123), we can show that $[1/p_s + 1/s_s] = 25/8[1/p_s - 1/s_s]^2 + 7/25$.

For this simple case there is a point on the boundary for every value of μ. But as μ approaches +1 both $1/p_{s,\mu 1}$ and $1/s_{s,\mu 1}$ approach infinity. The imbeddings of the source that lead to the points a and b on the source-region boundary are shown in Fig. 27.

V. OPTIMUM PERFORMANCE OF A MULTITERMINAL-PAIR AMPLIFIER USED WITH A MULTITERMINAL-PAIR SOURCE

In Section IV we imbedded a multiterminal-pair source network and examined the noise-to-signal ratio and exchangeable signal power that could be obtained at a single-output terminal pair through such a lossless reduction. We found that, in general, a whole region of values of these parameters is available. We described this fact by defining the source region in the noise-to-signal ratio and reciprocal exchangeable signal power plane – the noise-performance plane. We showed that we can obtain the outer boundary of this region from a simple eigenvalue equation (Eq. 101). We gave a complete interpretation of this equation and showed in section 4.5 that it was valid even for semidefinite signal cross spectral-density matrices.

We shall now examine the general optimization problem. We shall determine the noise performance that can be achieved by interconnecting an m-terminal-pair source and an n-terminal-pair amplifier network in the most general way. In section 5.1 we shall show that any noise performance that can be achieved by imbedding the source and amplifier networks in a common imbedding network can also be achieved by imbedding the source network and the amplifier independently to reduce both networks to one-terminal-pair networks and by combining the two resulting one-terminal-pair networks.

We use this fact in section 5.2 to examine the performance of a multiterminal-pair source network with a noisy resistor. It is then a simple matter to describe the general performance of the multiterminal-pair source with a multiterminal-pair amplifier. This problem is considered in section 5.3. A simple example is discussed in section 5.4.

5.1 REALIZATION OF THE OPTIMAL NETWORK

We shall prove that any signal-to-noise ratio and exchangeable signal power that can be achieved through a general lossless imbedding of a source and amplifier, such as that

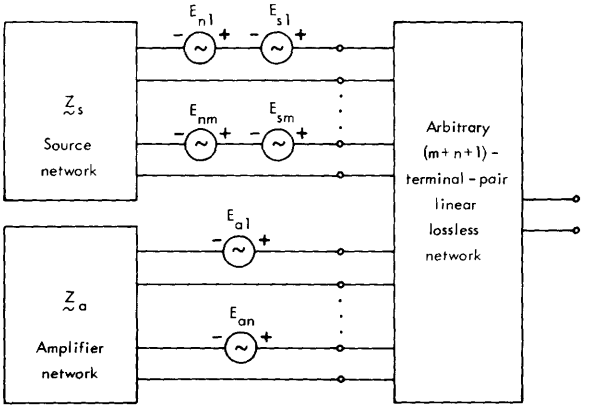

Fig. 28. General imbedding of an m-terminal-pair source and an n-terminal-pair amplifier.

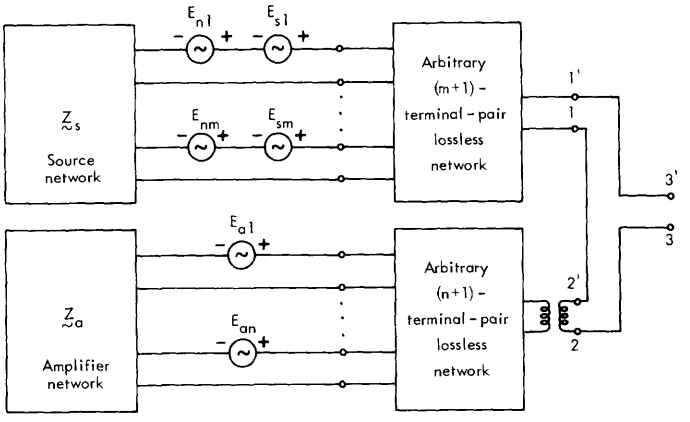

Fig. 29. Independent imbedding of an m-terminal-pair source and an n-terminal-pair amplifier.

shown in Fig. 28, can also be achieved by independently imbedding the source and amplifier as in Fig. 29.

Let us first consider the imbedding of Fig. 28. We may regard this as an imbedding of the composite network consisting of the source and amplifier networks. This composite network has a cross spectral-density matrix, $\overline{\underset{\sim}{E}\underset{\sim}{E}^\dagger}$, given by

$$\overline{\underset{\sim}{E}\underset{\sim}{E}^\dagger} = \begin{bmatrix} \overline{\underset{\sim}{E}_s\underset{\sim}{E}_s^\dagger} + \overline{\underset{\sim}{E}_n\underset{\sim}{E}_n^\dagger} & \vdots & 0 \\ \cdots\cdots\cdots\cdots & \vdots & \cdots\cdots \\ 0 & \vdots & \overline{\underset{\sim}{E}_a\underset{\sim}{E}_a^\dagger} \end{bmatrix} \tag{124}$$

and an impedance matrix $\underset{\sim}{Z}$ given by

$$\underset{\sim}{Z} = \begin{bmatrix} \underset{\sim}{Z}_s & \vdots & \underset{\sim}{0} \\ \cdots & \vdots & \cdots \\ \underset{\sim}{0} & \vdots & \underset{\sim}{Z}_a \end{bmatrix}. \tag{125}$$

From Eq. 26 we may write the exchangeable power at the output terminal pair as

$$P_{e,i} = \frac{\underset{\sim}{x}^\dagger \overline{\underset{\sim}{E}\underset{\sim}{E}^\dagger} \underset{\sim}{x}}{2\underset{\sim}{x}^\dagger(\underset{\sim}{Z}+\underset{\sim}{Z}^\dagger)\underset{\sim}{x}},$$

where $\underset{\sim}{x}$ is an arbitrary (m+n)-dimensional vector for this case. Since $\underset{\sim}{x}$ is completely arbitrary, we may partition it into two arbitrary vectors $\underset{\sim}{x}_1$ and $\underset{\sim}{x}_2$, where $\underset{\sim}{x}_1$ is an m-dimensional vector and $\underset{\sim}{x}_2$ is an n-dimensional vector.

$$\underset{\sim}{x} = \begin{bmatrix} \underset{\sim}{x}_1 \\ \cdots \\ \underset{\sim}{x}_2 \end{bmatrix} \tag{126}$$

Using Eqs. 124, 125, and 126 we may write Eq. 26 in an expanded form as

$$P_{e,i} = \frac{\underset{\sim}{x}_1^\dagger \overline{\underset{\sim}{E}_s \underset{\sim}{E}_s^\dagger} \underset{\sim}{x}_1 + \underset{\sim}{x}_1^\dagger \overline{\underset{\sim}{E}_n \underset{\sim}{E}_n^\dagger} \underset{\sim}{x}_1 + \underset{\sim}{x}_2^\dagger \overline{\underset{\sim}{E}_a \underset{\sim}{E}_a^\dagger} \underset{\sim}{x}_2}{2\underset{\sim}{x}_1^\dagger \left(\underset{\sim}{Z}_s + \underset{\sim}{Z}_s^\dagger\right) \underset{\sim}{x}_1 + 2\underset{\sim}{x}_2^\dagger \left(\underset{\sim}{Z}_a + \underset{\sim}{Z}_a^\dagger\right) \underset{\sim}{x}_2}. \tag{127}$$

From Eq. 127 we see that the exchangeable signal power at the output is given by

$$p_o = \frac{\underset{\sim}{x}_1^\dagger \overline{\underset{\sim}{E}_s \underset{\sim}{E}_s^\dagger} \underset{\sim}{x}_1}{2\underset{\sim}{x}_1^\dagger \left(\underset{\sim}{Z}_s + \underset{\sim}{Z}_s^\dagger\right) \underset{\sim}{x}_1 + 2\underset{\sim}{x}_2^\dagger \left(\underset{\sim}{Z}_a + \underset{\sim}{Z}_a^\dagger\right) \underset{\sim}{x}_2}. \tag{128}$$

The exchangeable signal-to-noise ratio at this output is given by

$$s_o = \frac{\underset{\sim}{x}_1^\dagger \overline{\underset{\sim}{E}_s \underset{\sim}{E}_s^\dagger} \underset{\sim}{x}_1}{\underset{\sim}{x}_1^\dagger \overline{\underset{\sim}{E}_n \underset{\sim}{E}_n^\dagger} \underset{\sim}{x}_1 + \underset{\sim}{x}_2^\dagger \overline{\underset{\sim}{E}_a \underset{\sim}{E}_a^\dagger} \underset{\sim}{x}_2}. \tag{129}$$

On the other hand, for the network of Fig. 29 we see from Eq. 94 that the exchangeable signal power at the terminal pair 1 - 1' is

$$p_s = \frac{\underset{\sim}{x}_1^\dagger \overline{\underset{\sim}{E}_s \underset{\sim}{E}_s^\dagger} \underset{\sim}{x}_1}{2\underset{\sim}{x}_1^\dagger \left(\underset{\sim}{Z}_s + \underset{\sim}{Z}_s^\dagger\right) \underset{\sim}{x}_1}, \tag{130}$$

and from Eq. 95 that the exchangeable signal-to-noise ratio is

$$s_s = \frac{\underset{\sim}{x}_1^\dagger \overline{\underset{\sim}{E}_s \underset{\sim}{E}_s^\dagger} \underset{\sim}{x}_1}{2\underset{\sim}{x}_1^\dagger \overline{\underset{\sim}{E}_n \underset{\sim}{E}_n^\dagger} \underset{\sim}{x}_1}. \tag{131}$$

In these two expressions the vector $\underset{\sim}{x}_1$ is completely arbitrary and depends on the source imbedding network. Similarly, the exchangeable noise power at the terminal pair 2 - 2' of Fig. 29 is given by

$$-\lambda = \frac{\underset{\sim}{x}_2^\dagger \overline{\underset{\sim}{E}_a \underset{\sim}{E}_a^\dagger} \underset{\sim}{x}_2}{2\underset{\sim}{x}_2^\dagger \left(\underset{\sim}{Z}_a + \underset{\sim}{Z}_a^\dagger\right) \underset{\sim}{x}_2}. \tag{132}$$

From Eq. 130 we conclude that the mean-square signal voltage appearing at the terminal pair 3 - 3' is $\underset{\sim}{x}_1^\dagger \overline{\underset{\sim}{E}_s \underset{\sim}{E}_s^\dagger} \underset{\sim}{x}_1$, and from Eqs. 130 and 132 we see that the real part of the impedance looking into this terminal pair is $(1/2)\, \underset{\sim}{x}_1^\dagger \left(\underset{\sim}{Z}_s + \underset{\sim}{Z}_s^\dagger\right) \underset{\sim}{x}_1 + (1/2)\, \underset{\sim}{x}_2^\dagger \left(\underset{\sim}{Z}_a + \underset{\sim}{Z}_a^\dagger\right) \underset{\sim}{x}_2$. Hence the exchangeable signal power at terminal pair 3 - 3' may be written as Eq. 128:

$$p_o = \frac{\underset{\sim}{x}_1^\dagger \overline{\underset{\sim}{E}_s \underset{\sim}{E}_s^\dagger}\, \underset{\sim}{x}_1}{2\underset{\sim}{x}_1^\dagger \left(\underset{\sim}{Z}_s + \underset{\sim}{Z}_s^\dagger\right) \underset{\sim}{x}_1 + 2\underset{\sim}{x}_2^\dagger \left(\underset{\sim}{Z}_a + \underset{\sim}{Z}_a^\dagger\right) \underset{\sim}{x}_2}.$$

Similarly, from Eqs. 131 and 132 we see that the mean-square noise voltage appearing at the terminal pair 3 - 3' is $\underset{\sim}{x}_1^\dagger \overline{\underset{\sim}{E}_n \underset{\sim}{E}_n^\dagger}\, \underset{\sim}{x}_1 + \underset{\sim}{x}_2^\dagger \overline{\underset{\sim}{E}_a \underset{\sim}{E}_a^\dagger}\, \underset{\sim}{x}_2$. The exchangeable signal-to-noise ratio at this terminal pair is, therefore, given by Eq. 129:

$$s_o = \frac{\underset{\sim}{x}_1^\dagger \overline{\underset{\sim}{E}_s \underset{\sim}{E}_s^\dagger}\, \underset{\sim}{x}_1}{\underset{\sim}{x}_1^\dagger \overline{\underset{\sim}{E}_n \underset{\sim}{E}_n^\dagger}\, \underset{\sim}{x}_1 + \underset{\sim}{x}_2^\dagger \overline{\underset{\sim}{E}_a \underset{\sim}{E}_a^\dagger}\, \underset{\sim}{x}_2}.$$

Thus, we see that we can achieve the same results by varying the lossless networks in Fig. 29 as we could by varying the single network of Fig. 28. While an actual system would probably be realized in a form such as that of Fig. 28, the form of realization in Fig. 29 is more suitable for theoretical discussions. In the realization of Fig. 29 we can see how to make the specific adjustments necessary to optimize the performance of the system. By varying the imbedding of the source network, we can adjust the way in which we are using the source network. By varying the imbedding network of the amplifier we can adjust the way in which we are using the amplifier network. Finally, by varying the turns ratio of the transformer shown as part of the amplifier network imbedding we can vary the extent to which we are using the amplifier by varying its impedance level relative to the source. This last variation is equivalent to varying the exchangeable gain of the amplifier. While we can perform similar variations by varying the imbedding network in Fig. 28, the effect of a particular network variation is not brought into evidence as it is in the realization of Fig. 29. We have therefore established the following theorem.

THEOREM 8: Any values of signal-to-noise ratio and exchangeable signal power that can be obtained at a single-output terminal pair through a general lossless imbedding of a source network and an amplifier network can also be obtained by independently imbedding the source network and the amplifier network and combining the two resultant one-terminal-pair networks.

5.2 OPTIMUM PERFORMANCE OF A MULTITERMINAL-PAIR SOURCE USED WITH A NOISY RESISTOR

We shall work up to the problem of the optimum performance of a multiterminal-pair amplifier used with a multiterminal-pair source network by several stages. We shall now analyze the optimum performance of a single noisy resistor used in conjunction with a multiterminal-pair source network. We shall also consider briefly what can be achieved with two independently noisy resistors. With this background the solution to the general problem can be derived almost by inspection.

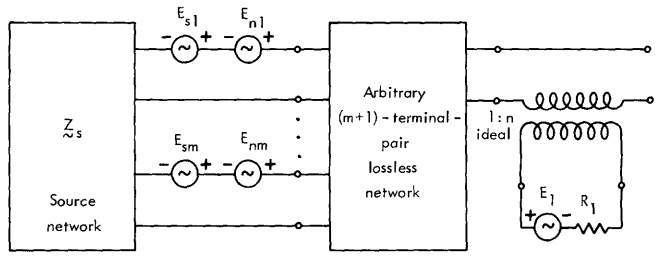

Fig. 30. Imbedding of an m-terminal-pair source network and a single noisy resistance.

The problem that we consider in this section is illustrated by Fig. 30. We use an arbitrary lossless imbedding network to reduce the multiterminal-pair source to a one-terminal-pair source and we then combine this one-terminal-pair source with the noisy resistor in an arbitrary way. The noisy resistor has a resistance R_1 and a noise voltage E_1. Since this noise voltage is statistically independent of the source voltages, we may achieve this arbitrary combination by means of an ideal transformer as shown in Fig. 30. For any particular imbedding network the exchangeable signal power of the source and exchangeable signal-to-noise ratio of the source are given by Eqs. 130 and 131, respectively, where the vector $\underset{\sim}{x}_1$ is completely determined by the particular imbedding network. But we have already solved the problem of the performance of a one-terminal-pair source used with a one-terminal-pair amplifier. In section 3.2 we showed that the output noise-to-signal ratio, $1/s_o$, for such a combination is given by (see Eq. 70)

$$\frac{1}{s_o} = \frac{1}{s_s} + \frac{\overline{|E_1|^2}}{4R_1}\left[\frac{1}{p_o} - \frac{1}{p_s}\right], \tag{133}$$

where p_o is the output exchangeable signal power. From Eqs. 129 and 131 we can show that (133) is valid only for

$$\frac{1}{s_o} \geqslant \frac{1}{s_s}. \tag{134}$$

Let us assume for simplicity that the source in Fig. 31 has a signal-voltage matrix $\overline{\underset{\sim}{E}_s \underset{\sim}{E}_s^\dagger}$ that is positive definite, and a $\underset{\sim}{Z}_s + \underset{\sim}{Z}_s^\dagger$ matrix that is positive definite. Assume that the source region for this source is as shown in Fig. 31. We shall also assume for the moment that R_1 is a negative resistance ($R_1 < 0$) with an exchangeable noise power $-\lambda_1$.

$$-\lambda_1 = \frac{\overline{|E_1|^2}}{4R_1} < 0. \tag{135}$$

Any given imbedding network in Fig. 31 determines a point within the source region such as the point a in Fig. 32. By subsequently introducing the resistor R_1 ($R_1 < 0$) and varying the transformer ratio n, we can achieve at the output any noise-to-signal ratio

and exchangeable signal power corresponding to a point on the line through a with a slope $-\lambda_1$, as shown in Fig. 32. This may be seen from Eq. 133; but from (134) we see that we can only achieve points on the half of this line that lies above the noise-to-signal ratio of the source. For different imbedding networks we obtain other lines, each having the same slope but terminating on different points in the source region.

It is apparent from Fig. 31 that the best source reduction for this resistor (amplifier) is the one corresponding to point b, where point b is one of the points on the outer boundary of the source region where the slope is $-\lambda_1$. For this particular source reduction we obtain the minimum noise-to-signal ratio achievable with this source and amplifier at large values of exchangeable power (or negative exchangeable power) by varying the transformer ratio n in Fig. 30. Similarly, the worst noise-to-signal ratios achievable with this source and amplifier at large exchangeable powers are obtained when the reduced source is characterized by the coordinates of point d in Fig. 31. Point d is the other point on the outer boundary of the source region where the slope is $-\lambda_1$. We have described how to obtain the points b and d from Eq. 101. If we solve Eq. 101 with $\mu = -\lambda_1$, we obtain a set of eigenvalues, σ_{1i}, and a set of eigenvectors, $\underset{\sim}{x}_1^{(1i)}$. (We use the first subscript, 1, to indicate that these are solutions corresponding to $\mu = -\lambda_1$.) We order these eigenvalues as shown in Fig. 20 so that $1/\sigma_{11} < 1/\sigma_{1i} < 1/\sigma_{1m}$. When the eigenvector $\underset{\sim}{x}_1^{(11)}$ is applied to the expressions in (130) and (131), the values of signal-to-noise ratio and exchangeable signal power obtained give the coordinates of point b in Fig. 31. But more important, the eigenvalue for this solution σ_{11} may now be interpreted as the maximum signal-to-noise ratio achievable at infinite exchangeable power. Likewise the eigenvector $\underset{\sim}{x}_1^{(1m)}$ yields the coordinates of the point d and the eigenvalue σ_{1m} is the minimum signal-to-noise ratio achievable with this source and amplifier at infinite exchangeable power. Finally, we note that the region of values of noise-to-signal ratio and exchangeable signal power achievable by imbedding the given source and noisy resistor is the region enclosed by the two straight lines terminating at b and d and by the segment b c d of the outer boundary of the source region.

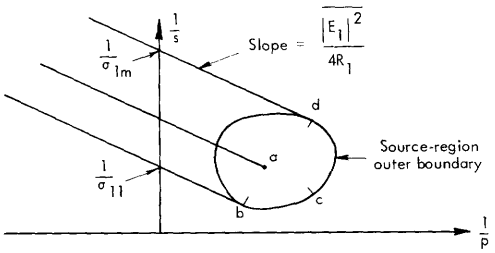

Fig. 31. Performance curves for a multiterminal source and a noisy negative resistance.

By similar means we can consider what we can achieve by combining a noisy positive resistance with the m-terminal-pair source of Fig. 30. Assume that we have a noisy positive resistance R_2 ($R_2 > 0$) with a noise voltage E_2. The exchangeable noise power of this resistance is

$$-\lambda_2 = \frac{\overline{|E_2|^2}}{4R_2} > 0.$$

The region of values of exchangeable noise-to-signal ratio and exchangeable signal power that we may obtain by combining this resistor with the source is shown in Fig. 32. By adjusting the imbedding network of the source and the coupling to the resistance as before, we may obtain at the output any point in the region bounded by the two straight lines of slope $-\lambda_2$ terminating at c and e and the segment of the source region boundary c b e. The points c and e are the two points on the source-region outer boundary where the slope is $-\lambda_2$. These points may be obtained from Eq. 101 as before. The only difference between this case with a positive resistance and the case with the negative resistance considered before is that the eigenvalues $1/\sigma_{21}$ and $1/\sigma_{2m}$ may not be interpreted as signal-to-noise ratios at infinite exchangeable power. It is apparent from Fig. 32, and also from physical considerations, that we cannot achieve infinite exchangeable power by combining a passive source with a positive resistance. We shall describe the general conditions that must be satisfied for an eigenvalue of Eq. 101 to be interpretable as an achievable signal-to-noise ratio at infinite exchangeable power.

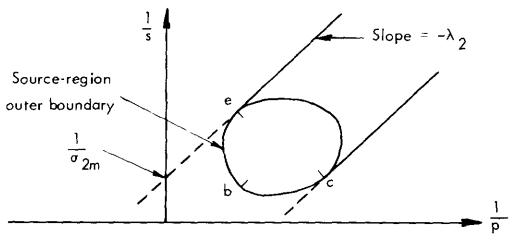

Fig. 32. Performance curves for a multiterminal source and a noisy positive resistance.

Before concluding this section we should discuss what can be achieved by combining both a positive and a negative resistance with the m-terminal-pair source. The region

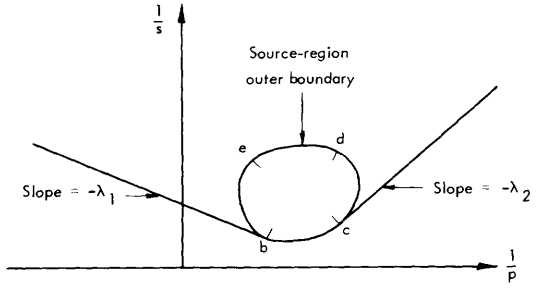

Fig. 33.
Performance of a multiterminal source used with a negative resistance and a positive resistance.

of the noise-performance plane that may be achieved at the output can be derived from an argument similar to that used in section 3.3. This region is shown in Fig. 33 for the source and two resistors that we are now considering. We may achieve any noise-to-signal ratio and exchangeable signal power in the region lying above the curve consisting of the straight line of slope $-\lambda_1$ terminating at b, the section b c of the source-region outer boundary, and the straight line of slope $-\lambda_2$ terminating at c. This region

may also be obtained by noting that any combination of the negative resistance R_1 and the m-terminal-pair source may be considered as a new source having as its source region the entire region shown in Fig. 31. By subsequently introducing the positive resistance R_2, we see that any point in the region shown in Fig. 33 may be obtained.

5.3 SOLUTIONS TO THE GENERAL OPTIMIZATION PROBLEM

We are now in a position to consider the solution to the general problem of the optimum performance of a multiterminal-pair amplifier used with a multiterminal-pair

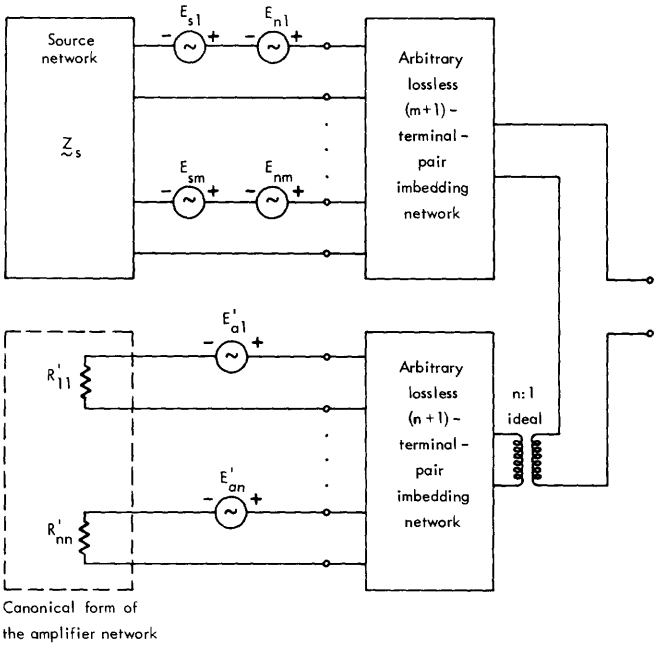

Fig. 34.
Realization for obtaining solutions to the optimization problem.

source. We have shown (Theorem 8) that we could always realize the optimum performance by individually imbedding the source and amplifier as in Fig. 29. This is a convenient form for the realization, for we have shown (section 2.6) that any exchangeable power that can be achieved by imbedding the amplifier as in Fig. 29 can also be achieved by imbedding the canonical form of the amplifier in some other lossless network. This is a consequence of the fact stated in Theorem H&A-2 that the eigenvalues of the characteristic noise matrix of the amplifier are invariant under lossless transformations that preserve the number of terminal pairs. Without loss of generality, then, we may examine the solution to the general noise-performance problem by considering the canonical form of the amplifier as shown in Fig. 34.

We denote the negative of the exchangeable noise power of the first element of the canonical form by $-\lambda_1$, that of the second element by $-\lambda_2$, etc. It will be recalled that the set of numbers $\lambda_1, \ldots \lambda_n$, are the eigenvalues of the characteristic noise matrix, $\underset{\sim}{N} = -\frac{1}{2}\left(\underset{\sim}{Z}_a + \underset{\sim}{Z}_a^\dagger\right) \overline{\underset{\sim}{E}_n \underset{\sim}{E}_n^\dagger}$, of the amplifier, or the eigenvalues of the equation

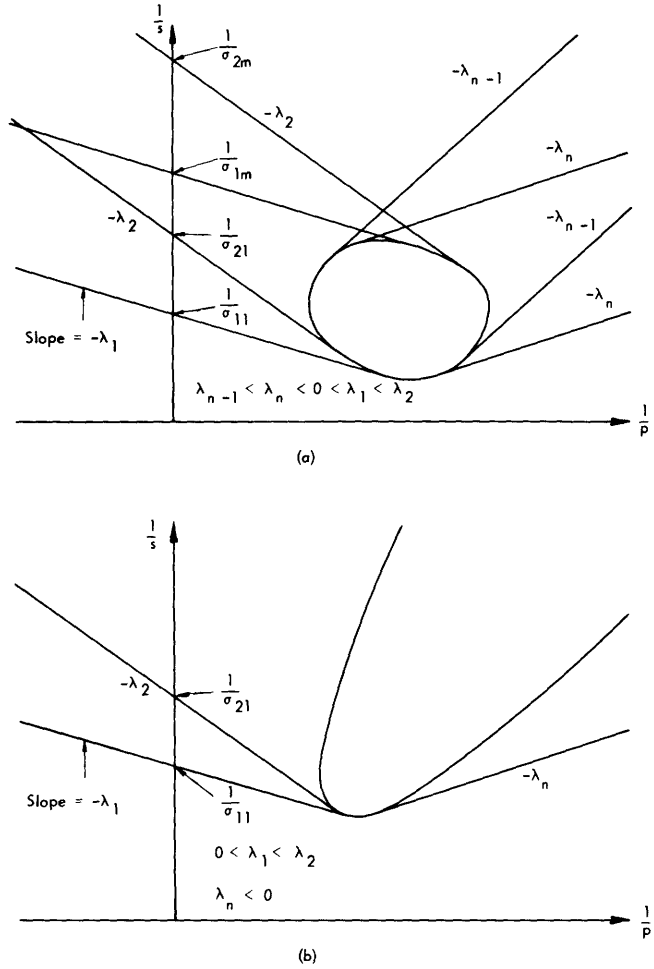

Fig. 35. (a) Solution lines for a source with $\underset{\sim}{Z}_s + \underset{\sim}{Z}_s^\dagger$ and $\overline{\underset{\sim}{E}_s \underset{\sim}{E}_s^\dagger}$ positive definite.

(b) Solution lines for a source with $\underset{\sim}{Z}_s + \underset{\sim}{Z}_s^\dagger$ positive definite and $\overline{\underset{\sim}{E}_s \underset{\sim}{E}_s^\dagger}$ positive semidefinite.

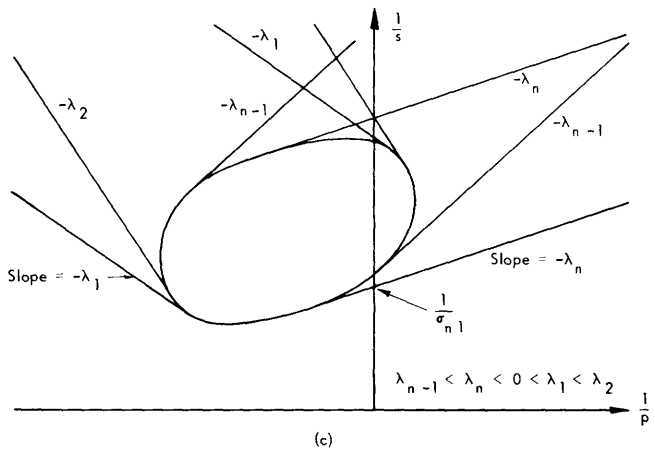

(c)

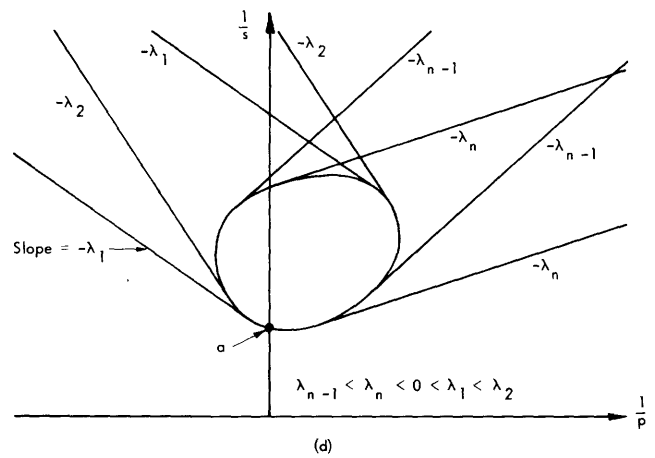

(d)

Fig. 35. (c) Solution lines for source with $\underset{\sim}{Z}_s + \underset{\sim}{Z}_s^\dagger$ indefinite, $\overline{\underset{\sim}{E}_s \underset{\sim}{E}_s^\dagger}$ positive definite.

(d) Solution lines for source with $\underset{\sim}{Z}_s + \underset{\sim}{Z}_s^\dagger$ indefinite, $\overline{\underset{\sim}{E}_s \underset{\sim}{E}_s^\dagger}$ positive definite.

$$\overline{\underset{\sim}{E}_a \underset{\sim}{E}_a^\dagger}\ \underset{\sim}{x}_2 + 2\lambda\left(\underset{\sim}{Z}_a + \underset{\sim}{Z}_a^\dagger\right)\underset{\sim}{x}_2 = 0. \tag{136}$$

We assume that (136) has both positive and negative eigenvalues, and that we have arranged the canonical form to agree with the ordering of these eigenvalues shown in Fig. 4c so that $0 < \lambda_1 < \lambda_2 < \lambda_3$, etc., and $0 > \lambda_n > \lambda_{n-1}$, etc.

We shall show what may be achieved through the realization of Fig. 34 by plotting the extremal performance lines for each of the elements of the canonical form of the amplifier with the given source, as we did in Figs. 31 and 32. Here we determine the positions of the extremal lines for the i^{th} element of the canonical form by solving Eq. 101 for $\mu = -\lambda_i$. That is, we solve the equation

$$\overline{\underset{\sim}{E}_s \underset{\sim}{E}_s^\dagger}\ \underset{\sim}{x}_1 - \sigma\left[\overline{\underset{\sim}{E}_n \underset{\sim}{E}_n^\dagger} + 2\lambda_i\left(\underset{\sim}{Z}_s + \underset{\sim}{Z}_s^\dagger\right)\right]\underset{\sim}{x}_1 = 0. \tag{137}$$

We denote the j^{th} eigenvalue of (137) σ_{ij}, and the corresponding eigenvector $\underset{\sim}{x}_1^{(ij)}$. We number the set of eigenvalues obtained for each λ_i as in Fig. 20 or Fig. 25 so that $1/\sigma_{i1}$ is the minimum value of the function $1/\sigma_\mu$ of Eq. 106 for $\mu = -\lambda_i$. When the eigenvector $\underset{\sim}{x}_1^{(ij)}$ is applied to the expressions in (130) and (131), we obtain the coordinates of the source point corresponding to the eigenvalue σ_{ij}; these coordinates are denoted $1/p_{s,ij}$ and $1/s_{s,ij}$. From Eqs. 133 and 134 we see that the two extremal performance lines obtainable with the i^{th} element of the canonical form of the amplifier are given by

$$\frac{1}{s_o} = \frac{1}{s_{s,ij}} - \lambda_i\left[\frac{1}{p_o} - \frac{1}{p_{s,ij}}\right]; \qquad j = 1, \text{ or } m \tag{138}$$

with the constraint that

$$\frac{1}{s_o} \geqslant \frac{1}{s_{s,ij}}. \tag{139}$$

For a number of sources, then, we shall plot the two lines given by (138) for each of four elements of the canonical form of the amplifier. We limit ourselves to four to keep the plots from becoming too complicated, at the same time providing enough of these lines for comparison. The four elements chosen are that corresponding to λ_1, the smallest positive eigenvalue of the characteristic noise matrix, $\underset{\sim}{N}$; that corresponding to λ_2, the next to the smallest eigenvalue of the characteristic noise matrix; that corresponding to λ_n, the smallest negative eigenvalue of $\underset{\sim}{N}$; and that corresponding to λ_{n-1}, the next to the smallest negative eigenvalue of $\underset{\sim}{N}$.

The plots described above are shown for four different source networks in Fig. 35. The source networks corresponding to the source regions in Fig. 35a, 35c, and 35d have positive definite signal-voltage matrices $\underset{\sim}{E}_s \underset{\sim}{E}_s^\dagger$; the source corresponding to the source region in Fig. 35b has a positive semidefinite signal-voltage matrix. The $\underset{\sim}{Z}_s + \underset{\sim}{Z}_s^\dagger$ matrix of the sources in Fig. 35a and 35b are positive definite, while that for the sources of Fig. 35c and 35d is indefinite. From our discussion above we see that we can achieve any point in the characteristic noise plane above the lower lines of

slopes $-\lambda_1$ and $-\lambda_n$, and some segment of the source-region outer boundary for each of the cases shown.

Let us discuss these four plots briefly. For the source whose region is shown in Fig. 35a, the best noise-to-signal ratio at large exchangeable power is obtained when the source is coupled only to the element of the canonical form of the amplifier whose exchangeable noise power is $-\lambda_1$. The optimum signal-to-noise ratio at large exchangeable power is given for this case by σ_{11}. The same statement may be made for the case illustrated in Fig. 35b. But for the source whose region is shown in Fig. 35c we find a different result. Here the minimum noise-to-signal ratio at large exchangeable power is obtained when this source is coupled only to the element of the canonical form of the amplifier corresponding to λ_n. That is, we obtain optimum noise performance when we couple only to the least noisy dissipative element of the canonical form of the amplifier. The optimum signal-to-noise ratio for this case is given by the eigenvalue σ_{n1}. Another situation that can occur is shown in Fig. 35d. For the source corresponding to this region the best signal-to-noise ratio achievable at large values of exchangeable power is obtained without using the given amplifier. For this source region the best signal-to-noise ratio at large exchangeable power is obtained merely by using the lossless imbedding network

5.4 COMMENTS ON THE SOLUTIONS TO THE GENERAL PROBLEM

We have shown that if the source region of a given source network is completely specified, and if all of the eigenvalues of the characteristic noise matrix of a given amplifier are known, we can easily determine the optimum performance of the source with the amplifier. We can determine whether we should couple only to the element of the canonical form of the amplifier corresponding to the smallest positive eigenvalue of the characteristic noise matrix, or whether we should couple only to the element corresponding to the smallest negative eigenvalue of the characteristic noise matrix, or whether it is better not to use the amplifier at all. While it is not too difficult in general to find the smallest positive and smallest negative eigenvalues of the characteristic noise matrix of an amplifier, the complete determination of the source region is quite a difficult procedure. The principal quantity of interest is the minimum noise-to-signal ratio at large exchangeable power, and this noise-to-signal ratio is usually the reciprocal of one of the eigenvalues of Eq. 137. Yet every eigenvalue of (137) may not be interpreted as an achievable signal-to-noise ratio at large exchangeable power. Consequently, it is desirable to determine the conditions for which an eigenvalue of (137) may be interpreted as an exchangeable signal-to-noise ratio at infinite exchangeable power.

For one particular case we do not have to formulate these conditions in detail. If we are considering a source having a $\underset{\sim}{Z}_s + \underset{\sim}{Z}_s^\dagger$ matrix that is positive definite, we know that the source region always lies completely in the right-hand half of the noise-performance plane. If we want to obtain large, or infinite, exchangeable signal power

we must couple to an active device – a negative resistance. Since a negative resistance has a positive noise measure or a positive value of λ, any eigenvalue of (137) for λ_i positive may be interpreted as a signal-to-noise ratio at infinite exchangeable power. In particular, if the value of λ_i is the least positive eigenvalue of the characteristic noise matrix of the amplifier, the largest eigenvalue of (137) is the maximum signal-to-noise ratio achievable with this source and amplifier at infinite exchangeable power. This important result may be stated as a theorem.

THEOREM 9: Consider the optimum noise performance of a multiterminal-pair amplifier used with a multiterminal-pair source having an impedance matrix with a positive definite Hermitian part. The optimum noise performance that can be achieved by using these two networks is limited by λ_1, the smallest positive eigenvalue of the amplifier. The maximum signal-to-noise ratio at large exchangeable power is given by the σ_{11}, the largest eigenvalue of the source equation (Eq. 101) for $\mu = -\lambda_1$.

When we investigate parametric devices we shall find, however, that many of our source regions will be indefinite. For such a source region we need a more general criterion. When we assume a value for λ_i in Eq. 137, we imply that we have a resistance with an exchangeable noise power $-\lambda_i$. If we then solve (137) for a given λ_i, we obtain a set of eigenvalues σ_{ij} and a set of eigenvectors $\underset{\sim}{x}_1^{(ij)}$. The eigenvectors tell us that we can reduce the source network with a lossless imbedding to a one-terminal-pair source with an exchangeable signal power $p_{s,ij}$ and an exchangeable signal-to-noise ratio $s_{s,ij}$. If subsequently we combine this reduced source with the resistor whose exchangeable power is $-\lambda_i$, we find that the new values of signal-to-noise ratio, s_o, and exchangeable signal power, p_o, are given by Eq. 138 under the constraint of (139). Thus we see that if it is possible to obtain infinite exchangeable signal power ($1/p_o = 0$) by combining this reduced source and this resistance, the corresponding value of noise-to-signal ratio, $1/s_{o,i\infty}$, in this limit is

$$\frac{1}{s_{o,i\infty}} = \frac{1}{s_{s,ij}} + \frac{\lambda_i}{p_{s,ij}}. \tag{140}$$

Comparing Eq. 140 with Eq. 106, we see that $1/s_{o,i\infty}$ is equal to the reciprocal of the eigenvalue σ_{ij}:

$$\frac{1}{s_{o,i\infty}} = \frac{1}{\sigma_{ij}}. \tag{141}$$

Using (141) in the constraint given by (139), we see that we may obtain infinite exchangeable power, if and only if,

$$\frac{1}{\sigma_{ij}} \geqslant \frac{1}{s_{s,ij}}. \tag{142}$$

Using (142) with (141) in (140), we see that an alternative of this inequality is

$$\frac{\lambda_i}{p_{s,ij}} \geq 0. \tag{143}$$

Another useful form of this inequality may be derived from Eq. 111. In terms of λ, where $\lambda = -\mu$, Eq. 111 is written

$$\frac{1}{p_{s,ij}} = \left[\frac{\partial}{\partial\lambda}\left(\frac{1}{\sigma_{\lambda j}}\right)\right]_{\lambda=\lambda_i}. \tag{144}$$

Hence a third expression equivalent to the inequality (142) is derived from (143) and (144):

$$\left[\lambda \frac{\partial}{\partial\lambda}\left(\frac{1}{\sigma_{\lambda j}}\right)\right]_{\lambda=\lambda_i} \geq 0. \tag{145}$$

We conclude that an eigenvalue of Eq. 137 may be interpreted as an achievable signal-to-noise ratio at infinite exchangeable power only if one of the inequalities (142), (143) or (145) is satisfied. The eigenvalue is the optimum signal-to-noise ratio at infinite exchangeable power only if $1/\sigma_{ij}$ is the minimum value of $1/\sigma_\mu$ for $\mu = -\lambda_i$, and if λ_i is the smallest positive or smallest negative eigenvalue of the characteristic noise matrix of the amplifier. We may, therefore, state the following theorem.

THEOREM 10: Consider the optimum noise performance of a multiterminal-pair amplifier used with a multiterminal-pair source having an impedance matrix with an indefinite Hermitian part. The optimum noise performance that can be achieved may be limited by λ_1 or λ_n, where λ_1 is the smallest positive eigenvalue of the characteristic noise matrix $\underset{\sim}{N}$ of the amplifier, and λ_n is the smallest negative eigenvalue of $\underset{\sim}{N}$. If the performance is limited by one of these eigenvalues, the maximum signal-to-noise ratio at large exchangeable power is given by the largest eigenvalue of the source equation (137) for $\lambda_i = \lambda_1$ or $\lambda_i = \lambda_n$. If neither of these cases yields a realizable signal-to-noise ratio at large exchangeable power, the optimum performance may be achieved without using the amplifier. In this case the maximum signal-to-noise ratio at large exchangeable power is given by the largest eigenvalue of the source equation for some value of λ_i that is greater than λ_n and less than λ_1 (that is, for $\lambda_n < \lambda_i < \lambda_1$, where $\lambda_n < 0$ and $\lambda_1 > 0$).

The optimization presented in section 5.3 can be generalized to include more than one amplifier and lossy imbeddings. In particular, interconnection of any number of independently noisy amplifiers with a given multiterminal-pair noisy source cannot produce a larger signal-to-noise ratio at large exchangeable power than the optimal lossless connection of the best amplifier with the source. This statement can be most readily proved by regarding the imbedding network as a lossless interconnection of its canonical form with each of the amplifiers. We may then regard all of the amplifiers and the set of noisy resistors arising from the canonical representation of the lossy imbedding network as a new amplifier. This new amplifier has as the eigenvalues of its characteristic noise matrix all of the eigenvalues of the characteristic noise matrices

of each of the amplifiers and those of the characteristic noise matrix of the lossy imbedding network. Here, as before, the smallest positive or smallest negative one of these eigenvalues determines the optimum performance, which proves the statement made above.

There is, however, one possible exception to this statement. This exception can occur only for source regions such as those shown in Fig. 35c, and only under special conditions. If the canonical form of the dissipative imbedding network contains a resistor at a temperature T_d, such that the equivalent λ for this resistor, which is $\lambda_d = -kT_d\Delta f$, is smaller than the smallest negative eigenvalue of the characteristic noise matrix of any of the amplifiers, the best signal-to-noise ratio at large exchangeable power can be achieved only by using the dissipative imbedding network with the source and none of the amplifiers.

5.5 EXAMPLE OF THE OPTIMUM PERFORMANCE OF AN AMPLIFIER WITH A TWO-TERMINAL-PAIR SOURCE

To illustrate the principles that have just been described, we shall consider a simple example. The simplest example for which these principles are necessary is that of the two-terminal-pair source network shown in Fig. 36. We shall assume that this source

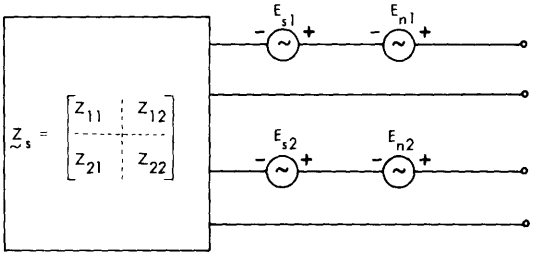

Fig. 36. Source network for example.

network contains only coherent signal generators. Then statistical averaging is unnecessary; $\overline{E_{s1}E_{s2}^*} = E_{s1}E_{s2}^*$. The signal-voltage matrix $\overline{\underset{\sim}{E}_s\underset{\sim}{E}_s^\dagger}$ is given explicitly:

$$\overline{\underset{\sim}{E}_s\underset{\sim}{E}_s^\dagger} \begin{bmatrix} |E_{s1}|^2 & E_{s1}E_{s2}^* \\ E_{s1}^*E_{s2} & |E_{s2}|^2 \end{bmatrix}. \tag{146}$$

The noise-voltage matrix, $\overline{\underset{\sim}{E}_n\underset{\sim}{E}_n^\dagger}$, is written explicitly

$$\overline{\underset{\sim}{E}_n\underset{\sim}{E}_n^\dagger} \begin{bmatrix} \overline{|E_{n1}|^2} & \overline{E_{n1}E_{n2}^*} \\ \overline{E_{n1}^*E_{n2}} & \overline{|E_{n2}|^2} \end{bmatrix}. \tag{147}$$

The impedance matrix is

$$\underset{\sim}{Z}_s = \left[\begin{array}{c:c} Z_{11} & Z_{12} \\ \hdashline Z_{12} & Z_{22} \end{array}\right]. \tag{148}$$

So the matrix $\underset{\sim}{Z}_s + \underset{\sim}{Z}_s^\dagger$ is given by

$$\underset{\sim}{Z}_s + \underset{\sim}{Z}_s^\dagger = 2\left[\begin{array}{c:c} R_{11} & Z'_{12} \\ \hdashline Z'^{*}_{12} & R_{22} \end{array}\right], \tag{149}$$

where R_{11} is the real part of Z_{11}, R_{22} is the real part of Z_{22}, and $Z'_{12} = (1/2)\left(Z_{12}+Z^*_{21}\right)$. We shall restrict ourselves to the case for which $\underset{\sim}{Z}_s + \underset{\sim}{Z}_s^\dagger$ is positive definite. The positive definiteness of this matrix ensures that

$$R_{11} > 0,\ R_{22} > 0 \qquad R_{11}R_{22} - |Z'_{12}|^2 > 0. \tag{150}$$

We do not assume that the source network is necessarily reciprocal. If it were reciprocal, we would have $Z_{12} = Z_{21}$, and $Z'_{12} = \mathrm{Re}\,[Z_{12}]$.

Furthermore, we assume that we are using this source with a multiterminal-pair amplifier. The smallest positive eigenvalue of the characteristic noise matrix of this amplifier is λ_1. If we realize the optimum network in the form shown in Fig. 29 we are essentially using the amplifier as a two-terminal-pair amplifier with a one-terminal-pair source. In accordance with Eq. 87 or Eq. 59, we define the optimum noise measure of this amplifier as

$$M_{e,\,opt} = \frac{\lambda_1}{kT_o\Delta f} \tag{151}$$

In Section VI we shall show that it is always possible to define a noise measure regardless of the form of the realization, and that the achievable optimum noise measure is $M_{e,\,opt}$.

Even for the simple source network described above, a complete description of the source region in general terms is extremely difficult to give and not particularly illuminating. For this reason, we shall derive only the optimum signal-to-noise ratio that can be achieved at infinite exchangeable power with the amplifier used. Since the source has a positive definite $\underset{\sim}{Z}_s + \underset{\sim}{Z}_s^\dagger$ matrix and λ_1 is positive, any solution to Eq. 137 for $\lambda_i = \lambda_1$ will be a realizable signal-to-noise ratio at infinite exchangeable power.

The eigenvalues of (137) are the eigenvalues of the matrix $\left[\overline{\underset{\sim}{E}_n\underset{\sim}{E}_n^\dagger} + 2\lambda_1\left(\underset{\sim}{Z}_s+\underset{\sim}{Z}_s^\dagger\right)\right]^{-1}\overline{\underset{\sim}{E}_s\underset{\sim}{E}_s^\dagger}$. For the source under consideration, the matrix $\overline{\underset{\sim}{E}_s\underset{\sim}{E}_s^\dagger}$ is of rank one; that is, its determinant is zero. The rank of the matrix $\left[\overline{\underset{\sim}{E}_n\underset{\sim}{E}_n^\dagger} + 2\lambda_1\left(\underset{\sim}{Z}_s+\underset{\sim}{Z}_s^\dagger\right)\right]^{-1}\overline{\underset{\sim}{E}_s\underset{\sim}{E}_s^\dagger}$ cannot be greater than the rank of its factors, so it also must be of rank one. From matrix theory we know that the trace (the sum of the diagonal elements) of a matrix is equal to the sum

of its eigenvalues, and a matrix of rank one has only one nonzero eigenvalue. Hence, for this example the one eigenvalue of (137) can be obtained either by solving (137) or, more simply, by computing the trace of the matrix $\left[\overline{\underset{\sim}{E}_n\underset{\sim}{E}_n^\dagger}+2\lambda\left(\underset{\sim}{Z}_s+\underset{\sim}{Z}_s^\dagger\right)\right]^{-1}\overline{\underset{\sim}{E}_s\underset{\sim}{E}_s^\dagger}$. With either method we find that the eigenvalue of (137), which corresponds to the maximum signal-to-noise ratio at large exchangeable power, is given by

$$\sigma_{11}=\frac{|E_{s1}|^2\left[\overline{|E_{n2}|^2}+4\lambda_1 R_{22}\right]+|E_{s2}|^2\left[\overline{|E_{n1}|^2}+4\lambda_1 R_{11}\right]-2\,\mathrm{Re}\left[E_{s1}^*E_{s2}\left(\overline{E_{n1}E_{n2}^*}+4\lambda_1 Z_{12}'\right)\right]}{\left[\overline{|E_{n1}|^2}+4\lambda_1 R_{11}\right]\left[\overline{|E_{n2}|^2}+4\lambda_1 R_{22}\right]-\left|\overline{E_{n1}E_{n2}^*}+4\lambda_1 Z_{12}'\right|^2}. \tag{152}$$

Equation 152 does not lend itself to simple discussions; therefore, we shall consider some special cases that are more meaningful. For these cases we define the quantities

$$\left.\begin{aligned} S_1&=\frac{|E_{s1}|^2}{4R_{11}}\\ N_1&=\frac{\overline{|E_{n1}|^2}}{4R_{11}}\\ S_2&=\frac{|E_{s2}|^2}{4R_{22}}\\ N_2&=\frac{\overline{|E_{n2}|^2}}{4R_{22}}\\ N_{12}&=\frac{\overline{E_{n1}E_{n2}^*}}{4R_{11}R_{22}}\end{aligned}\right\} \tag{153}$$

The quantity S_1 is the exchangeable signal power at the first terminal pair of the source shown in Fig. 36 when the second terminal pair is open-circuited; N_1 is the exchangeable noise power at this terminal pair under the same conditions. Similarly, S_2 and N_2 are the exchangeable signal power and the exchangeable noise power at the second terminal pair of the source shown in Fig. 36 when the first terminal pair is open-circuited. The quantity N_{12} is related to the correlation between the two noise voltages, and satisfies the inequality.

$$N_1N_2\geq|N_{12}|^2. \tag{154}$$

Case a: Consider the case in which only one signal voltage is present, the noise voltages are uncorrelated, and there is no transfer impedance Z'_{12}. For this case $\left(E_{s2} = 0, \overline{E_{n1}E_{n2}^*} = 0, Z'_{12} = 0\right)$, we find

$$\sigma_{11} = \frac{|E_{s1}|^2}{\overline{|E_{n1}|^2} + 4\lambda_1 R_{11}} \tag{155}$$

or, in terms of the quantities in (153) and (151),

$$\sigma_{11} = \frac{S_1}{N_1 + \lambda_1} = \frac{S_1}{N_1 + kT_o \Delta f M_{e,opt}}. \tag{156}$$

Comparing Eq. 156 with Eq. 86, we see that this is just the optimum signal-to-noise ratio that can be achieved with the given amplifier by combining it with the one-terminal-pair source consisting of the first terminal pair of the given source. This is exactly what we would expect because, under the given assumptions, the second terminal pair of the source is just an independently noisy positive resistance. If the noise of this second resistance is partially correlated with the noise of the first, we have the situation described by a second case.

Case b: In this case we also have only one signal voltage, and no transfer impedance Z'_{12}. That is, $E_{s2} = 0$, $Z'_{12} = 0$. Equation 152 becomes

$$\sigma_{11} = \frac{|E_{s1}|^2}{\overline{|E_{n1}|^2} + 4\lambda_1 R_{11}} \left[\frac{1}{1 - \frac{\overline{|E_{n1}E_{n2}^*|^2}}{\left[\overline{|E_{n1}|^2} + 4\lambda_1 R_{11}\right]\left[\overline{|E_{n2}|^2} + 4\lambda_1 R_{22}\right]}} \right]$$

$$\sigma_{11} = \frac{S_1}{N_1 + \lambda_1} \left[\frac{1}{1 - \frac{|N_{12}|^2}{(N_1+\lambda_1)(N_2+\lambda_1)}} \right]. \tag{157}$$

Comparing this signal-to-noise ratio with that obtained for Case a (Eq. 156), we see that the signal-to-noise ratio that is achievable at large exchangeable power may be improved if the two noise sources in the source network are partially correlated. This is to be expected because correlation between the noise voltages implies that we can use the noise of the resistor at the second terminal pair of the source to cancel part of the noise appearing at the first terminal pair, thereby improving the quality of the signal source driving the amplifier. The signal-to-noise ratio is improved by a factor equal to the quantity in brackets in Eq. 157. This factor is greater than unity for any value of correlation or N_{12}; it is a monotonically increasing function of $|N_{12}|$, reaching

its maximum value when the noise voltages are completely correlated $\left(N_1N_2 = |N_{12}|^2\right)$.

Case c: Another interesting case is encountered where there is only one signal voltage and the source noise is thermal at a temperature T_s. For this case, $\overline{\underset{\sim}{E}_n\underset{\sim}{E}_n^\dagger} = 2kT_s\Delta f\left(\underset{\sim}{Z}_s+\underset{\sim}{Z}_s^\dagger\right)$, and Eq. 152 becomes

$$\sigma_{11} = \frac{|E_{s1}|^2}{\overline{|E_{n1}|^2} + 4\lambda_1 R_{11}}\left[\frac{1}{1 - \dfrac{|Z'_{12}|^2}{R_{11}R_{22}}}\right]$$

$$\sigma_{11} = \frac{S_1}{N_1 + \lambda_1}\left[\frac{1}{1 - \dfrac{|Z'_{12}|^2}{R_{11}R_{22}}}\right] \tag{158}$$

The optimum signal-to-noise ratio achievable at large exchangeable power given by (158) is better for this case than for the case in which the noises are uncorrelated (Eq. 156) if Z'_{12} is not zero. If the source were reciprocal ($Z_{12}=Z_{21}$), we could have derived this result from a different standpoint. If the noise is thermal, the exchangeable noise power at the first terminal pair of the source is independent of any lossless loading of the second terminal pair. It can be seen, however, that lossless loadings of the second terminal pair of the source network do affect the real part of the impedance looking into the first terminal pair. If we attach a lossless element to the second terminal pair of the source, we can vary this to minimize the real part of the impedance looking into the first terminal pair. This minimum resistance is $R_{11} - \left(R_{12}^2/R_{22}\right)$, where R_{12} is the real part of $Z_{12} = Z_{21}$. Since the exchangeable signal power S_1 is inversely proportional to the resistance at this terminal pair, we would expect the signal-to-noise ratio for this case to be better than that of Case a by a factor of $1/\left(1 - R_{12}^2/R_{11}R_{22}\right)$; and this is just what we find. (For a nonreciprocal source impedance network a more general imbedding network must be considered; the net result is the same.)

Case d: The last case that we shall consider is that in which signal is present at both terminal pairs of the source, the noise voltages appearing at the two-terminal pairs are uncorrelated, and the transfer impedance, Z_{12}, is zero. Making use of these conditions in the expression (152), we find that the optimum signal-to-noise ratio at large exchangeable power is

$$\sigma_{11} = \frac{S_1}{N_1 + \lambda_1} + \frac{S_2}{N_2 + \lambda_1}$$

$$\sigma_{11} = \frac{S_1}{N_1 + kT_o\Delta fM_{e,opt}} + \frac{S_2}{N_2 + kT_o\Delta fM_{e,opt}}. \tag{159}$$

This is a very interesting result and can be obtained by taking a different viewpoint. We notice that the currents flowing in the two-terminal pairs of the source are uncoupled for this case. Consequently, we can attach to the first terminal pair an amplifier with large exchangeable gain and a noise measure $M_{e,opt}$. The exchangeable signal-to-noise ratio at the output is given by the first term of Eq. 159 or by Eq. 156. We can attach another identical amplifier with large exchangeable gain and the same noise measure to the second terminal pair. The exchangeable signal-to-noise ratio at the output of this second amplifier is given by the second term in (159). The noise voltages at the outputs of these two amplifiers are uncorrelated and the signals are completely correlated. Equation 159 tells us that the best signal-to-noise ratio that can be achieved is equal to the sum of the two signal-to-noise ratios appearing at the outputs of the two amplifiers. (The output exchangeable power of the combination is still large.) This is a well-known result.[8]

Other cases could be considered, but they are more complicated and do not really show anything new. Also, since we can simultaneously diagonalize two matrices one of which is positive definite, we can transform any two-terminal-pair source with coherent signal voltages and positive definite $\underset{\sim}{Z}_s + \underset{\sim}{Z}_s^\dagger$ matrix into a new source that is covered by Case d. We do this by imbedding the source in a lossless four-terminal-pair network to obtain a new network whose matrices $\underset{\sim}{Z}'_s + \underset{\sim}{Z}_s'^\dagger$ and $\overline{\underset{\sim}{E}'_n \underset{\sim}{E}_n'^\dagger}$ are diagonal (see Eqs. 23 and 24). In any event, the solution to the general problem is given by the expression in Eq. 152.

VI. CHARACTERIZATION OF THE NOISE PERFORMANCE OF MULTITERMINAL AMPLIFIERS

In Section V we were concerned with the optimum noise performance of a multiterminal amplifier used with a multiterminal source. Now we shall define and evaluate the noise performance of a prescribed system consisting of a source network connected to an amplifying network with one output terminal pair as shown in Fig. 37a. We shall show that it is possible to define a meaningful noise figure, noise measure, and exchangeable gain for such an amplifier. For two-terminal-pair devices this is done in the generally accepted way of comparing output parameters with source parameters. For such a device this approach is not possible because the source is characterized by a whole region of parameters. We shall show, however, that we can define meaningful criteria for amplifier performance by comparing the output parameters with the parameters of an equivalent source network. This equivalent source is a one-terminal-pair source derived from the m-terminal-pair source by imbedding it in a lossless network; this lossless network combines the source voltages in a way that is similar to the way in which the amplifier combines them. Thus we shall compare the performance of the amplifier (its noise-to-signal ratio and exchangeable signal power) with the performance of an equivalent "lossless amplifier" – the equivalent source network.

We shall first describe the source-amplifier system. Then for comparison we shall introduce two other systems in which some, or all, noise sources have been removed. One of these systems contains the ideal noiseless equivalent of the actual amplifier; the other system is the equivalent reduced source. We derive expressions for the exchangeable signal power and signal-to-noise ratio of each of these three systems. We define the equivalent reduced source of the amplifier and discuss the significance of using this source as a basis of comparison.

Next, we use these ideas to give generalized definitions for noise figure, noise measure, and exchangeable gain which are logical extensions of the usual definitions for two-terminal-pair amplifiers. We interpret these quantities in the noise-performance plane to show that they are directly related to the quantities that were defined for a two-terminal-pair amplifier in section 3.1. We also show that if we have a cascade of multiterminal amplifiers, we can define a noise figure for each stage in the cascade. The noise figure of the over-all amplifier is given by the usual formula for the noise figure of amplifiers in cascade.

Finally, we describe a simple method for determining each of the above-mentioned quantities. Also, we determine the additional information that must be known, and/or the additional measurements that must be made in order to completely specify the noise-to-signal ratio and the exchangeable signal power at the output.

6.1 BASES OF COMPARISON

The system that we shall evaluate is shown in Fig. 37a, in which a linear noisy m-terminal-pair signal source is connected to an (m+1)-terminal-pair amplifier. The

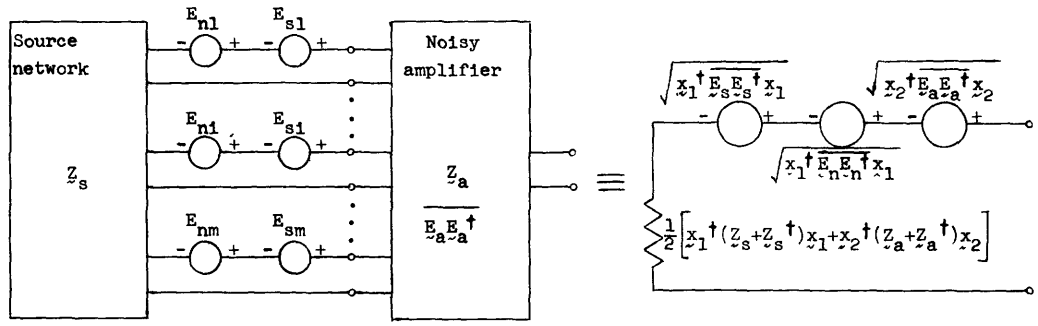

(a) Amplifying system

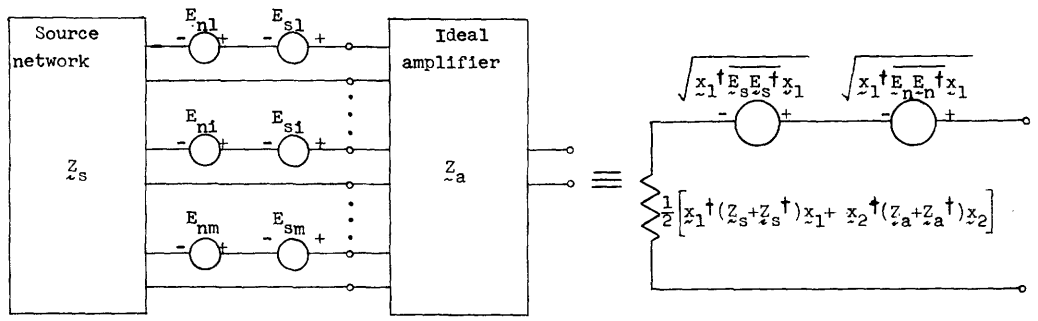

(b) Ideal amplifying system

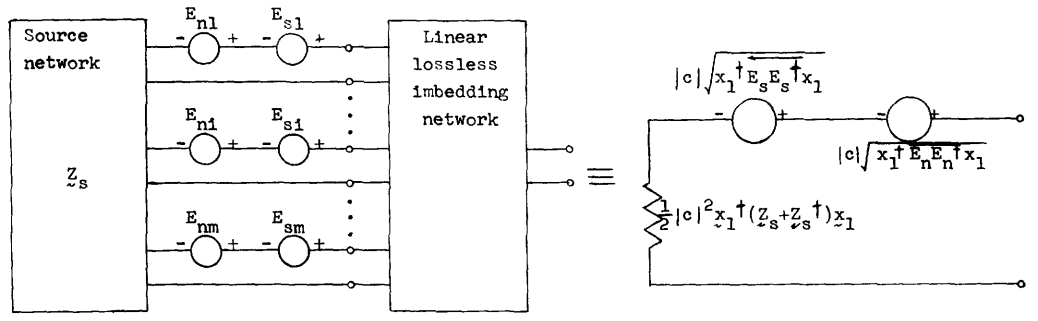

(c) Equivalent reduced source

Fig. 37. Amplifying systems for comparison.

Thévenin equivalent of this system is also shown. We shall also describe two noiseless parallels to this system – one that includes "gain," and another that does not. We shall refer to the last system as the "equivalent reduced source." We shall derive expressions for the signal-to-noise ratio and exchangeable signal power at the outputs of each of these systems. These expressions will be useful when noise figure, exchangeable-power gain, and noise measure are defined by comparing the actual system with the equivalent reduced source.

In Fig. 37b we show the system of Fig. 37a with the amplifier replaced by an ideal amplifier. The ideal amplifier is identical to the amplifier shown in Fig. 37a, except that is has no internal noise sources. The Thévenin equivalent for this system is also shown. The system shown in Fig. 37c, together with its Thévenin equivalent, is the equivalent reduced source. This system is derived from the system of Fig. 37a by replacing the amplifier with a lossless network that combines the voltages of the source network in a similar way as the amplifier. We shall discuss the equivalent reduced source in more detail when we discuss its noise-to-signal ratio and its exchangeable signal power.

The source network in Fig. 37 is characterized by its impedance matrix, $\underset{\sim}{Z}_s$; by the cross-power spectral-density matrix of its open-circuit signal voltages, $\overline{\underset{\sim}{E}_s\underset{\sim}{E}_s^\dagger}$; and by the cross-power spectral-density matrix of its open-circuit noise voltages $\overline{\underset{\sim}{E}_n\underset{\sim}{E}_n^\dagger}$. The amplifier is characterized by its impedance matrix $\underset{\sim}{Z}_a$, and by the cross-power spectral-density matrix of its open-circuit noise voltages, $\overline{\underset{\sim}{E}_a\underset{\sim}{E}_a^\dagger}$. We shall show that when two such networks are connected in a linear lossless manner the exchangeable signal power and signal-to-noise ratio at an output must be expressible in the forms

$$p_o = \frac{\underset{\sim}{x}_1^\dagger \overline{\underset{\sim}{E}_s\underset{\sim}{E}_s^\dagger}\, \underset{\sim}{x}_1}{2\underset{\sim}{x}_1^\dagger\left(\underset{\sim}{Z}_s+\underset{\sim}{Z}_s^\dagger\right)\underset{\sim}{x}_1 + 2\underset{\sim}{x}_2^\dagger\left(\underset{\sim}{Z}_a+\underset{\sim}{Z}_a^\dagger\right)\underset{\sim}{x}_2} \tag{160}$$

and

$$s_o = \frac{\underset{\sim}{x}_1^\dagger \overline{\underset{\sim}{E}_s\underset{\sim}{E}_s^\dagger}\, \underset{\sim}{x}_1}{\underset{\sim}{x}_1^\dagger \overline{\underset{\sim}{E}_n\underset{\sim}{E}_n^\dagger}\, \underset{\sim}{x}_1 + \underset{\sim}{x}_2^\dagger \overline{\underset{\sim}{E}_a\underset{\sim}{E}_a^\dagger}\, \underset{\sim}{x}_2}, \tag{161}$$

respectively. The interconnection of the source and amplifier in Fig. 37a is of this kind. Hence its output exchangeable signal power and signal-to-noise ratio are given by (160) and (161). For the interconnection shown the components of the vectors $\underset{\sim}{x}_1$ and $\underset{\sim}{x}_2$ are functions only of the elements of the matrices $\underset{\sim}{Z}_s$ and $\underset{\sim}{Z}_a$.

It should be pointed out that there is an arbitrary normalization in these expressions. That is, if we multiply both the vector $\underset{\sim}{x}_1$ and the vector $\underset{\sim}{x}_2$ by the same arbitrary complex constant, neither the exchangeable signal power, p_o, nor the signal-to-noise ratio,

s_o, is changed. We may remove this arbitrariness by identifying the quantity of $\underset{\sim}{x}_1^\dagger \overline{\underset{\sim}{E}_s \underset{\sim}{E}_s^\dagger}\, \underset{\sim}{x}_1$ as the mean-square signal voltage at the output of the system of Fig. 37a. This means that the real part of the output impedance of the system is given by $\frac{1}{2}\left[\underset{\sim}{x}_1^\dagger\left(\underset{\sim}{Z}_s+\underset{\sim}{Z}_s^\dagger\right)\underset{\sim}{x}_1+\underset{\sim}{x}_2^\dagger\left(\underset{\sim}{Z}_a+\underset{\sim}{Z}_a^\dagger\right)\underset{\sim}{x}_2\right]$, the contribution of the noise generators in the source network to the mean-square noise voltage at the output is $\underset{\sim}{x}_1^\dagger \overline{\underset{\sim}{E}_n \underset{\sim}{E}_n^\dagger}\, \underset{\sim}{x}_1$, and the contribution of the noise generators in the amplifier to the mean-square noise voltage at the output is $\underset{\sim}{x}_2^\dagger \overline{\underset{\sim}{E}_a \underset{\sim}{E}_a^\dagger}\, \underset{\sim}{x}_2$.

From the form of (160) and (161) we see that the components of the vector $\underset{\sim}{x}_1$ may be interpreted as voltage transfer ratios relating the open-circuit voltages of the source to the open-circuit voltage at the output. It is apparent that for the system of Fig. 37a these ratios are all measurable. For instance, the first component of $\underset{\sim}{x}_1$ is the ratio of the portion of the open-circuit voltage at the output, which is due to the open-circuit voltage at the first terminal pair of the source network, to the open-circuit voltage at the first terminal pair of the source network. Thus with all sources in the system of Fig. 37a dead or accounted for, we may determine x_{11}, the first component of $\underset{\sim}{x}_1$, by introducing a voltage e_1 in series with the first terminal pair of the source network. The complex open-circuit voltage appearing at the output terminal pair because of this voltage is $x_{11}e_1$. The other components of the vector $\underset{\sim}{x}_1$ are similarly defined.

Now let us consider the equivalent reduced source. The equivalent reduced source combines the open-circuit voltages of the multiterminal-pair source in a similar way as the amplifier does. Thus the lossless network of Fig. 37c must have a set of voltage-transfer ratios y_i that are proportional to the voltage-transfer ratios x_{1i} of the amplifier. Defining the vector

$$\underset{\sim}{y} = c\underset{\sim}{x}_1, \tag{162}$$

where c is a complex number, we find that the mean-square signal voltage at the output of the equivalent reduced source is $\underset{\sim}{y}^\dagger \overline{\underset{\sim}{E}_s \underset{\sim}{E}_s^\dagger}\, \underset{\sim}{y}$. By analogy (Eqs. 94 and 95), we conclude that the exchangeable signal power and signal-to-noise ratio at the output of the equivalent reduced source are

$$p_s = \frac{\underset{\sim}{y}^\dagger \overline{\underset{\sim}{E}_s \underset{\sim}{E}_s^\dagger}\, \underset{\sim}{y}}{2\underset{\sim}{y}^\dagger\left(\underset{\sim}{Z}_s+\underset{\sim}{Z}_s^\dagger\right)\underset{\sim}{y}} = \frac{\underset{\sim}{x}_1^\dagger \overline{\underset{\sim}{E}_s \underset{\sim}{E}_s^\dagger}\, \underset{\sim}{x}_1}{2\underset{\sim}{x}_1^\dagger\left(\underset{\sim}{Z}_s+\underset{\sim}{Z}_s^\dagger\right)\underset{\sim}{x}_1} \tag{163}$$

and

$$s_s = \frac{\underset{\sim}{y}^\dagger \overline{\underset{\sim}{E}_s \underset{\sim}{E}_s^\dagger}\, \underset{\sim}{y}}{\underset{\sim}{y}^\dagger \overline{\underset{\sim}{E}_n \underset{\sim}{E}_n^\dagger}\, \underset{\sim}{y}} = \frac{\underset{\sim}{x}_1^\dagger \overline{\underset{\sim}{E}_s \underset{\sim}{E}_s^\dagger}\, \underset{\sim}{x}_1}{\underset{\sim}{x}_1^\dagger \overline{\underset{\sim}{E}_n \underset{\sim}{E}_n^\dagger}\, \underset{\sim}{x}_1}. \tag{164}$$

By adjusting the lossless network in Fig. 37c, we may realize any vector $\underset{\sim}{y}$. By adjusting

the constant c in (162) we are merely adjusting the impedance level of the equivalent reduced source; however, the impedance levels in a system are usually prescribed. That is, the impedance looking into the source is usually the same as that looking into the output. Therefore we shall arbitrarily fix the impedance level of the equivalent reduced source so that the real part of its impedance is the same as the real part of the output impedance of the amplifier. If the system has an output impedance with a negative real part, and if the source network is passive, this condition cannot be satisfied. But we can make the output resistance of the equivalent reduced source equal to the magnitude of the output resistance of the amplifying system; this is an arbitrary, but convenient, normalization. Comparing (163) with (160), we see that the constant c must be given by

$$|c|^2 = \left| 1 + \frac{\underset{\sim}{x}_2^\dagger \left(\underset{\sim}{Z}_a + \underset{\sim}{Z}_a^\dagger\right) \underset{\sim}{x}_2}{\underset{\sim}{x}_1^\dagger \left(\underset{\sim}{Z}_s + \underset{\sim}{Z}_s^\dagger\right) \underset{\sim}{x}_1} \right|. \tag{165}$$

Thus we define the equivalent reduced source of an amplifying system as follows: The equivalent reduced source of a linear amplifying system with a single output is the one-terminal-pair source that is obtained when the amplifier is replaced by a linear lossless network that combines the open-circuit voltages of the source into a single-output terminal pair in the same ratio as the amplifier combines these voltages into its output terminal pair. The impedance level of the equivalent reduced source is such that the real part of its output impedance has the same magnitude as the magnitude of the real part of the output impedance of the amplifying system.

The ideal amplifying system shown in Fig. 37b is identical to the original amplifying system, except for the absence of amplifier noise. It is apparent, then, that the exchangeable signal power for this system is given by p_o in Eq. 160, and that the signal-to-noise ratio is given by s_s in Eq. 164. The points defined in the noise-performance plane by the three systems of Fig. 37 are shown in Fig. 38.

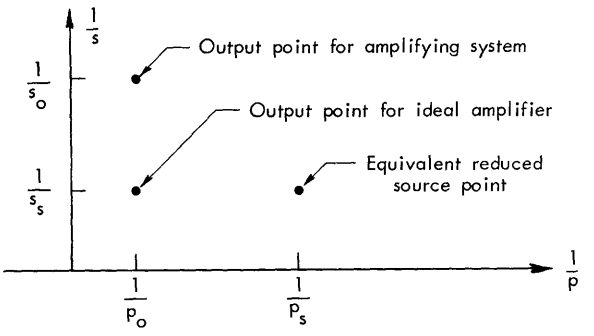

Fig. 38. Points determined in the noise-performance plane by the three systems in Fig. 37.

We shall give definitions for noise figure, exchangeable-power gain, and noise measure by comparing the actual amplifying system with its equivalent reduced source. This is a reasonable comparison for several reasons. Since the imbedding network of the equivalent reduced source is lossless, it conserves power at all frequencies. It seems reasonable, therefore, to regard the reduced source as equivalent to the amplifying system in the absence of amplifier gain and noise. On

this basis, any increase in the noise-to-signal ratio above that of the reduced source is attributable to the addition of noise in the amplification process, and any increase in the exchangeable signal power at the output of the amplifying system over the exchangeable signal power of the reduced source is attributable to the gain of the amplifier.

Thus we see that in comparing the amplifying system with the reduced source we are separating the voltage-combining process of the amplifier from the gain or amplification process. We are charging against the amplifier only the noise that it adds in producing gain. This separation of voltage-combining functions and amplification functions appears explicitly in the realization of Fig. 29. In order to evaluate the question of how near a system has come to being optimum we must not only compare its noise measure with its optimum noise measure, but we must also see where the point determined in the noise-performance plane by the equivalent reduced source lies with respect to the outer boundary of the source region. This comparison tells us how much we can improve the performance of a given amplifier by changing its voltage-combining operations (at constant noise measure) to accommodate a given distribution of noise and signal sources in the source network.

6.2 GENERALIZED DEFINITIONS OF NOISE FIGURE, EXCHANGEABLE-POWER GAIN, AND NOISE MEASURE

We shall define the noise figure, equivalent exchangeable gain, and the noise measure of the amplifying device shown in Fig. 37a. We shall also investigate the interpretation of these parameters in the noise-performance plane. We shall compare the output point whose coordinates are specified by the reciprocals of the output parameters given in (160) and (161) with the equivalent input point whose coordinates are specified by the reciprocals of the parameters of the equivalent reduced source as given in (163) and (164) (see Fig. 38). For a one-terminal-pair source used with a two-port amplifier, or an m-terminal-pair source that has been losslessly reduced to a one-terminal-pair source before being used with the amplifier, the point defined by the equivalent reduced source is identical to that defined by the actual source or input network.

(a) Noise Figure

The noise figure, at a specified output frequency, is defined as the ratio of the total noise power per unit bandwidth exchangeable at the output port when the only source of noise in the source network is thermal noise at standard temperature (T_o=290°K) to that portion of the total noise power engendered at this frequency by the thermal noise of the source.

Let us express this in terms of the quantities in Eqs. 160, 161, 163, and 164. If the noise sources in the source network are thermal at temperature T_o, $\overline{\underset{\sim}{E}_n \underset{\sim}{E}_n^\dagger} = 2kT_o\Delta f\left(\underset{\sim}{Z}_s+\underset{\sim}{Z}_s^\dagger\right)$. Then the total noise power per unit bandwidth exchangeable at the output port, when the only source of noise present in the source network is thermal

noise, is

$$N_T = \frac{1}{\Delta f} \frac{2kT_o \Delta f \, \underset{\sim}{x}_1^\dagger \left(\underset{\sim}{Z}_s + \underset{\sim}{Z}_s^\dagger\right) \underset{\sim}{x}_1 + \underset{\sim}{x}_2^\dagger \overline{\underset{\sim}{E}_a \underset{\sim}{E}_a^\dagger} \, \underset{\sim}{x}_2}{2\underset{\sim}{x}_1^\dagger \left(\underset{\sim}{Z}_s + \underset{\sim}{Z}_s^\dagger\right) \underset{\sim}{x}_1 + 2\underset{\sim}{x}_2^\dagger \left(\underset{\sim}{Z}_a + \underset{\sim}{Z}_a^\dagger\right) \underset{\sim}{x}_2}. \tag{166}$$

The portion of the power of (166) resulting solely from the thermal noise of the source is

$$N_o = \frac{1}{\Delta f} \frac{2kT_o \Delta f \, \underset{\sim}{x}_1^\dagger \left(\underset{\sim}{Z}_s + \underset{\sim}{Z}_s^\dagger\right) \underset{\sim}{x}_1}{2\underset{\sim}{x}_1^\dagger \left(\underset{\sim}{Z}_s + \underset{\sim}{Z}_s^\dagger\right) \underset{\sim}{x}_1 + 2\underset{\sim}{x}_2^\dagger \left(\underset{\sim}{Z}_a + \underset{\sim}{Z}_a^\dagger\right) \underset{\sim}{x}_2}. \tag{167}$$

The exchangeable noise figure is given by (166) divided by (167):

$$F_e = 1 + \frac{1}{kT_o \Delta f} \frac{\underset{\sim}{x}_2^\dagger \overline{\underset{\sim}{E}_a \underset{\sim}{E}_a^\dagger} \, \underset{\sim}{x}_2}{2\underset{\sim}{x}_1^\dagger \left(\underset{\sim}{Z}_s + \underset{\sim}{Z}_s^\dagger\right) \underset{\sim}{x}_1} \tag{168}$$

and the excess exchangeable noise figure is

$$F_e - 1 = \frac{1}{kT_o \Delta f} \frac{\underset{\sim}{x}_2^\dagger \overline{\underset{\sim}{E}_a \underset{\sim}{E}_a^\dagger} \, \underset{\sim}{x}_2}{2\underset{\sim}{x}_1^\dagger \left(\underset{\sim}{Z}_s + \underset{\sim}{Z}_s^\dagger\right) \underset{\sim}{x}_1}. \tag{169}$$

From Eqs. 161 and 164, we have

$$\frac{1}{s_o} - \frac{1}{s_s} = \frac{\underset{\sim}{x}_2^\dagger \overline{\underset{\sim}{E}_a \underset{\sim}{E}_a^\dagger} \, \underset{\sim}{x}_2}{\underset{\sim}{x}_1^\dagger \overline{\underset{\sim}{E}_s \underset{\sim}{E}_s^\dagger} \, \underset{\sim}{x}_1} \tag{170}$$

and from this and Eq. 163 we see that we may write (169)

$$F_e - 1 = \frac{1}{kT_o \Delta f} \frac{\frac{1}{s_o} - \frac{1}{s_s}}{\frac{1}{p_s}}. \tag{171}$$

This is identical to the expression for the noise figure for a two-terminal-pair amplifier given in Eq. 57.

(b) Equivalent Exchangeable-Power Gain

The equivalent exchangeable-power gain is defined as the ratio of the exchangeable signal power at the output terminal pair to the exchangeable signal power of the equivalent reduced source. This gives

$$G_e = \frac{p_o}{p_s} = \frac{\frac{1}{p_s}}{\frac{1}{p_o}}, \tag{172}$$

or, from Eqs. 160 and 163,

$$G_e = \frac{\underset{\sim}{x}_1^\dagger \left(\underset{\sim}{Z}_s + \underset{\sim}{Z}_s^\dagger\right) \underset{\sim}{x}_1}{\underset{\sim}{x}_1^\dagger \left(\underset{\sim}{Z}_s + \underset{\sim}{Z}_s^\dagger\right) \underset{\sim}{x}_1 + \underset{\sim}{x}_2^\dagger \left(\underset{\sim}{Z}_a + \underset{\sim}{Z}_a^\dagger\right) \underset{\sim}{x}_2}. \tag{173}$$

(c) Noise Measure

We can give two definitions for noise measure. One, based on two previous definitions, is that the noise measure of an amplifier is equal to the excess exchangeable noise figure divided by unity minus the reciprocal of the equivalent exchangeable power gain. That is,

$$M_e = \frac{F_e - 1}{1 - \frac{1}{G_e}}. \tag{174}$$

Using (169) and (173) in (174) we may also write

$$M_e = \frac{1}{kT_o\Delta f}\left[-\frac{\underset{\sim}{x}_2^\dagger \overline{\underset{\sim}{E}_a \underset{\sim}{E}_a^\dagger}\, \underset{\sim}{x}_2}{\underset{\sim}{x}_2^\dagger \left(\underset{\sim}{Z}_a + \underset{\sim}{Z}_a^\dagger\right) \underset{\sim}{x}_2}\right]. \tag{175}$$

But in terms of the quantities in Eqs. 160-164 this may be written

$$M_e = \frac{1}{kT_o\Delta f}\left[-\frac{\frac{1}{s_o} - \frac{1}{s_s}}{\frac{1}{p_o} - \frac{1}{p_s}}\right]. \tag{176}$$

Equation 176 is a mathematical statement of another definition of noise measure described in section 3. 1.

The noise measure of an amplifier is equal to the difference in the noise-to-signal ratio at the output and the noise-to-signal ratio of the equivalent reduced source divided by the reciprocal of the exchangeable signal power of the source minus the reciprocal of the exchangeable signal power at the output when this ratio is normalized to $kT_o\Delta f$ (the exchangeable power of a resistor at standard temperature over the same output bandwidth). Again we see that the expression for the noise measure of a multiterminal-pair amplifier agrees with that of a two-terminal-pair amplifier as given in Eq. 59. Also, we see from Eqs. 171, 172, and 176 that the noise figure of an amplifier approaches the noise measure of this amplifier as the exchangeable gain approaches infinity, or as $1/p_o$ approaches zero.

It should be pointed out that the three quantities that we have defined, exchangeable noise figure, equivalent exchangeable power gain, and noise measure, are independent of the actual noise and signal voltages present in the source network. This is evident from Eqs. 169, 173, and 175, respectively. Thus we only have to specify $\underset{\sim}{Z}_s$, the

impedance matrix of the source network, in order to evaluate these parameters. This is also true for two-terminal-pair amplifiers. For instance, a radio receiver (two-terminal-pair network) connected to an antenna has a perfectly well-defined noise figure. The quality of the receiver output (its signal-to-noise ratio) depends on whether the antenna is directed toward a source of signal. While a misdirected antenna will adversely affect the output signal-to-noise ratio, we do not charge this effect against the receiver. Similarly, for a generalized multiterminal-pair source there is a best way to combine the signal and noise voltages for use with a given amplifier as we have shown. The viewpoint that we have taken in defining noise figure, noise measure, and exchangeable gain is that we can always describe a nonoptimum combination of the source voltages as a poor utilization of the source. To evaluate the manner in which we are using the source, we must see where the equivalent source point is located in the noise-performance plane with respect to the outer boundary of the source region of the given source network.

Let us see what information we must have in addition to the noise figure and exchangeable gain of the amplifier in order to determine the signal-to-noise ratio and exchangeable signal power at the output. To fix these two quantities we must specify all of the open-circuit signal voltages of the source and their correlations. Then by determining the components of $\underset{\sim}{x}_1$ we can calculate $\underset{\sim}{x}_1^\dagger \overline{\underset{\sim}{E}_s \underset{\sim}{E}_s^\dagger}\, \underset{\sim}{x}_1$ and $\underset{\sim}{x}_1^\dagger \overline{\underset{\sim}{E}_n \underset{\sim}{E}_n^\dagger}\, \underset{\sim}{x}_1$. We must also know the real part of the output impedance of the amplifier, $(1/2)\left[\underset{\sim}{x}_1^\dagger \left(\underset{\sim}{Z}_s+\underset{\sim}{Z}_s^\dagger\right)\underset{\sim}{x}_1+ \underset{\sim}{x}_2^\dagger \left(\underset{\sim}{Z}_a+\underset{\sim}{Z}_a^\dagger\right)\underset{\sim}{x}_2\right]$. From knowledge of these quantities we can determine s_s, the signal-to-noise ratio of the equivalent reduced source as given by Eq. 164, and p_o, the exchangeable signal power at the output as given by Eq. 160. Then from Eq. 172 we can calculate p_s, the exchangeable signal power of the equivalent reduced source. In terms of these quantities we find that the noise-to-signal ratio at the output is given by Eq. 171:

$$\frac{1}{s_o} = \frac{1}{s_s} + \frac{kT_o\Delta f}{p_s}(F_e-1). \tag{177}$$

The viewpoint that we have taken also enables us to treat cascades of amplifiers. Consider the cascade of two amplifiers shown in Fig. 39. Even though the first amplifier in this casecade is not of the form of the amplifier in Fig. 37a, we can still define a

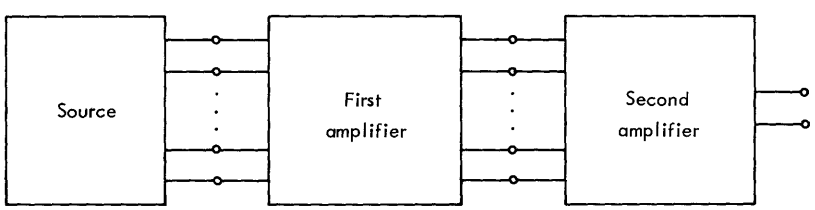

Fig. 39. Two multiterminal-pair amplifiers in cascade.

noise figure for this amplifier. Consider the composite amplifier consisting of both amplifiers. If we denote the signal-to-noise ratio and exchangeable power of the equivalent reduced source as s_{s1} and p_{s1}, in accordance with Eq. 171, we have

$$F_{e12} - 1 = \frac{\frac{1}{s_o} - \frac{1}{s_1}}{kT_o \Delta f \frac{1}{p_{s1}}}. \tag{178}$$

Similarly, the network to the left of the second is the source for this amplifier. This source has an equivalent reduced source with a signal-to-noise ratio of s_{s2} and exchangeable signal power of p_{s2}. The excess noise figure for this amplifier, in accordance with Eq. 171, then is

$$F_{e2} - 1 = \frac{\frac{1}{s_o} - \frac{1}{s_{s2}}}{kT_o \Delta f \frac{1}{p_{s2}}}. \tag{179}$$

Defining the second-stage source point $(1/p_{s2}, 1/s_{s2})$, as the equivalent output of the first stage, we can write the excess noise figure of the first amplifier as

$$F_{e1} - 1 = \frac{\frac{1}{s_{s2}} - \frac{1}{s_{s1}}}{kT_o \Delta f \frac{1}{p_{s1}}}. \tag{180}$$

From these three expressions, then, we see that the noise figure obeys the usual cascading formula

$$F_{e12} - 1 = F_{e1} - 1 + (F_{e2} - 1)/G_{e1}, \tag{181}$$

where G_{e1} is the equivalent exchangeable gain of the first amplifier

$$G_{e1} = \frac{p_{s2}}{p_{s1}}. \tag{182}$$

This procedure can be extended to cover any number of stages. The viewpoint that we are using does not even require that the number of terminal pairs appearing at each interstage be the same. There is one drawback to the application of these definitions to cascades of amplifiers, which is a consequence of the fact that we are essentially normalizing to the way in which we are finally combining the source voltages. Therefore we cannot define the noise figure of the first amplifier until we have specified the manner in which we are combining the outputs in the last stage to obtain a single output. That is, we cannot define the equivalent reduced source until we have seen how the voltages of the source are combined.

6.3 EXPERIMENTAL DETERMINATION OF NOISE FIGURE, EXCHANGEABLE-POWER GAIN, AND NOISE MEASURE

The standardized methods of measuring noise figure[26] are not directly applicable to the multiterminal case because, in general, they require a calibrated source. To use these methods, one would have to know the source impedance of the equivalent reduced source. This determination would be an involved procedure, since it would require, first, that we determine all elements of the source impedance matrix and, then, measure all voltage transfer ratios x_{1i}. Then we could evaluate $\underset{\sim}{x}_1^\dagger \left(\underset{\sim}{Z}_s+\underset{\sim}{Z}_s^\dagger\right) \underset{\sim}{x}_1$. We would also need information concerning the noise voltages present in the source in order to evaluate $\underset{\sim}{x}_1^\dagger \overline{\underset{\sim}{E}_n \underset{\sim}{E}_n^\dagger}\, \underset{\sim}{x}_1$, the mean-square noise voltage appearing at the output caused by noise in the source. Such a method, besides being tedious, is prone to large cumulative errors.

A much simpler method is the following. If there is no signal present in the source network, and if the only noise present in the source network is thermal noise at temperature T, then $\overline{\underset{\sim}{E}_n \underset{\sim}{E}_n^\dagger} = 2kT\Delta f \left(\underset{\sim}{Z}_s+\underset{\sim}{Z}_s^\dagger\right)$, and $\overline{\underset{\sim}{E}_s \underset{\sim}{E}_s^\dagger} = 0$. Under these conditions, let us cool (or heat) the source to temperature T_1 and measure P_1, the exchangeable power at the output in a band Δf wide. Then let us cool (or heat) the source to a temperature T_2 and measure P_2, the exchangeable power at the output, in a band Δf wide. This gives

$$P_1 = \frac{2kT_1\Delta f \underset{\sim}{x}_1^\dagger \left(\underset{\sim}{Z}_s+\underset{\sim}{Z}_s^\dagger\right) \underset{\sim}{x}_1 + \underset{\sim}{x}_2^\dagger \overline{\underset{\sim}{E}_a \underset{\sim}{E}_a^\dagger}\, \underset{\sim}{x}_2}{2\underset{\sim}{x}_1^\dagger \left(\underset{\sim}{Z}_s+\underset{\sim}{Z}_s^\dagger\right) \underset{\sim}{x}_1 + 2\underset{\sim}{x}_2^\dagger \left(\underset{\sim}{Z}_a+\underset{\sim}{Z}_a^\dagger\right) \underset{\sim}{x}_2} \tag{183}$$

and

$$P_2 = \frac{2kT_2\Delta f \underset{\sim}{x}_1^\dagger \left(\underset{\sim}{Z}_s+\underset{\sim}{Z}_s^\dagger\right) \underset{\sim}{x}_1 + \underset{\sim}{x}_2^\dagger \overline{\underset{\sim}{E}_a \underset{\sim}{E}_a^\dagger}\, \underset{\sim}{x}_2}{2\underset{\sim}{x}_1^\dagger \left(\underset{\sim}{Z}_s+\underset{\sim}{Z}_s^\dagger\right) \underset{\sim}{x}_1 + 2\underset{\sim}{x}_2^\dagger \left(\underset{\sim}{Z}_a+\underset{\sim}{Z}_a^\dagger\right) \underset{\sim}{x}_2}. \tag{184}$$

Then taking the difference between these two equations and using Eq. 173, we find

$$P_1 - P_2 = k\Delta f(T_1-T_2)\, G_e \tag{185}$$

or

$$G_e = \frac{P_1 - P_2}{k\Delta f(T_1-T_2)}. \tag{186}$$

Using (169) and (173) in (183), we can write

$$P_1 = kT_1\Delta f G_e + kT_o\Delta f G_e(F_e-1); \tag{187}$$

then

$$F_e - 1 = \frac{P_1 - kT_1\Delta f G_e}{G_e kT_o \Delta f}. \tag{188}$$

With the help of Eq. 186 this becomes

$$F_e - 1 = \frac{1}{T_o} \frac{T_1 P_2 - T_2 P_1}{P_1 - P_2}. \tag{189}$$

Now we use Eqs. 186 and 189 in the defining equation for M_e (Eq. 174) to obtain

$$M_e = \frac{1}{T_o} \frac{T_1 P_2 - T_2 P_1}{(P_1 - P_2) - k\Delta f(T_1 - T_2)}. \tag{190}$$

Then with these two sets of readings we may determine the excess noise figure, Eq. 189; the equivalent exchangeable power gain, Eq. 186; and the noise measure, Eq. 190, of the amplifying device that is being used. It should be pointed out that it might not be possible to perform this experiment in practice. In particular, if the source in question consists of the elements of an antenna array, we would have to replace the system of antennas by its equivalent circuit, that is, a circuit that has the same impedance matrix, in order to obtain a circuit whose temperature can be uniformly regulated.

Another problem with this method is that we may not be able to produce a large enough exchangeable power level at the output to obtain a reliable reading by cooling the network. In this case we could use an additional stage of known noise measure in cascade, or we could resort to the following procedure. We know that the network with an impedance matrix $\underset{\sim}{Z}_s$ containing only thermal noise can be transformed into a canonical form consisting of a set of independent noisy resistors by an appropriate lossless transformation network. Also, we know that there is an inverse canonical transformation that carries this canonical network back into the original network. Thus with our source, for testing purposes, we could imbed a set of independent noise generators (gas-discharge tubes, thermionic noise diodes, etc.), all at the same temperature, T_a, in the inverse canonical transformation network to give us a source that is identical to the original source network when the only source of noise present is thermal noise at temperature T_a. Using this aritficial source at two temperatures, we could make the desired measurements. In fact, once we have constructed this inverse canonical transformation network, we can use any of the methods of measurement that are standard for two-port devices, but we would still have to measure all of the elements of the impedance matrix of the source in order to construct this calibrated source network.

If we wish to evaluate how well we are utilizing the source, we must completely specify the signal-voltage matrix, $\overline{\underset{\sim}{E}_s \underset{\sim}{E}_s^\dagger}$, and the noise-voltage matrix, $\overline{\underset{\sim}{E}_n \underset{\sim}{E}_n^\dagger}$, as well as the impedance matrix, $\underset{\sim}{Z}_s$, of the source. With a complete knowledge of these three matrices, we can determine the source-region outer boundary as described in Section IV. By determining the voltage-transfer ratios in $\underset{\sim}{x}_1$ we can calculate the signal-to-noise ratio and exchangeable signal power for the amplifying system and for the reduced source by the method already described. We can then compare the source point obtained with the source-region boundary to see how much we could have improved the performance by utilizing the source more effectively.

On the other hand, if one is not interested in how well the source is being utilized, but only in the output signal-to-noise ratio, this involved procedure is not necessary. One may measure the output signal-to-noise ratio directly. The exchangeable power at the output may be measured with both the signal and noise present in the source. If it is also possible to measure the exchangeable power at the output with the signal sources dead and the same noise sources, the exchangeable signal power is equal to the difference of these two power readings. The signal-to-noise ratio at the output is then given by the ratio of this difference to the second reading.

VII. MULTIFREQUENCY NETWORKS COUPLED WITH LOSSLESS PARAMETRIC DEVICES

We shall now apply the theory that has been developed to a system in which signal voltages are present at more than one frequency. We shall consider the optimum noise performance that can be achieved in such a system when the terminals at different frequencies are coupled by a device that obeys the Manley-Rowe relations.

More precisely, we would like to consider a source that has a large number of accessible terminal pairs. The frequencies of the signals present at each of these terminal pairs may be different, but all of the frequencies will be expressible in the form $n\omega_\alpha + m\omega_\beta$, where m and n are integers. We shall also consider that we have a number of amplifiers (including positive and negative resistors) at each of these frequencies. We would like to know how to combine these elements with the source, using a device obeying the Manley-Rowe relations, to obtain the best signal-to-noise ratio at a single-output terminal pair (and hence at a given output frequency) for large values of exchangeable signal power.

We shall begin by discussing the Manley-Rowe relations and the constraints that they impose upon the coupling network under consideration. We shall then show that if we choose new current and voltage variables in a particular way, the constraints imposed on these new variables are the same as the constraints imposed upon the currents and voltages of a linear lossless network. This is not to say that the parametric coupling network is a lossless network. In general we shall extract more signal power from this network than we supply to it; the difference in powers is supplied by a pump. In this sense the coupling network may be considered as an "amplifier."

By expressing the terminal realtions of the source and amplifier networks in terms of the new variables, we shall find that, mathematically at least, we have the same problem as the one that we solved for the single-frequency case. We shall show how to set up this equivalent problem. We shall then use these techniques to investigate the noise performance of a one-terminal-pair source coupled by a lossless Manley-Rowe device to resistors (both positive and negative) at several frequencies. We solve the problem of a two-terminal-pair source – that is, a source with signal at two frequencies which has uncorrelated noise voltages. Finally, we examine the effects of noise correlation upon the results obtained for the last problem.

7.1 MANLEY-ROWE FORMULAS AND CONSTRAINTS

We know that for a linear lossless network the conservation of power requires the net power delivered to the network at each frequency to be zero. For a nonlinear lossless network, on the other hand, power that is delivered to the network at one frequency can be extracted at another frequency. Such a network obviously does not conserve power in the same fashion as the linear system. It has been shown[2] that if a nonlinear lossless capacitor is so excited that its current and voltage have components at a number

of frequencies of the form $m\omega_a + n\omega_\beta$, where m and n are integers, then

$$\sum_{m=-\infty}^{\infty} \sum_{n=1}^{\infty} \frac{nP_{mn}}{m\omega_a + n\omega_\beta} = 0 \tag{191}$$

$$\sum_{n=-\infty}^{\infty} \sum_{m=1}^{\infty} \frac{mP_{mn}}{m\omega_a + n\omega_\beta} = 0, \tag{192}$$

where P_{mn} is the power input at frequency $m\omega_a + n\omega_\beta$. Equations 191 and 192 are the Manley-Rowe formulas. Although they were originally proved for a nonlinear capacitor, they are also applicable to many types of nonlinear lossless systems.[27]

It is customary to operate such a device by "pumping" it at one of the given frequencies. That is, we drive it very hard and well into its nonlinear range with a cw source, known as the pump, at one of the frequencies which is then called the "pump frequency." The signals at the other frequencies, known as the "sideband frequencies," are assumed to be much smaller than the pump. In this case the device behaves, at the sideband frequencies, as a time-variant linear element instead of a nonlinear element. These conditions greatly simplify matters, since they allow us to write a linear relation between the sideband voltages and currents. Consequently, if we represent the device at the sideband frequencies as shown in Fig. 40, with power at only one frequency flowing at each terminal pair, we may write

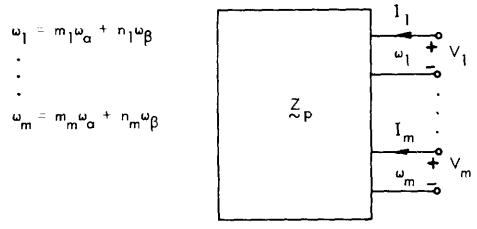

Fig. 40. Lossless parametric device.

$$\underset{\sim}{V} = \underset{\sim}{Z}_P \underset{\sim}{I}. \tag{193}$$

Here, $\underset{\sim}{V}$ is the vector composed of the voltages $V_1, V_2, \ldots V_m$, and $\underset{\sim}{I}$ is the vector composed of the currents $I_1, I_2, \ldots I_m$. The voltage V_1 and the current I_1 are at one of the sideband frequencies, which we label $\omega_1 = |m_1\omega_a + n_1\omega_\beta|$, since we are using ω to designate positive frequencies. (We shall use the symbol ν_1 to designate the (possibly negative) frequency, $m_1\omega_a + n_1\omega_\beta$, appearing in the Manley-Rowe formulas.) The voltage V_i and current I_i are at frequency ω_i, etc. Although only one frequency is present at each terminal pair, any given frequency may be found at several terminal pairs. We have shown no noise sources in (193), since the only source of noise is through the pump input; generally the noise introduced in this manner is negligible.

Let us assume that we pump a device, which obeys the Manley-Rowe formulas, at ω_β. We see that (192) gives us a relation between the power flowing into the network at each of the sideband frequencies appearing in this summation; usually we only allow

power to enter and leave the device at a finite number of these frequencies. Similarly, if we pump at ω_a, Eq. 191 gives us the relation between the powers flowing at the sideband frequencies. Although it is not customary, we may also pump at a frequency which appears in both (191) and (192). In this case we eliminate this frequency between the two equations to get a relation between the sideband powers similar to that above. In any case, we can obtain a relation among the sideband powers that is written

$$\sum_{\substack{\text{i sideband} \\ \text{frequencies}}} \frac{P_i}{\nu_i} = 0, \tag{194}$$

where P_i is the power into the device at the i^{th} terminal pair at frequency ω_i, and ν_i is equal to plus or minus ω_i. (If we are pumping at ω_a, we have from (191) and (194) $\nu_i = (m_i\omega_a + n_i\omega_\beta)/n_i$. For linearity we limit ourselves to sidebands with $n_i = 1$. Hence $\nu_i = \omega_\beta + m_i\omega_a$, where m_i is a positive or negative integer.)

Now let us express (194) in terms of the voltages and currents of the network of Fig. 40. We see that the power into the first terminal pair is

$$P_1 = \text{Re}\,[V_1 I_1^*] = \tfrac{1}{2}[V_1^* I_1 + V_1 I_1^*]. \tag{195}$$

The power into the i^{th} terminal pair is

$$P_i = \text{Re}\,[V_i I_i^*] = \tfrac{1}{2}[V_i^* I_i + V_i I_i^*], \text{ etc.} \tag{196}$$

Let us define a diagonal matrix $\underset{\sim}{K}$ whose i^{th} element along the diagonal is ν_i, the normalized frequency at the i^{th} terminal pair. We may then write Eq. 194

$$\underset{\sim}{V}^\dagger \underset{\sim}{K}^{-1} \underset{\sim}{I} + \underset{\sim}{I}^\dagger \underset{\sim}{K}^{-1} \underset{\sim}{V} = 0. \tag{197}$$

We can also define a matrix $\underset{\sim}{K}^{1/2}$ whose i^{th} element along its diagonal is the positive square root of the corresponding element of the matrix $\underset{\sim}{K}$. If ν_i is negative, the i^{th} element of $\underset{\sim}{K}^{1/2}$ will be $j\sqrt{|\nu_i|}$, where j is the square root of -1. We may now define new "current" and "voltage" variables:

$$\underset{\sim}{I}' = \underset{\sim}{K}^{-1/2} \underset{\sim}{I} \tag{198}$$

$$\underset{\sim}{V}' = [\underset{\sim}{K}^{-1/2}]^\dagger \underset{\sim}{V}. \tag{199}$$

Let us write (197) as

$$\underset{\sim}{V}^\dagger \underset{\sim}{K}^{-1/2} \underset{\sim}{K}^{-1/2} \underset{\sim}{I} + \underset{\sim}{I}^\dagger [\underset{\sim}{K}^{-1/2}]^\dagger [\underset{\sim}{K}^{-1/2}]^\dagger \underset{\sim}{V} = 0. \tag{200}$$

We see that by using Eqs. 198 and 199 in Eq. 200 we obtain

$$\underset{\sim}{V}'^\dagger \underset{\sim}{I}' + \underset{\sim}{I}'^\dagger \underset{\sim}{V}' = 0. \tag{201}$$

Equation 201 is the constraint imposed by the Manley-Rowe formulas upon the frequency-normalized current and voltage variables $\underset{\sim}{I}'$ and $\underset{\sim}{V}'$ at the terminals of the equivalent circuit of a lossless parametric device. This relation is identical to the constraint that losslessness imposes upon the currents and voltages at the terminals of a linear lossless network (see Eq. 10). This does not imply that the network of Fig. 40 is lossless. Indeed, from Eq. 194 we see that at the sidebands the network may have more power leaving at sideband frequencies than is flowing in at these frequencies — the difference in these powers is supplied by the pump. Thus we see that in using the variables $\underset{\sim}{V}'$ and $\underset{\sim}{I}'$ we are merely enabling ourselves to write (194) in a simple form. We see that if we express the terminal relations of the source and amplifiers in terms of their frequency-normalized variables we shall have an optimization problem that is identical to the one we have already solved for single-frequency networks.

7.2 FORMULATION OF THE OPTIMIZATION PROBLEM

We shall now describe how to set up the optimization problem in the primed variables. We begin by considering the m-terminal-pair source network shown in Fig. 41. The open-circuit signal voltage at the first terminal pair in a band Δf wide about a frequency ω_1 is E_{s1}, the open-circuit signal voltage at the second terminal pair in a band Δf wide about frequency ω_2 is E_{s2}, etc. We may, then, define the signal-voltage vector $\underset{\sim}{E}_s$ whose i^{th} element is E_{si}. Similarly, we define a noise-voltage-generator vector, $\underset{\sim}{E}_n$. We also define a terminal-voltage vector $\underset{\sim}{V}$ whose i^{th} element is the terminal voltage V_i at the i^{th} terminal pair. The terminal voltages are related to the currents through the impedance matrix $\underset{\sim}{Z}_s$.

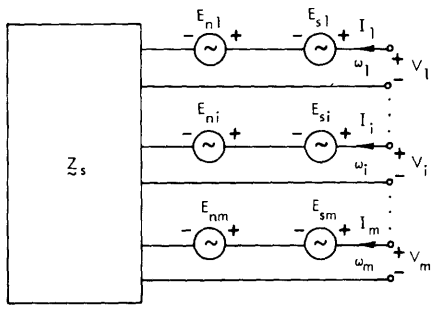

Fig. 41. Multiterminal-pair multifrequency source network.

$$\underset{\sim}{V} = \underset{\sim}{Z}_s \underset{\sim}{I} + \underset{\sim}{E}_s + \underset{\sim}{E}_n \tag{202}$$

Now we consider imbedding the source in an (m+1)-terminal-pair (not counting the pump terminals) parametric network as shown in Fig. 42. In order to be used with the source network, the frequencies at the first m-terminal pairs must match the corresponding source frequencies. The frequency of the remaining output terminal need not be specified but will be designated as ω_o for convenience. After we have designated a pump frequency, we may write out Eq. 194. From this equation we may determine the normalized frequency that is related to each ω_i. This set of numbers in turn enables

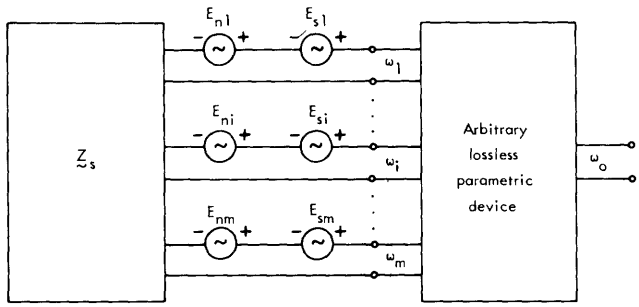

Fig. 42. Imbedding of multifrequency source.

us to determine the matrix $\underset{\sim}{K}_S$ whose i^{th} diagonal element is ν_i.

We may now express Eq. 202 in terms of $\underset{\sim}{V}'$ and $\underset{\sim}{I}'$ by premultiplying it by $[\underset{\sim}{K}_S^{-1/2}]^\dagger$. This gives

$$\left[\underset{\sim}{K}_S^{-1/2}\right]^\dagger \underset{\sim}{V} = \left[\underset{\sim}{K}_S^{-1/2}\right]^\dagger \underset{\sim}{Z}_S\underset{\sim}{K}_S\underset{\sim}{K}_S^{-1/2}\underset{\sim}{K}_S^{-1/2}\underset{\sim}{I} + \left[\underset{\sim}{K}_S^{-1/2}\right]^\dagger \underset{\sim}{E}_S + \left[\underset{\sim}{K}_S^{-1/2}\right]^\dagger \underset{\sim}{E}_n. \tag{203}$$

Using (198) and (199) in (202), we obtain the relation

$$\underset{\sim}{V}' = \left[\underset{\sim}{K}_S^{-1/2}\right]^\dagger \underset{\sim}{Z}_S'\underset{\sim}{K}_S^{-1/2}\underset{\sim}{I}' + \left[\underset{\sim}{K}_S^{-1/2}\right]^\dagger \underset{\sim}{E}_S + \left[\underset{\sim}{K}_S^{-1/2}\right]^\dagger \underset{\sim}{E}_n, \tag{204}$$

where

$$\underset{\sim}{Z}_S' = \underset{\sim}{Z}_S\underset{\sim}{K}_S. \tag{205}$$

Equation 204 is the equation relating the frequency-normalized source variables. Before we make use of this equation we must clear up one point. For a one-terminal-pair source we defined exchangeable power as the stationary value of the power output from the source obtained by arbitrary variation of the terminal current or voltage. In frequency-normalized variables $\underset{\sim}{V}'$ and $\underset{\sim}{I}'$ the quantity analogous to power is $\mathrm{Re}[V'I'^*]$ which is power divided by the frequency ν. Thus when we derive "power" expressions from Eq. 204 we shall not really obtain power but power normalized to ν. Such a normalization reverses the sense of power flow at terminal pairs at the lower sidebands. (For a device pumped at ω_α, where $\omega_\alpha > \omega_\beta$, we find from (191) and (194) that the ν_i's are given by $\nu_i = \omega_\beta + m_i\omega_\alpha$. For lower sidebands m_i is a negative integer and ν_i is negative.) Thus a noisy positive resistance at a lower sideband frequency performs in the frequency-normalized variables as a negative resistance does in the single-frequency problems considered previously.

Comparing Fig. 43 with Fig. 17, we see that the lossless parametric network of Fig. 43 performs the same function in the primed variables as the lossless network in Fig. 17 does in the voltage and current variables. In section 4.2 we derived an

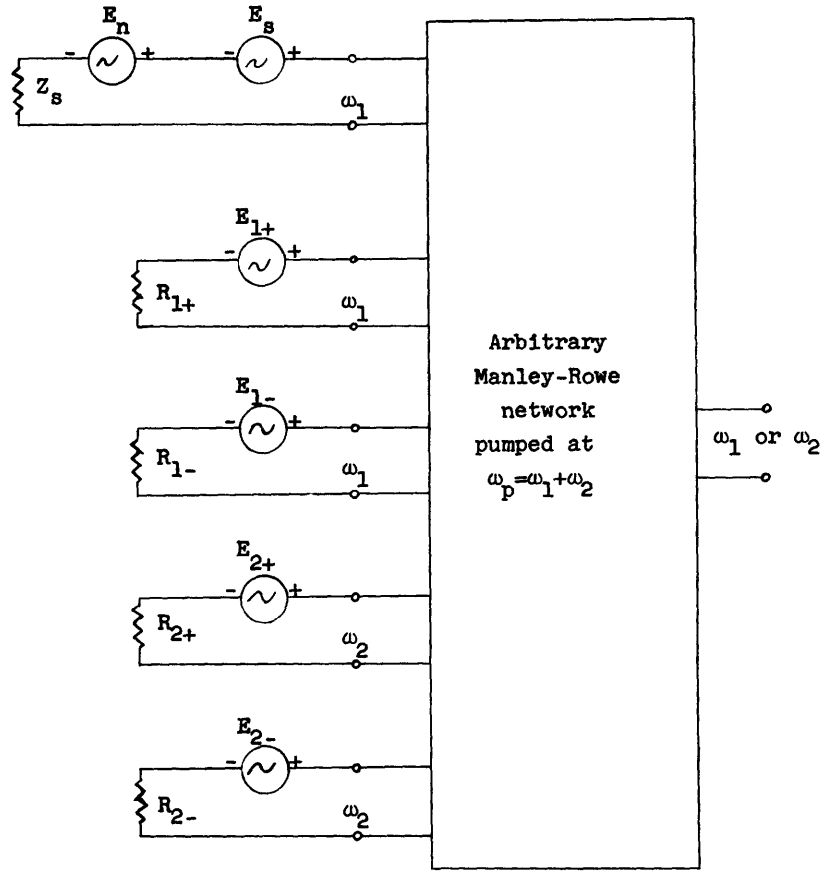

Fig. 43. One-terminal-pair source coupled to noisy resistors by a lossless Manley-Rowe network.

expression for the exchangeable signal power at the output of the network of Fig. 17 (Eq. 94) from Eq. 1; by similar arguments we may deduce from Eq. 204 that the exchangeable signal power at the output of the network in Fig. 42 divided by the frequency ν_o is given by

$$p'_s = \frac{\underset{\sim}{x}_1'^{\dagger}\left[\underset{\sim}{K}_s^{-1/2}\right]^{\dagger}\overline{\underset{\sim}{E}_s\underset{\sim}{E}_s^{\dagger}}\left[\underset{\sim}{K}_s^{-1/2}\right]\underset{\sim}{x}_1'}{2\underset{\sim}{x}_1'^{\dagger}\left[\underset{\sim}{K}_s^{-1/2}\right]^{\dagger}\left(\underset{\sim}{Z}_s+\underset{\sim}{Z}_s^{\dagger}\right)\left[\underset{\sim}{K}_s^{-1/2}\right]\underset{\sim}{x}_1'}, \tag{206}$$

where the vector $\underset{\sim}{x}_1'$ depends on the exact form of the parametric coupling network. It is convenient to define a new vector

$$\underset{\sim}{x}_1 = \left[\underset{\sim}{K}^{-1/2}\right]\underset{\sim}{x}_1'. \tag{207}$$

Using (207) in (206), we obtain

$$p'_s = \frac{\underset{\sim}{x}_1^{\dagger}\overline{\underset{\sim}{E}_s\underset{\sim}{E}_s^{\dagger}}\,\underset{\sim}{x}_1}{2\underset{\sim}{x}_1^{\dagger}\left(\underset{\sim}{Z}_s+\underset{\sim}{Z}_s^{\dagger}\right)\underset{\sim}{x}_1}. \tag{208}$$

By analogy with the single-frequency case, we may state that the vector $\underset{\sim}{x}_1$ is completely arbitrary. That is, by varying the parametric coupling network, any vector $\underset{\sim}{x}_1$ can be achieved. To perform arbitrary variations of the lossless parametric device, for instance, we would vary the capacitance-voltage characteristic of a lossless nonlinear capacitor if we were using such a capacitor as our parametric device. Also, it is more desirable to express the normalized exchangeable signal power in terms of the vector $\underset{\sim}{x}_1$ as in Eq. 208, since we may interpret the components of $\underset{\sim}{x}_1$ in the same way that we interpreted the components of $\underset{\sim}{x}_1$ for the single-frequency case (see discussion in conjunction with Eq. 27). Referring again to Fig. 42, if all sources except E_{si} are short-circuited, the open-circuit voltage at the output terminal pair would be $x_{1i}E_{si}$, where x_{1i} is the i^{th} component of the vector $\underset{\sim}{x}_1$.

The ratio of exchangeable signal power to exchangeable noise power at the output in Fig. 43 is the same as the ratio of these same quantities, with each normalized to ν_o. Thus, the signal-to-noise ratio is given by

$$s_s = \frac{\underset{\sim}{x}_1^\dagger \overline{\underset{\sim}{E}_s \underset{\sim}{E}_s^\dagger} \underset{\sim}{x}_1}{\underset{\sim}{x}_1^\dagger \overline{\underset{\sim}{E}_n \underset{\sim}{E}_n^\dagger} \underset{\sim}{x}_1}. \tag{209}$$

Using the quantities defined in Eqs. 208 and 209, we can define a source region in the same way that we did for the single-frequency case in Section IV. All of the equations derived there are applicable to the present case; the only necessary modification is to replace the unprimed quantities with their appropriate primed counter parts. If we want to obtain performance in a region of the 1/2-1/p' plane outside the source region, we must consider the use of an independently noisy network with the multifrequency source; we shall refer to this network as an amplifier as in the single-frequency case. Our amplifier network might consist of two-port or multiport amplifiers at any of the frequencies that are involved in Eq. 194. It might also consist of single positive or negative resistances at any of these frequencies; this latter type of device we shall frequently refer to as an "external termination." We may consider our amplifier network, then, to consist of any or all these devices that we have available. We need only to order the terminal pairs to define a noise-voltage-generator column matrix, $\underset{\sim}{E}_a$, and an impedance matrix, $\underset{\sim}{Z}_a$.

The procedure, now, is to imbed both the source and amplifier networks in an appropriate parametric network. As in the case of the source network above, we define a matrix $\underset{\sim}{K}_a$ appropriate to the amplifier network. We then define the matrix

$$\underset{\sim}{Z}'_a = \underset{\sim}{Z}_a \underset{\sim}{K}_a. \tag{210}$$

Then using $\underset{\sim}{Z}'_a$, rather than $\underset{\sim}{Z}_a$, and λ' (or μ'), rather than λ (or μ), all mathematical operations and discussions of Section V are now applicable to this problem.

As we have mentioned, for the case under consideration, we display the solutions

to the optimization problem on a normalized plot with coordinates of noise-to-signal ratio and the reciprocal of exchangeable signal power normalized to the output frequency ν_o - a 1/s-1/p' plot. Before we go on to some examples there are two observations we should make concerning this normalized-noise plot. First, we note that once we have plotted the solutions to the optimization equation in the normalized-noise plane, we can obtain the solutions that are appropriate at a given output frequency, ω_j, merely by dividing all coordinates on the 1/p' axis by ν_j (where ν_j may be positive or negative). Thus we have the advantage of being able to display the solutions to a large number of problems on a single diagram. Second, as a consequence of this relationship between the plots at various frequencies, we see that the stationary values of signal-to-noise ratio at infinite exchangeable signal power are independent of the frequency at which the output is taken.

7.3 EXAMPLE OF A ONE-TERMINAL-PAIR SOURCE

We shall examine the noise performance of the system shown in Fig. 43. We assume that at frequency ω_1 the one-terminal-pair source has an impedance Z_s with a positive real part R_s, and that the exchangeable signal power and signal-to-noise ratio are p_s and s_s, respectively. We assume that we have a lossless nonlinear device that obeys the Manley-Rowe relations and is pumped at the frequency ω_p ($\omega_p > \omega_1$). We shall see what we can achieve by using this device to couple to a positive and negative resistance at frequency ω_1 and a positive and negative resistance at frequency $\omega_2 = \omega_p - \omega_1$. For $\omega_p = \omega$, Eqs. 191 and 194 give us the relation

$$\frac{P_1}{\omega_1} + \frac{P_2}{-\omega_2} = 0,$$

where P_1 is the power into the coupling network at ω_1, and P_2 is the power into the coupling network at ω_2. We conclude that $\nu_1 = \omega_1$ and $\nu_2 = -\omega_2$.

We shall now see what can be accomplished by coupling to each of the noisy resistances shown in Fig. 43 one at a time. In considering coupling to these resistors one at a time we are essentially solving a problem similar to the one considered in section 3.2. We showed in Fig. 13 that a noisy resistor used with a one-terminal-pair source determined a half-line in the noise-performance plane with a slope equal to the exchangeable noise power of the resistor. In the frequency-normalized noise-performance plane a noisy resistor used with a one-terminal-pair source defines a half-line with a slope equal to its frequency-normalized exchangeable noise power (that is, its exchangeable noise power divided by ν). Thus a resistor at a frequency ω_1 determines a line with a slope equal to its exchangeable noise power divided by ω_1; a resistor at a frequency ω_2 determines a line with a slope equal to its exchangeable noise power divided by $-\omega_2 = \nu_2$. We shall show subsequently how these performance curves appear on the (unnormalized) noise-performance plane when the output is at the frequency ω_1 and when the output is at the frequency ω_2.

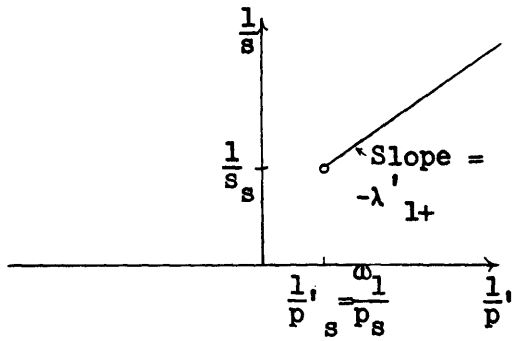

(a) Frequency normalized

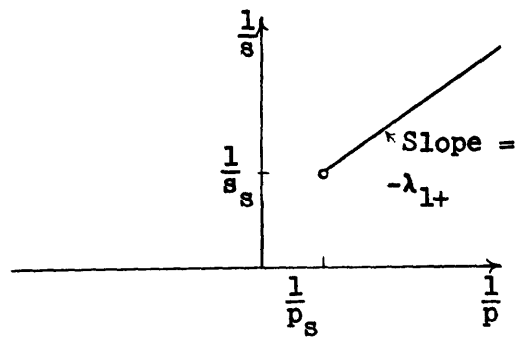

(b) Output at ω_1

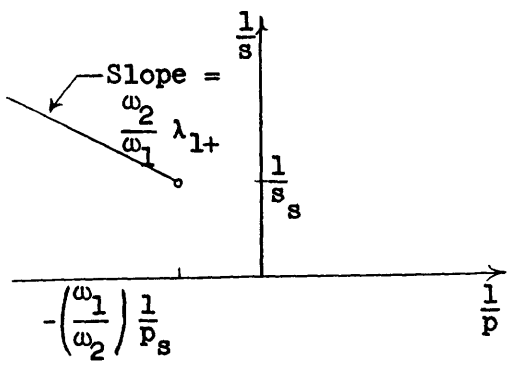

(c) Output at ω_2

Fig. 44. Performance of a positive resistance at ω_1.

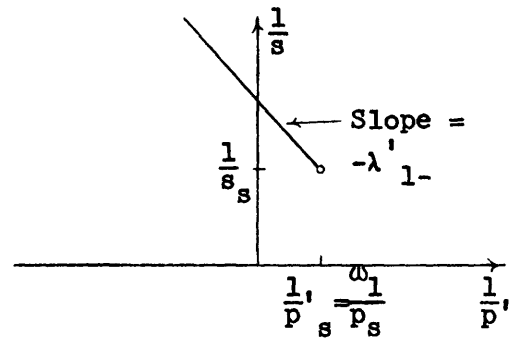

(a) Frequency normalized

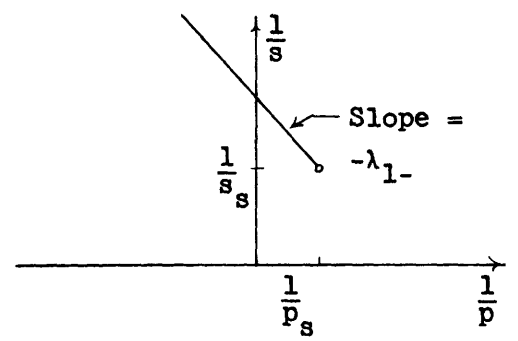

(b) Output at ω_1

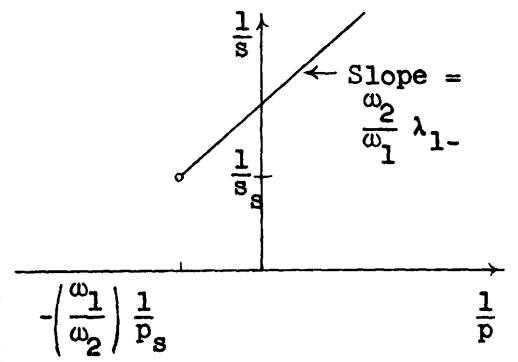

(c) Output at ω_2

Fig. 45. Performance of a negative resistance at ω_1.

a. Coupling Only to a Positive Resistance at ω_1

We shall consider coupling to the impedance Z_{1+} which has a positive real part R_{1+} and a mean-square noise voltage $\overline{|E_{1+}|^2}$ at the frequency ω_1. The exchangeable noise power of this impedance is

$$-\lambda_{1+} = \frac{\overline{|E_{1+}|^2}}{4R_{1+}} > 0.$$

The exchangeable power normalized to ω_1 is just

$$-\lambda'_{1+} = \frac{-\lambda_{1+}}{\omega_1}.$$

The performance curve for this resistor in the frequency-normalized noise performance plane is shown in Fig. 44a. If we are interested in taking our output at ω_1, we can multiply the powers in Fig. 44a by ω_1. The resulting performance curve shown in Fig. 44b is similar to that shown in Fig. 13b, since only one frequency is involved. If we are interested in what may be achieved at an output at frequency ω_2, we multiply all of the powers in Fig. 44a by $-\omega_2$. This gives the plot shown in Fig. 44c.

b. Coupling Only to a Negative Resistance at ω_1

Let us consider what can be accomplished by coupling to the impedance Z_{1-} in Fig. 43. This impedance has a negative real part R_{1-} and a mean-square noise voltage $\overline{|E_{1-}|^2}$. The exchangeable noise power of this impedance is

$$-\lambda_{1-} = \frac{\overline{|E_{1-}|^2}}{4R_{1-}} < 0,$$

and the exchangeable power normalized to ω_1 is

$$-\lambda'_{1-} = -\frac{\lambda_{1-}}{\omega_1} < 0.$$

The performance curve for this resistor in the frequency-normalized noise-performance plane is shown in Fig. 45a. If we are interested in taking our output at ω_1, we can multiply the powers in Fig. 45a by ω_1. The resulting performance curve, shown in Fig. 45b, is similar to that shown in Fig. 13a, since only one frequency is involved. If we are interested in determining what can be achieved at an output at frequency ω_2, we multiply all of the powers in Fig. 45a by $-\omega_2$. This gives the plot shown in Fig. 45c.

c. Coupling Only to a Positive Resistance at ω_2

The performance curves obtained when we couple to an impedance that has a positive real part R_{2+} and a mean-square noise voltage $\overline{|E_{2+}|^2}$ at frequency ω_2 are shown

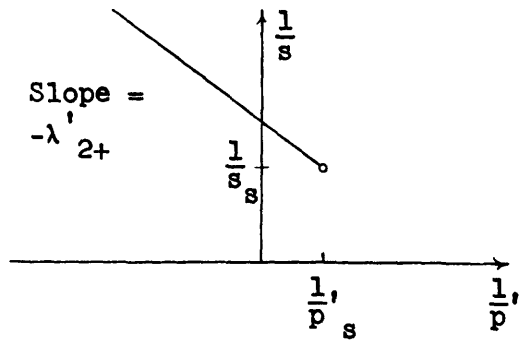

(a) Frequency normalized

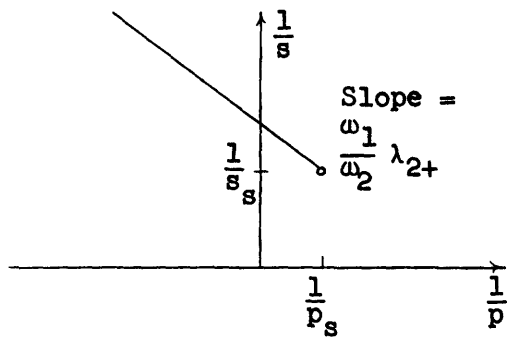

(b) Output at ω_1

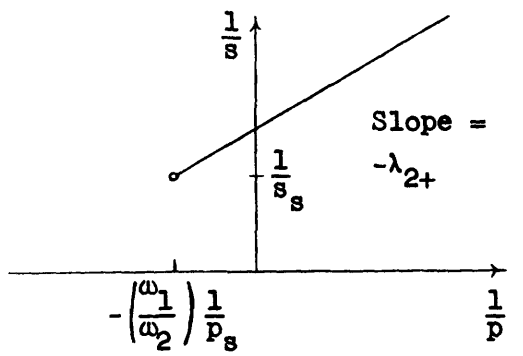

(c) Output at ω_2

Fig. 46. Performance of a positive resistance at ω_2.

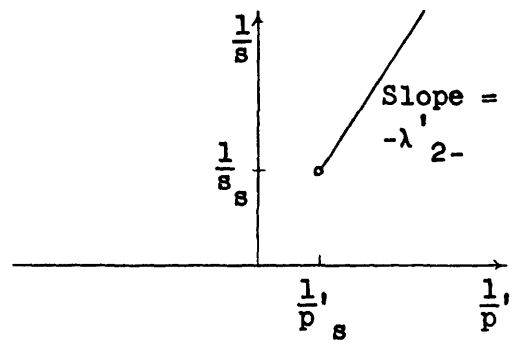

(a) Frequency normalized

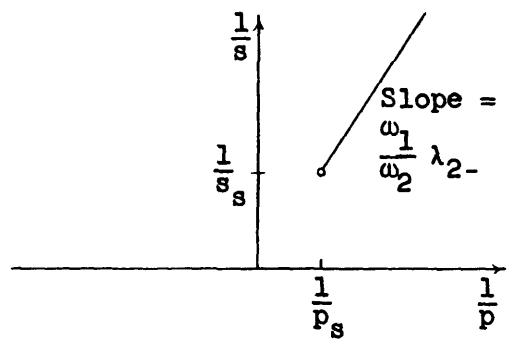

(b) Output at ω_1

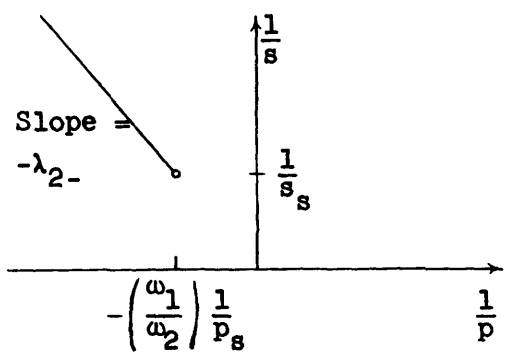

(c) Output at ω_2

Fig. 47. Performance of a negative resistance at ω_2.

in Fig. 46. The exchangeable noise power for this resistance is

$$-\lambda_{2+} = \frac{\overline{|E_{2+}|^2}}{4R_{2+}} > 0,$$

and the exchangeable power normalized to ν_2 is

$$-\lambda'_{2+} = \frac{\lambda_{2+}}{\omega_2} < 0.$$

d. Coupling Only to a Negative Resistance at ω_2

Similarly, Fig. 47 shows the performance curves obtained when we couple to an impedance that has a negative real part R_{2-} and a mean-square noise voltage $\overline{|E_{2-}|^2}$ at frequency ω_2. The exchangeable power of this resistance is

$$-\lambda_{2-} = \frac{\overline{|E_{2-}|^2}}{4R_{2-}} < 0,$$

and the exchangeable power normalized to ν_2 is

$$-\lambda'_{2-} = \frac{\lambda_{2-}}{\omega_2} > 0.$$

To summarize, we see that the performance curves in Figs. 44b and 45b are identical to those shown in Figs. 13b and 13a, respectively. Thus Figs. 44a and 45a merely show how these performance curves appear in the frequency-normalized noise-performance plane. On the other hand, Figs. 44c and 45c show the ranges of performance that can be achieved if we convert to frequency ω_2.

When the frequency of the source and resistance are different, we have a slightly different interpretation. From Fig. 46b we see that a positive resistance at ω_2 converts to a negative resistance at ω_1; similarly, from Fig. 47b we see that a negative resistance at ω_2 converts to a positive resistance at ω_1. On the other hand, when we are examining the performance of the system as a converter (output at ω_2), Figs. 46c and 47c apply. Here we are essentially converting our source at ω_1 to a negative-resistance source at ω_2, and subsequently connecting it to noisy resistance at ω_2. Therefore the performance curves of Figs. 46c and 47c are identical to those of Figs. 13c and 13d, respectively.

If we are interested in achieving the best performance at large exchangeable power we would use the positive resistance at ω_2 if $-(\omega_1/\omega_2)\lambda_{2+}$ is less than λ_{1-}. For this case this gives the best performance as a parametric amplifier or as a converter. If λ_{1-} is less than $-(\omega_1/\omega_2)\lambda_{2+}$, we would couple only the negative resistance at ω_1. If we are taking our output at ω_1, this means that our amplifier at ω_1 (the negative resistance) is

better than the parametric amplifier that we can construct by coupling to the positive resistance at ω_2. If we are taking our output at ω_2, it means that our amplifier is better than our converter. This implies that we should first amplify our source at ω_1 to obtain large exchangeable power and then convert to frequency ω_2.

7.4 EXAMPLE OF A TWO-FREQUENCY SOURCE WITH UNCORRELATED NOISE

We shall consider the optimal utilization of the source shown in Fig. 48. A source such as this could be representative of an antenna system receiving a modulated signal

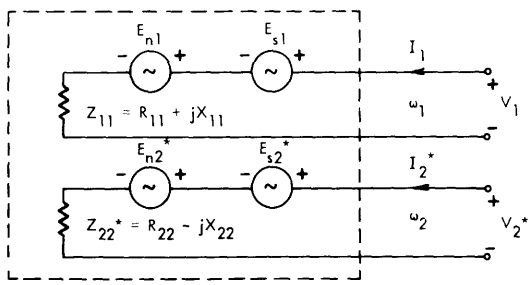

Fig. 48. Two-frequency source.

with a carrier frequency of $\omega_p/2$, an upper sideband at frequency ω_1, and a lower sideband at frequency $\omega_2 = \omega_p - \omega_1$. To take into account the nature of the coupling between the two sidebands, we must use the complex conjugates of the amplitudes of voltage and current at the positive frequency ω_2. Therefore the source voltages and currents are related by

$$\begin{bmatrix} V_1 \\ \cdots \\ V_2^* \end{bmatrix} = \begin{bmatrix} Z_{11} & \vdots & 0 \\ \cdots & \vdots & \cdots \\ 0 & \vdots & Z_{22}^* \end{bmatrix} \begin{bmatrix} I_1 \\ \cdots \\ I_2^* \end{bmatrix} + \begin{bmatrix} E_{s1} \\ \cdots \\ E_{s2}^* \end{bmatrix} + \begin{bmatrix} E_{n1} \\ \cdots \\ E_{n2}^* \end{bmatrix}. \tag{211}$$

We shall assume that the real parts of Z_{11} and Z_{22}^* are positive. Also, we shall assume that the signal voltages are completely correlated and that the noise voltages are completely uncorrelated. Thus the voltage cross-spectral matrices are

$$\overline{\underset{\sim}{E}_s \underset{\sim}{E}_s^\dagger} = \begin{bmatrix} |E_{s1}|^2 & \vdots & E_{s1}E_{s2} \\ \cdots & \vdots & \cdots \\ E_{s1}^* E_{s2}^* & \vdots & |E_{s2}|^2 \end{bmatrix} \tag{212}$$

and

$$\overline{\underset{\sim}{E}_n \underset{\sim}{E}_n^\dagger} = \begin{bmatrix} \overline{|E_{n1}|^2} & \vdots & 0 \\ \cdots & \vdots & \cdots \\ 0 & \vdots & \overline{|E_{n2}|^2} \end{bmatrix}. \tag{213}$$

If we assume that we are going to use a lossless parametric device pumped at ω_p, we find that for $\omega_p = \omega_\alpha$ and $\omega_1 = \omega_\beta$ Eq. 194 gives the relationship that we desire.

$$\frac{P_1}{\omega_1} + \frac{P_2}{-\omega_2} = 0. \tag{214}$$

Then

$$\underset{\sim}{K}_s = \begin{bmatrix} \omega_1 & \vdots & 0 \\ \cdots & \vdots & \cdots \\ 0 & \vdots & -\omega_2 \end{bmatrix}. \tag{215}$$

In accordance with Eq. 205, then, we find

$$\underset{\sim}{Z}'_s = \begin{bmatrix} Z_{11} & \vdots & 0 \\ \cdots & \vdots & \cdots \\ 0 & \vdots & Z^*_{22} \end{bmatrix} \begin{bmatrix} \omega_1 & \vdots & 0 \\ \cdots & \vdots & \cdots \\ 0 & \vdots & -\omega_2 \end{bmatrix} = \begin{bmatrix} Z_{11}\omega_1 & \vdots & 0 \\ \cdots & \vdots & \cdots \\ 0 & \vdots & -Z^*_{22}\omega_2 \end{bmatrix}. \tag{216}$$

The source optimization equation analogous to Eq. 137 is

$$\overline{\underset{\sim}{E}_s \underset{\sim}{E}_s^\dagger}\, \underset{\sim}{x}_1 - \sigma\left[\overline{\underset{\sim}{E}_n \underset{\sim}{E}_n^\dagger} + 2\lambda'\left(\underset{\sim}{Z}'_s + \underset{\sim}{Z}'^\dagger_s\right)\right] \underset{\sim}{x}_1 = 0. \tag{217}$$

Using Eqs. 212, 213, and 216 in Eq. 217, we obtain

$$\begin{aligned} \left[|E_{s1}|^2 - \sigma\left(\overline{|E_{n1}|^2} + 4\lambda'\omega_1 R_{11}\right)\right] x_{11} + E_{s1}E_{s2}x_{12} &= 0 \\ E^*_{s1}E^*_{s2}x_{11} + \left[|E_{s2}|^2 - \sigma\left(\overline{|E_{n2}|^2} - 4\lambda'\omega_2 R_{22}\right)\right] x_{12} &= 0. \end{aligned} \tag{218}$$

These two equations (218) have a nontrivial solution only if the determinant of the coefficient matrix is identically zero. This occurs for

$$\sigma = 0$$

and for

$$\sigma = \sigma_{\lambda 1} = \frac{|E_{s1}|^2}{\overline{|E_{n1}|^2} + 4\lambda'\omega_1 R_{11}} + \frac{|E_{s2}|^2}{\overline{|E_{n2}|^2} - 4\lambda'\omega_2 R_{22}}. \tag{219}$$

For convenience we shall define the following quantities, which are exchangeable powers and exchangeable power normalized to (positive) frequency,

$$S_1 = \frac{|E_{s1}|^2}{4R_{11}} \qquad S_1' = \frac{S_1}{\omega_1}$$

$$S_2 = \frac{|E_{s2}|^2}{4R_{22}} \qquad S_2' = \frac{S_2}{\omega_2} \tag{220}$$

$$N_1 = \frac{\overline{|E_{n1}|^2}}{4R_{11}} \qquad N_1' = \frac{N_1}{\omega_1}$$

$$N_2 = \frac{\overline{|E_{n2}|^2}}{4R_{22}} \qquad N_2' = \frac{N_2}{\omega_2} \quad .$$

In terms of these quantities Eq. 219 becomes

$$\sigma_{\lambda' 1} = \frac{S_1'}{N_1' + \lambda'} + \frac{S_2'}{N_2' - \lambda'}. \tag{221}$$

In (221) we have an expression of $\sigma_{\lambda' 1}$ as a function of λ'. We see that since there is only one nonzero eigenvalue to (218), $\sigma_{\lambda' 1}$, the source region is described by a single curve in 1/s-1/p' space. That is, for any λ' (where $-\lambda'$ is a slope) there is one eigenvalue, $\sigma_{\lambda' 1}$, and one eigenvector, $\underset{\sim}{x}_1^{(1)}$. We use the eigenvector in

$$s_s = \frac{\underset{\sim}{x}_1^\dagger \overline{\underset{\sim}{E}_s \underset{\sim}{E}_s^\dagger} \underset{\sim}{x}_1}{\underset{\sim}{x}_1^\dagger \overline{\underset{\sim}{E}_n \underset{\sim}{E}_n^\dagger} \underset{\sim}{x}_1} \tag{222}$$

and

$$p_s' = \frac{\underset{\sim}{x}_1^\dagger \overline{\underset{\sim}{E}_s \underset{\sim}{E}_s^\dagger} \underset{\sim}{x}_1}{2\underset{\sim}{x}_1^\dagger \left(\underset{\sim}{Z}_s' + \underset{\sim}{Z}_s^\dagger\right) \underset{\sim}{x}_1} \tag{223}$$

to define a point in the 1/s-1/p' plane. If we do this for each value of λ', we shall trace out the boundary of the source region.

Let us proceed along these lines. Substituting (221) in either of Eqs. 218, we find that the ratio of the components of the eigenvector $\underset{\sim}{x}_1^{(1)}$ is given by

$$\frac{x_{12}^{(1)}}{x_{11}^{(1)}} = \frac{E_{s2}^* \omega_1 R_{11}}{E_{s1} \omega_2 R_{22}} \frac{N_1' + \lambda'}{N_2' - \lambda'}. \tag{224}$$

Using (224) in (222) and (223), we find

$$\frac{1}{s_{s,\lambda'1}} = \frac{1}{(\sigma_{\lambda'1})^2}\left[\frac{N_1'S_1'}{(N_1'+\lambda')^2} + \frac{N_2'S_2'}{(N_2'-\lambda')^2}\right] \tag{225}$$

$$\frac{1}{p'_{s,\lambda'1}} = \frac{1}{(\sigma_{\lambda'1})^2}\left[\frac{S_1'}{(N_1'+\lambda')^2} - \frac{S_2'}{(N_2'-\lambda')^2}\right]. \tag{226}$$

From (226) we see that the source region is indefinite since $1/p'_{s,\lambda'1}$ is positive for λ' near $-N_1'$ and is negative for λ' near N_2'. The general properties of the source-region outer boundary may be obtained by determining the points on the source-region boundary curve where the slope is zero, and where the curve crosses the $1/s$ axis.

To obtain the point on the source-region boundary where the slope is zero, we evaluate the expressions (221), (220), and (226) for $\lambda' = 0$. This yields

$$\frac{1}{\sigma_{01}} = \frac{N_1'N_2'}{N_2'S_1' + N_1'S_2'} = \frac{1}{s_{s,01}} \tag{227}$$

and

$$\frac{1}{p'_{s,01}} = \frac{S_1'N_2'^2 - S_2'N_1'^2}{(S_1'N_2'+S_2'N_1')^2}. \tag{228}$$

In order to locate the points on the source-region boundary where $1/p'_{s,\lambda'1}$ is zero, we must find the values of λ' that makes $1/p'_{s,\lambda'1}$, as given by (226), zero. This condition gives us two values of λ',

$$\lambda'_a = \frac{N_2'\sqrt{S_1'} - N_1'\sqrt{S_2'}}{\sqrt{S_1'} + \sqrt{S_2'}} \tag{229}$$

and

$$\lambda'_b = \frac{N_2'\sqrt{S_1'} + N_1'\sqrt{S_2'}}{\sqrt{S_1'} - \sqrt{S_2'}}. \tag{230}$$

The values of noise-to-signal ratio that correspond to these two values of λ' may be obtained from (221) or (225):

$$\frac{1}{s_{s,a1}} = \frac{N_1' + N_2'}{[\sqrt{S_1'}+\sqrt{S_2'}]^2} \tag{231}$$

and

$$\frac{1}{\sigma_{s,bl}} = \frac{N_1' + N_2'}{[\sqrt{S_1'} - \sqrt{S_2'}]^2}, \tag{232}$$

respectively. We see that the noise-to-signal ratio corresponding to λ_a' is always less than that corresponding to λ_b'. But from Eqs. 229 and 230 we see that four distinct cases may be differentiated. These are

Case I: $N_2'\sqrt{S_1'} > N_1'\sqrt{S_2'}$; $\sqrt{S_1'} > \sqrt{S_2'}$

Case II: $N_2'\sqrt{S_1'} > N_1'\sqrt{S_2'}$; $\sqrt{S_1'} < \sqrt{S_2'}$

Case III: $N_2'\sqrt{S_1'} < N_1'\sqrt{S_2'}$; $\sqrt{S_1'} < \sqrt{S_2'}$

Case IV: $N_2'\sqrt{S_1'} < N_1'\sqrt{S_2'}$; $\sqrt{S_1'} > \sqrt{S_2'}$

The normalized source regions for each of these four cases are shown in Fig. 49.

The optimum noise-to-signal ratio that can be achieved at infinite exchangeable power for each of these cases may be determined by inspection. For Cases I and II the best noise-to-signal ratio is given by the value of $1/\sigma_{s,al}$ of Eq. 231, unless there is available an independently noisy device at a related frequency characterized by a value of λ' which is positive but less than λ_a'. If such a device is available, we may achieve the signal-to-noise ratio given by Eq. 221. For Cases III and IV the best noise-to-signal ratio is also given by Eq. 231, unless there is available an independently noisy device at a related frequency characterized by a value of λ' which is negative but greater than λ_a'.

We shall now show that, at least in principle, we always have available a device with an arbitrarily small positive or negative λ'. Consider a resistor at a temperature T_i in a bandwidth Δf about a frequency ω_i, where

$$\omega_i = |m_i\omega_1 + n_i\omega_p|, \qquad n_i = 1. \tag{233}$$

Let us imbed this in the parametric coupling network together with the source as shown in Fig. 50. Since the parametric network admits power at this frequency, Eq. 194 becomes

$$\frac{P_1}{\omega_1} + \frac{P_2}{-\omega_2} + \frac{n_i P_i}{n_i\omega_1 + m_i\omega_p} = 0. \tag{234}$$

Then the matrix $\underset{\sim}{K}_a$ is a number

$$K_a = \omega_1 + \left(\frac{m_i}{n_i}\right)\omega_p. \tag{235}$$

Consequently, the amplifier equation analogous to Eq. 136 is

$$(4kT_iR_i\Delta f)\, x_2 + 2\lambda'(2R_iK_a)\, x_2 = 0. \tag{236}$$

This yields

$$\lambda' = \frac{-kT_i\Delta f}{\omega_1 + \left(\frac{m_i}{n_i}\right)\omega_p}. \tag{237}$$

By choosing ω_i such that m_i/n_i is a sufficiently large quantity (m_i is an integer, n_i = 1), we can make λ' an arbitrarily small negative number. Similarly, by choosing ω_i so that m_i/n_i is a sufficiently large negative quantity, we can make λ' an arbitrarily small positive quantity. By this means we can approach the limit of noise-to-signal

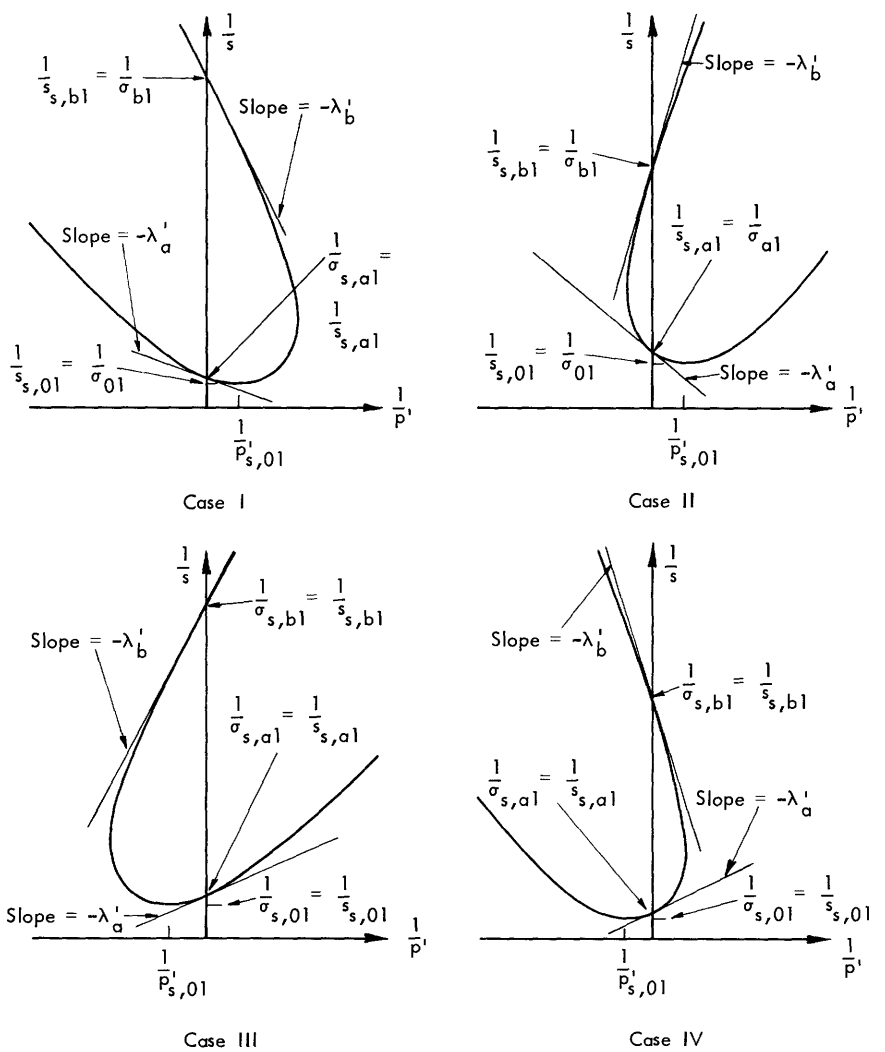

Fig. 49. Source regions.

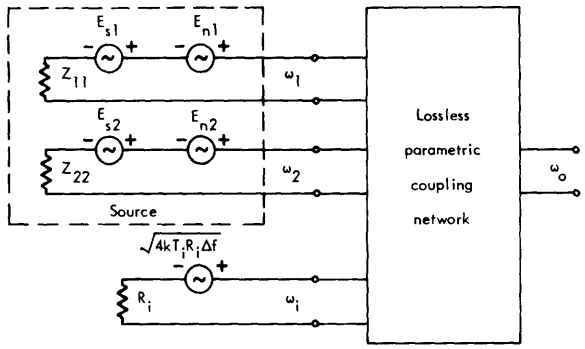

Fig. 50. Optimum amplification with a noisy resistance.

ratio at infinite exchangeable output power equal to that given by Eq. 227. In practice it would be difficult to achieve such operation because such operation is highly susceptible to spurious responses. Also, in practical devices the parasitic losses become very important at high frequencies and would cancel out the apparent gains.

7.5 EXAMPLE OF A TWO-FREQUENCY SOURCE WITH CORRELATED NOISE

We shall consider the same source that we considered in the preceding section, the one shown in Fig. 48, except that we shall allow the noise voltages to be correlated. The noise-voltage cross-spectral matrix is now given by

$$\overline{\underset{\sim}{E}_n\underset{\sim}{E}_n^\dagger} = \begin{bmatrix} \overline{|E_{n1}|^2} & \vdots & \overline{E_{n1}E_{n2}} \\ \cdots\cdots & \vdots & \cdots\cdots \\ \overline{E_{n1}E_{n2}^*} & \vdots & \overline{|E_{n2}|^2} \end{bmatrix} \tag{238}$$

rather than by Eq. 213. The matrices given in (212) and (216) remain unchanged. When we use this new $\overline{\underset{\sim}{E}_n\underset{\sim}{E}_n^\dagger}$ matrix in (217) we find that the source optimization equation becomes

$$\begin{aligned} &\left[|E_s|^2-\sigma\left(\overline{|E_{n1}|^2}+4\lambda'\omega_1R_{11}\right)\right]x_{11}+\left[E_{s1}E_{s2}-\sigma\overline{E_{n1}E_{n2}}\right]x_{12}=0 \\ &\left[E_{s1}^*E_{s2}^*-\sigma\overline{E_{n1}E_{n2}^*}\right]x_{11}+\left[|E_{s2}|^2-\sigma\left(\overline{|E_{n2}|^2}-4\lambda'\omega_2R_{22}\right)\right]x_{12}=0\ . \end{aligned} \tag{239}$$

Equations 239 have a nontrivial solution only if the determinant of the coefficient matrix is zero. This occurs for $\sigma = 0$ and for

$$\sigma = \sigma_{\lambda'1}^{(c)} = \frac{|E_{s2}|^2\left[\overline{|E_{n1}|^2}+4\lambda'R_{11}\omega_1\right]+|E_{s1}|^2\left[\overline{|E_{n2}|^2}-4\lambda'R_{22}\omega_2\right]-\left[E_{s1}^*E_{s2}^*\overline{E_{n1}E_{n2}}+E_{s1}E_{s2}\overline{E_{n1}E_{n2}^*}\right]}{\left[\overline{|E_{n1}|^2}+4\lambda'R_{11}\omega_1\right]\left[\overline{|E_{n2}|^2}-4\lambda'R_{22}\omega_2\right]-\overline{|E_{n1}E_{n2}|^2}}. \tag{240}$$

It is helpful to define the quantity

$$\rho = \frac{\overline{E_{n1}E_{n2}}}{\sqrt{\overline{|E_{n1}|^2}\,\overline{|E_{n2}|^2}}} \frac{E_{s1}^* E_{s2}^*}{|E_{s1}E_{s2}|} = |\rho|\, e^{j\theta}. \tag{241}$$

If the phase of $E_{s1}^* E_{s2}^*$ is zero, the quantity ρ is the noise-voltage correlation coefficient. Thus if we introduce phase shifters at one or both of the terminal pairs of the source, and if we adjust these phase shifters so that the phases of E_{s1} and E_{s2}^* are the same, the quantity ρ is the noise-voltage correlation that would be measured under these conditions. Consequently, we may regard ρ, in general, as the noise-voltage correlation coefficient referred to the phase of the signal-voltage correlation coefficient – the magnitude of the signal-voltage correlation coefficient is unity, since the signals are fully correlated. The magnitude of ρ, on the other hand, is between zero and one.

$$0 \leq |\rho| \leq 1. \tag{242}$$

Using Eqs. 220 and 241, we may rewrite Eq. 240 as

$$\sigma_{\lambda' 1}^{(c)} = \frac{S_1'(N_2'-\lambda') + S_2'(N_1'+\lambda') - 2\sqrt{N_1'N_2'S_1'S_2'}\,|\rho|\,\cos\theta}{(N_1'+\lambda')(N_2'-\lambda') - N_1'N_2'|\rho|^2}. \tag{243}$$

The reciprocal of this in expended form is

$$\frac{1}{\sigma_{\lambda' 1}^{(c)}} = \frac{N_1'N_2'(1-|\rho|^2) + (N_2'-N_1')\lambda' - \lambda'^2}{N_2'S_1' + N_1'S_2' - 2\sqrt{N_1'N_2'S_1'S_2'}\,|\rho|\,\cos\theta + \lambda'(S_2'-S_1')}. \tag{244}$$

In (243) we have an expression for $\sigma_{\lambda' 1}^{(c)}$ as a function of λ' that is similar to the expression of (218) for $\sigma_{\lambda' 1}$ in the uncorrelated case. (We use a bracketed superscript c to differentiate between expressions pertaining to the correlated case and expressions analogous to the uncorrelated case.) Since there is only one nonzero eigenvalue to Eqs. 239, $\sigma_{\lambda' 1}^{(c)}$, we conclude that the source region is described by a single outer-boundary curve in the 1/s-1/p' plane. Then, for any λ', where $-\lambda'$ is a slope, there is one eigenvalue, $\sigma_{\lambda' 1}^{(c)}$, and one eigenvector $\underset{\sim}{x}_1^{(1)}$. We could use the eigenvector in the expressions for the signal-to-noise ratio and exchangeable signal power given in Eqs. 222 and 223 to define a point in the 1/s-1/p' plane. If we were to do this for every value of λ', we would trace out the boundary of the source region; but the expressions rapidly become so involved as to be practically useless.

Although the mathematics becomes very involved, the results are qualitatively the same as those obtained for the uncorrelated case considered above. We demonstrated that the source region could assume any one of the four typical shapes shown in Fig. 49. On the other hand, we showed that the expression for the minimum noise-to-signal ratio

at infinite exchangeable power, $1/\sigma_{a1}$ of Eq. 231, was the same for all cases. Moreover, the slope of the source-region boundary at this point, $-\lambda'_a$, was also the same for all cases. The situation for the source with correlated noise is similar. Therefore, we shall determine the minimum noise-to-signal ratio that can be obtained at large (infinite) values of exchangeable signal power by using this source only with a lossless parametric network.

We proceed to find the slope of the outer boundary of the source region at the points where this boundary curve crosses the noise-to-signal ratio axis. We may use Eq. 111 for this calculation, substituting $-\lambda'$ for the slope μ. Thus, we are looking for the values of λ' that satisfy

$$\frac{\partial}{\partial\lambda'}\left[\frac{1}{\sigma^{(c)}_{\lambda' 1}}\right] = 0. \tag{245}$$

Using (244) in (245), we find two values of λ' that satisfy (245):

$$\lambda'^{(c)}_a = \frac{(S'_1+S'_2)(N'_1+N'_2)}{(S'_1-S'_2)}\left\{\frac{N'_2S'_1 + N'_1S'_2 - 2\sqrt{N'_1N'_2S'_1S'_2}\,|\rho|\cos\theta}{(S'_1+S'_2)(N'_1+N'_2)}\right.$$

$$\left. -\frac{1}{2}\sqrt{\left[1-\frac{16\sqrt{N'_1N'_2S'_1S'_2}\,|\rho|\cos\theta}{(S'_1+S'_2)(N'_1+N'_2)}\right]^2 - \left[\frac{S'_1-S'_2}{S'_1+S'_2}\right]^2\left[1-\frac{4N'_1N'_2|\rho|^2}{(N'_1+N'_2)^2}\right]}\right\} \tag{246}$$

and

$$\lambda'^{(c)}_b = \frac{(S'_1+S'_2)(N'_1+N'_2)}{(S'_1-S'_2)}\left\{\frac{N'_2S'_1 + N'_1S'_2 - 2\sqrt{N'_1N'_2S'_1S'_2}\,|\rho|\cos\theta}{(S'_1+S'_2)(N'_1+N'_2)}\right.$$

$$\left. +\frac{1}{2}\sqrt{\left[1-\frac{16\sqrt{N'_1N'_2S'_1S'_2}\,|\rho|\cos\theta}{(S'_1+S'_2)(N'_1+N'_2)}\right]^2 - \left[\frac{S'_1-S'_2}{S'_1+S'_2}\right]^2\left[1-\frac{4N'_1N'_2|\rho|^2}{(N'_1+N'_2)^2}\right]}\right\}. \tag{247}$$

From (246) and (247) we could derive the conditions on the source parameters under which each of the four cases of Fig. 44 applies. These conditions are not very interesting and it is not necessary to determine them. What we are really interested in is the smallest value of noise-to-signal ratio at infinite exchangeable power. Substituting $\lambda'^{(c)}_a$ and $\lambda'^{(c)}_b$ in Eq. 244 we find the two extremal values of noise-to-signal ratio at infinite exchangeable power. These values are $1/\sigma^{(c)}_{a1}$ and $1/\sigma^{(c)}_{b1}$. Let it suffice to say that it can be shown that $1/\sigma^{(c)}_{b1}$ is always greater than $1/\sigma^{(c)}_{a1}$. Consequently the minimum

noise-to-signal ratio at infinite exchangeable power is obtained for all cases by substituting $\lambda_a'^{(c)}$ into Eq. 244. After several pages of algebra one can show that

$$\frac{1}{\sigma_{a1}^{(c)}} = \frac{N_1' + N_2'}{[\sqrt{S_1'}+\sqrt{S_2'}]^2} \frac{1}{1 - b_s} \left[1-b_s b_n |\rho| \cos\theta \right.$$

$$\left. - \sqrt{\left[1-b_s b_n |\rho| \cos\theta\right]^2 - \left[1-b_s^2\right]\left[1-b_n^2|\rho|^2\right]} \right] \tag{248}$$

where

$$b_s = \frac{2\sqrt{S_1' S_2'}}{S_1' + S_2'} = \frac{2}{\sqrt{\frac{S_1'}{S_2'}} + \sqrt{\frac{S_2'}{S_1'}}} \tag{249}$$

$$b_n = \frac{2\sqrt{N_1' N_2'}}{N_1' + N_2'} = \frac{2}{\sqrt{\frac{N_1'}{N_2'}} + \sqrt{\frac{N_2'}{N_1'}}} . \tag{250}$$

The two constants b_s and b_n are a measure of the symmetry or balance of the source. That is, b_s is unity if $\sqrt{S_1'}/\sqrt{S_2'} = 1$ and falls off monotonically to zero as the ratio $\sqrt{S_1'}/\sqrt{S_2'}$ is increased or decreased from unity. Similarly, the constant b_n is unity if $\sqrt{N_1'}/\sqrt{N_2'} = 1$ and falls off monotonically to zero as the ratio $\sqrt{N_1'}/\sqrt{N_2'}$ is increased or decreased from unity. Consequently,

$$0 \leq b_s \leq 1$$

$$0 \leq b_n \leq 1 .$$

The first multiplicative factor in (248), $(N_1'+N_2')/[\sqrt{S_1'}+\sqrt{S_2'}]^2$, is just the noise-to-signal ratio that the source would have at infinite exchangeable power if there were no correlation ($|\rho| = 0$) as given by $1/\sigma_{a1}$ in Eq. 231. Therefore, we shall plot the ratio of $1/\sigma_{a1}^{(c)}$ to $1/\sigma_{a1}$ to evaluate the effects of noise correlation. We plot

$$\frac{\frac{1}{\sigma_{a1}^{(c)}}}{\frac{1}{\sigma_{a1}}} = \frac{1}{1 - b_s} \left[1-b_s b_n |\rho| \cos\theta - \sqrt{(1-b_s b_n |\rho| \cos\theta)^2 - \left(1-b_s^2\right)\left(1-b_n^2|\rho|^2\right)} \right] \tag{251}$$

in Fig. 51 as a function of $b_n|\rho|$ for several values of b_s and several values of $\cos\theta$.

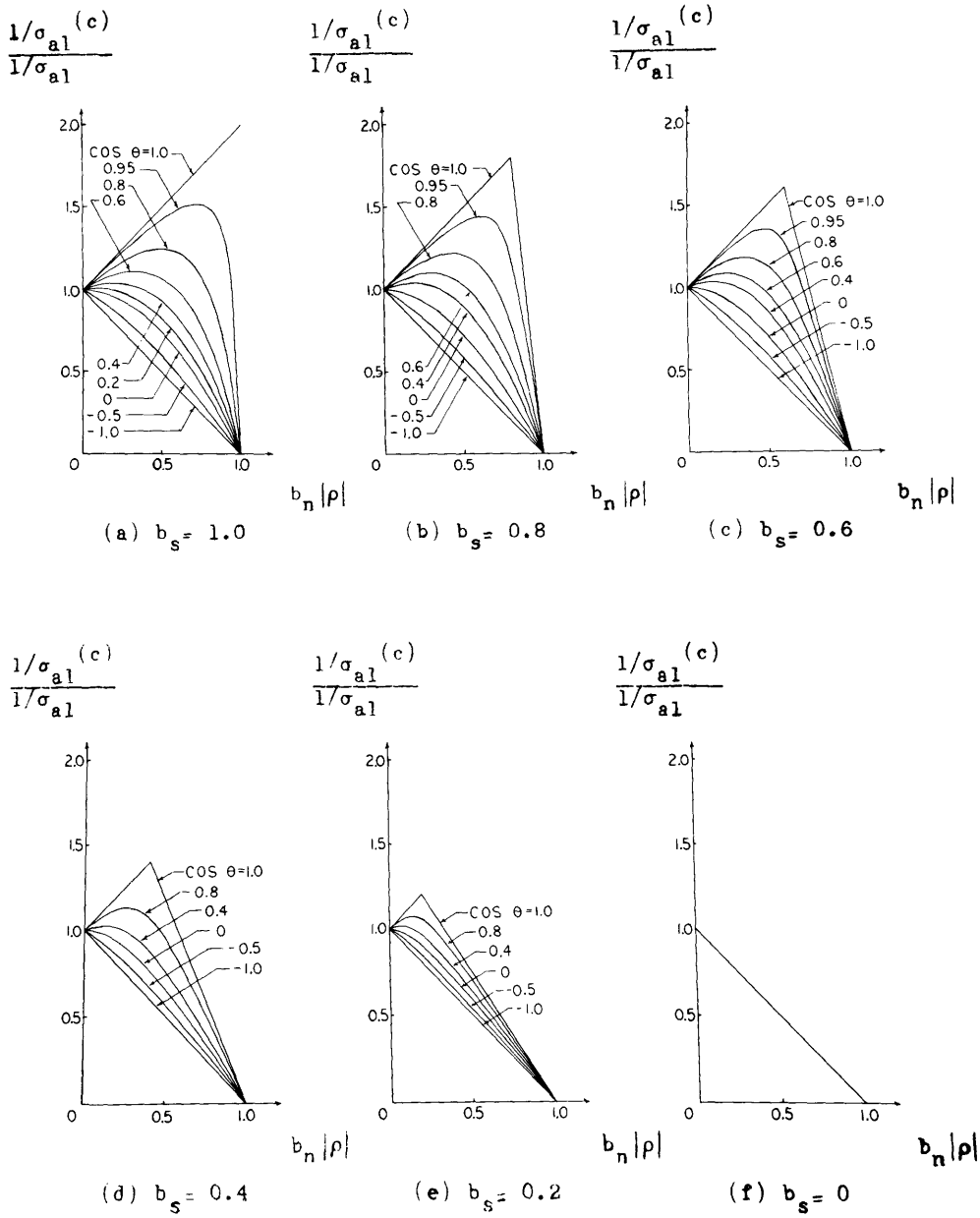

Fig. 51. Plots of Eq. 251.

Using the plots in Fig. 51, we can evaluate the best noise-to-signal ratio at large exchangeable power that can be achieved with a given two-frequency two-terminal-pair source with coherent signals used in conjunction with a lossless parametric device. We may be able to achieve better noise-to-signal ratio at large exchangeable power if we have a device (such as the resistor that has been considered) characterized by a value of λ' which has the same sign as $\lambda_a'^{(c)}$ of Eq. 246, but has a smaller magnitude. In this case the best noise-to-signal ratio achievable at infinite exchangeable power is obtained by evaluating $1/\sigma_{\lambda'}^{(c)}$ of Eq. 244 for this value of λ'.

VIII. CONCLUSIONS

A great deal of material has been covered in the last six sections. We shall conclude by summarizing our principal accomplishments and noting our most prominent omissions.

We set out to determine a criterion for the optimum noise performance of a multiterminal-pair amplifier used with a multiterminal-pair source, and to determine the amplifier and source parameters that set the limits for this performance. We began by examining the concept of exchangeable power and succeeded in increasing the utility of this concept. If one assumes that the primary purpose of amplifiers is to make large amounts of signal power available at the output, one can only conclude that the output of the amplifier should be characterized by a large positive value, or any negative value of exchangeable signal power. We proceeded to show that at large exchangeable power the ratio of exchangeable signal power to exchangeable noise power is equal to the ratio of signal power to noise power delivered to the load. We also showed that if we have a device with a negative exchangeable power at the output, the actual signal-to-noise ratio achieved in delivering power to a load can be no better than the best signal-to-noise ratio that can be obtained by combining the elements of the system in such a manner as to obtain infinite exchangeable power. This result leads us to conclude, on a pragmatic basis, of on no other, that the optimum noise performance of an amplifier should be a measure of how large a signal-to-noise ratio can be achieved at large (essentially infinite) values of exchangeable power by using the amplifier with a given source.

In order to see how to achieve the optimum performance, we examined the performance of our amplifiers on a plot with noise-to-signal ratio and the reciprocal of exchangeable signal power as coordinates – the noise-performance plane. These coordinates can be used in general to examine the noise performance of any linear system. By plotting the points determined by the outputs of successive stages on this plot, one can see exactly how each stage contributes to the over-all noise performance of any given system. For cascades of two-terminal-pair amplifiers this plot is equivalent to a plot of excess exchangeable noise figure against the reciprocal of exchangeable gain.

Using the characteristic noise plane, we showed that the eigenvalues of the characteristic noise matrix of a noisy network are the quantities that ultimately determine the quality of the noise performance of the network as an amplifier. For purely dissipative signal sources or signal sources with a positive definite impedance matrix, the smallest positive eigenvalue of the characteristic noise matrix of an amplifier determines how well the amplifier will perform with the source. For sources with indefinite impedance matrices, three cases are possible. The optimal performance of the system may be limited by the smallest positive eigenvalue of the characteristic noise matrix, or by the smallest negative eigenvalue of the characteristic noise matrix, or in some cases the performance is not limited by the amplifier at all but only by the source network itself.

The smallest positive eigenvalue of the characteristic noise matrix is just the negative of the exchangeable power of the least noisy negative resistance appearing in the

canonical form of the amplifier; the smallest negative eigenvalue of the characteristic noise matrix is just the negative of the exchangeable power of the least noisy positive resistance appearing in the canonical form of the amplifier. We also showed that the smallest positive and smallest negative eigenvalues are $kT_o\Delta f$ times the smallest positive and smallest negative values, respectively, of the noise measure that can be achieved by using the device as an amplifier.

In this context we extended the concepts of noise measure, noise figure, and exchangeable gain to multiterminal-pair amplifiers used with multiterminal-pair sources. We accomplished this by comparing the amplifier performance with the performance of a lossless network that combines the source voltages in the same way as the amplifier. We referred to this last system as the equivalent source. In making this comparison we are separating the amplifying function of the amplifier from the voltage combining function. The way in which the device amplifies is described by the extended noise measure, noise figure, and exchangeable gain. The way in which the amplifier combines the source voltages may be evaluated by examining the point determined in the noise-performance plane by the equivalent source. We did not define a quantitative measure of the effectiveness of the combining operation of the amplifier. What we did do, though, is provide a method of determining the outer boundary of the source region. By noting the position of the equivalent-source point with respect to the outer boundary of the source region, one can judge how effectively the amplifier has utilized the source.

The method that we chose for determining the outer boundary of the source region was a slope-intercept method. That is, we looked for the point on the source-region boundary where the slope had a given value. The reciprocal of the eigenvalue of the source optimization equation was shown to be the intercept of the tangent to the boundary at this point, with the noise-to-signal ratio axis in the noise-performance plane. An amplifier limits the noise performance of a system, however, only by the smallest positive or smallest negative value of its noise measure, and a line of constant noise measure is a line of constant slope in the noise-performance plane. Therefore the form of the source optimization equation is very convenient; for, the optimum signal-to-noise ratio at infinite exchangeable power achievable with a given amplifier and a given source is one of the eigenvalues of the source optimization equation. We devoted considerable attention to setting up criteria for determining which of the eigenvalues gives this optimum signal-to-noise ratio.

Although we have derived all of the optimization equations for networks characterized on an impedance basis, the results are valid for any basis. The eigenvalues of the characteristic noise matrix of the amplifier and the boundary of the source region in the noise-performance plane are invariants of the amplifier network and the source network, respectively. Therefore, if we had characterized our networks on any other basis, such as the admittance basis or wave basis, we would have obtained essentially the same optimization equations. The only difference would be a change in variables and a corresponding conjunctive transformation of all of the matrices in a given equation.[18] The

plots of solutions to these equations in the noise-performance plane would remain the same.

Finally, we showed how the optimization procedure could be modified to cover multiterminal-pair, multifrequency sources and amplifiers coupled by lossless networks that conserve power in the Manley-Rowe sense. These techniques have also been extended to cover linear or quasi-linear devices that couple several frequencies but do not obey the Manley-Rowe relations.[25] Unfortunately the resulting optimization equations become quite complicated without yielding very much insight into the problem.

The problem of optimizing the performance of a system over a broadband of frequencies may apparently be solved by using the spot-noise criteria. For a broadband system one could determine the maximum signal-to-noise ratio achievable at large exchangeable power at each frequency in the band. By making suitable approximations one could presumably construct a network that would come arbitrarily close to realizing this optimum performance. A network designed solely on this basis would also, presumably, be extremely complex, and there is no guarantee that it would be optimal or even desirable in any other respect. For, in a wideband system, one would also be concerned with the over-all stability, phase characteristics, transient response, and so forth, of the system. None of these factors is considered in the present theory.

These considerations raise the question of the over-all utility of the theory that we have presented. It is probable that the theory will be most useful in determining the extent to which a system that has been built to satisfy a number of other practical considerations fails to achieve its optimum noise performance. In other words, one might use the optimal performance criteria as a basis of comparison in designing a system. Through such a comparison one can determine when the point of diminishing returns has been reached with respect to improving both the noise performance of the amplifier and the way in which the amplifier utilizes the source.

APPENDIX A

PROOF OF THE SEMICONVEXITY OF THE SOURCE REGION OUTER BOUNDARY

We shall establish the fact that the source region outer boundary is semiconvex by considering a degeneracy in Eq. 101,

$$\overline{\underset{\sim}{E}_s\underset{\sim}{E}_s^\dagger}\,\underset{\sim}{x} - \sigma\left[\overline{\underset{\sim}{E}_n\underset{\sim}{E}_n^\dagger} - 2\mu\left(\underset{\sim}{Z}_s+\underset{\sim}{Z}_s^\dagger\right)\right]\underset{\sim}{x} = 0.$$

For simplicity, we rewrite this equation as

$$\underset{\sim}{A}\,\underset{\sim}{x} - \sigma[\underset{\sim}{B}-\mu\,\underset{\sim}{C}]\,\underset{\sim}{x} = 0, \tag{A-1}$$

in which the definitions of the matrixes $\underset{\sim}{A}$, $\underset{\sim}{B}$, and $\underset{\sim}{C}$ are obvious.

Although it is by no means obvious, the two vectors $\underset{\sim}{x}^{(aa)}$ and $\underset{\sim}{x}^{(ab)}$, to which we have referred, are very special vectors with very special properties, that is, if the source region really appears in part as shown in Fig. 21. Rather than prove that these vectors have special properties, we shall show that one can always construct two vectors that have these properties. At the end of the proof it becomes apparent that the two vectors that we have constructed, and denoted $\underset{\sim}{x}^{(aa)}$ and $\underset{\sim}{x}^{(ab)}$, are indeed the two vectors referred to before.

We begin by assuming that for $\mu = a$ there is a two-fold degeneracy in Eq. A-1. Consequently, there are two independent vectors, $\underset{\sim}{x}^{(ai)}$ and $\underset{\sim}{x}^{(aj)}$, that satisfy Eq. A-1 for the same eigenvalue, $\sigma_{ai} = \sigma_{aj}$. Thus

$$\underset{\sim}{A}\,\underset{\sim}{x}^{(ai)} - \sigma_{ai}[\underset{\sim}{B}-a\,\underset{\sim}{C}]\,\underset{\sim}{x}^{(ai)} = 0 \tag{A-2}$$

and

$$\underset{\sim}{A}\,\underset{\sim}{x}^{(aj)} - \sigma_{ai}[\underset{\sim}{B}-a\,\underset{\sim}{C}]\,\underset{\sim}{x}^{(aj)} = 0. \tag{A-3}$$

Let us consider two other vectors, $\underset{\sim}{x}^{(aa)}$ and $\underset{\sim}{x}^{(ab)}$, that are arbitrary linear combinations of these two vectors.

$$\underset{\sim}{x}^{(aa)} = \underset{\sim}{x}^{(ai)} + a\,\underset{\sim}{x}^{(aj)} \tag{A-4}$$

$$\underset{\sim}{x}^{(ab)} = \underset{\sim}{x}^{(ai)} + b\,\underset{\sim}{x}^{(aj)} \tag{A-5}$$

With the aid of Eq. A-4 we see that Eq. A-2 plus a multiplied by Eq. A-3 gives

$$\underset{\sim}{A}\,\underset{\sim}{x}^{(aa)} - \sigma_{ai}[\underset{\sim}{B}-a\,\underset{\sim}{C}]\,\underset{\sim}{x}^{(aa)} = 0. \tag{A-6}$$

Similarly, with the aid of Eq. A-5 we see that Eq. A-2 plus b multiplied by Eq. A-3 gives

$$\underset{\sim}{A}\,\underset{\sim}{x}^{(ab)} - \sigma_{ai}[\underset{\sim}{B}-a\,\underset{\sim}{C}]\,\underset{\sim}{x}^{(ab)} = 0. \tag{A-7}$$

We have done this in order to pick our degenerate vectors in such a way that they have specific properties. Since a and b are arbitrary numbers, we may adjust them so that the vectors $\underset{\sim}{x}^{(aa)}$ and $\underset{\sim}{x}^{(ab)}$ are orthogonal with respect to the matrix $\underset{\sim}{A}$.

$$\underset{\sim}{x}^{(aa)\dagger}\ \underset{\sim}{A}\,\underset{\sim}{x}^{(ab)} = 0. \tag{A-8}$$

If Eq. A-8 is satisfied, we see that by premultiplying Eq. A-7 by $\underset{\sim}{x}^{(aa)\dagger}$ we also have

$$\underset{\sim}{x}^{(aa)\dagger}\ \underset{\sim}{B}\,\underset{\sim}{x}^{(ab)} - a\,\underset{\sim}{x}^{(aa)\dagger}\ \underset{\sim}{C}\,\underset{\sim}{x}^{(ab)} = 0. \tag{A-9}$$

But we have imposed only one constraint on the two parameters a and b. Since we may impose a second constraint, we shall also require

$$\underset{\sim}{x}^{(aa)\dagger}\ \underset{\sim}{B}\,\underset{\sim}{x}^{(ab)} = 0. \tag{A-10}$$

If we have adjusted the two parameters a and b in Eqs. A-4 and A-5 to satisfy the two constraints given in Eq. A-8 and A-10, it follows from Eq. A-9 that

$$\underset{\sim}{x}^{(aa)\dagger}\ \underset{\sim}{C}\,\underset{\sim}{x}^{(ab)} = 0. \tag{A-11}$$

We shall assume now that the vectors $\underset{\sim}{x}^{(aa)}$ and $\underset{\sim}{x}^{(ab)}$ satisfy the constraints given by Eqs. A-8, A-10, and A-11.

When we imbed the source network in a lossless reduction network characterized by the vector $\underset{\sim}{x}^{(aa)}$, the noise-to-signal ratio and the reciprocal of the exchangeable signal power of the reduced source are given by

$$\frac{1}{s_{s,aa}} = \frac{\underset{\sim}{x}^{(aa)\dagger}\ \underset{\sim}{B}\,\underset{\sim}{x}^{(aa)}}{\underset{\sim}{x}^{(aa)\dagger}\ \underset{\sim}{A}\,\underset{\sim}{x}^{(aa)}} \tag{A-12}$$

and

$$\frac{1}{p_{s,aa}} = \frac{\underset{\sim}{x}^{(aa)\dagger}\ \underset{\sim}{C}\,\underset{\sim}{x}^{(aa)}}{\underset{\sim}{x}^{(aa)\dagger}\ \underset{\sim}{A}\,\underset{\sim}{x}^{(aa)}}, \tag{A-13}$$

respectively.

Similarly, when we imbed the source network in a lossless reduction network characterized by the vector $\underset{\sim}{x}^{(ab)}$, the noise-to-signal ratio and the reciprocal of the exchangeable signal powers of the reduced source are given by

$$\frac{1}{s_{s,ab}} = \frac{\underset{\sim}{x}^{(ab)\dagger}\ \underset{\sim}{B}\,\underset{\sim}{x}^{(ab)}}{\underset{\sim}{x}^{(ab)\dagger}\ \underset{\sim}{A}\,\underset{\sim}{x}^{(ab)}} \tag{A-14}$$

and

$$\frac{1}{p_{s,ab}} = \frac{\underset{\sim}{x}^{(ab)\dagger}\ \underset{\sim}{C}\,\underset{\sim}{x}^{(ab)}}{\underset{\sim}{x}^{(ab)\dagger}\ \underset{\sim}{A}\,\underset{\sim}{x}^{(ab)}}, \tag{A-15}$$

respectively.

If we premultiply Eq. A-6 by $\underset{\sim}{x}^{(aa)\dagger}$ and premultiply Eq. A-7 by $\underset{\sim}{x}^{(ab)\dagger}$, we can show, using the definitions of Eqs. A-12 through A-15, that

$$\frac{1}{\sigma_{ai}} = \frac{1}{s_{s,aa}} - \frac{a}{p_{s,aa}} = \frac{1}{s_{s,ab}} - \frac{a}{p_{s,ab}}. \tag{A-16}$$

Let us consider a third lossless reduction of the source network. Let this reduction network be characterized by the vector $\underset{\sim}{x}^{(ac)}$, where

$$\underset{\sim}{x}^{(ac)} = \underset{\sim}{x}^{(aa)} + c\,\underset{\sim}{x}^{(ab)}, \tag{A-17}$$

and c is an arbitrary parameter. The noise-to-signal ratio and the reciprocal of the exchangeable signal power of this reduced source are given by

$$\frac{1}{s_{s,ac}} = \frac{\underset{\sim}{x}^{(ac)\dagger}\,\underset{\sim}{\underset{\sim}{B}}\,\underset{\sim}{x}^{(ac)}}{\underset{\sim}{x}^{(ac)\dagger}\,\underset{\sim}{\underset{\sim}{A}}\,\underset{\sim}{x}^{(ac)}} \tag{A-18}$$

and

$$\frac{1}{p_{s,ac}} = \frac{\underset{\sim}{x}^{(ac)\dagger}\,\underset{\sim}{\underset{\sim}{C}}\,\underset{\sim}{x}^{(ac)}}{\underset{\sim}{x}^{(ac)\dagger}\,\underset{\sim}{\underset{\sim}{A}}\,\underset{\sim}{x}^{(ac)}}. \tag{A-19}$$

Using the definition in Eq. A-17 and the constraints in Eqs. A-8, A-10, and A-11, we may rewrite these two quantities as

$$\frac{1}{s_{s,ac}} = \frac{\underset{\sim}{x}^{(aa)\dagger}\,\underset{\sim}{\underset{\sim}{B}}\,\underset{\sim}{x}^{(aa)} + |c|^2\,\underset{\sim}{x}^{(ab)\dagger}\,\underset{\sim}{\underset{\sim}{B}}\,\underset{\sim}{x}^{(ab)}}{\underset{\sim}{x}^{(aa)\dagger}\,\underset{\sim}{\underset{\sim}{A}}\,\underset{\sim}{x}^{(aa)} + |c|^2\,\underset{\sim}{x}^{(ab)\dagger}\,\underset{\sim}{\underset{\sim}{A}}\,\underset{\sim}{x}^{(ab)}} \tag{A-20}$$

and

$$\frac{1}{p_{s,ac}} = \frac{\underset{\sim}{x}^{(aa)\dagger}\,\underset{\sim}{\underset{\sim}{C}}\,\underset{\sim}{x}^{(aa)} + |c|^2\,\underset{\sim}{x}^{(ab)\dagger}\,\underset{\sim}{\underset{\sim}{C}}\,\underset{\sim}{x}^{(ab)}}{\underset{\sim}{x}^{(aa)\dagger}\,\underset{\sim}{\underset{\sim}{A}}\,\underset{\sim}{x}^{(aa)} + |c|^2\,\underset{\sim}{x}^{(ab)\dagger}\,\underset{\sim}{\underset{\sim}{A}}\,\underset{\sim}{x}^{(ab)}}. \tag{A-21}$$

We may rewrite Eq. A-20 as

$$\frac{1}{s_{s,ac}} = \frac{\underset{\sim}{x}^{(aa)\dagger}\,\underset{\sim}{\underset{\sim}{B}}\,\underset{\sim}{x}^{(aa)}}{\underset{\sim}{x}^{(aa)\dagger}\,\underset{\sim}{\underset{\sim}{A}}\,\underset{\sim}{x}^{(aa)}} + \frac{|c|^2\left\{\underset{\sim}{x}^{(ab)\dagger}\,\underset{\sim}{\underset{\sim}{B}}\,\underset{\sim}{x}^{(ab)} - \dfrac{[\underset{\sim}{x}^{(aa)\dagger}\,\underset{\sim}{\underset{\sim}{B}}\,\underset{\sim}{x}^{(aa)}][\underset{\sim}{x}^{(ab)\dagger}\,\underset{\sim}{\underset{\sim}{A}}\,\underset{\sim}{x}^{(ab)}]}{\underset{\sim}{x}^{(aa)\dagger}\,\underset{\sim}{\underset{\sim}{A}}\,\underset{\sim}{x}^{(aa)}}\right\}}{\underset{\sim}{x}^{(aa)\dagger}\,\underset{\sim}{\underset{\sim}{A}}\,\underset{\sim}{x}^{(aa)} + |c|^2\,\underset{\sim}{x}^{(ab)\dagger}\,\underset{\sim}{\underset{\sim}{A}}\,\underset{\sim}{x}^{(ab)}}. \tag{A-22}$$

Using the definitions in Eqs. A-12 and A-14, we may write Eq. A-22 as

$$\frac{1}{s_{s,ac}} = \frac{1}{s_{s,aa}} + \left[\frac{1}{s_{s,ab}} - \frac{1}{s_{s,aa}}\right] f(|c|^2), \tag{A-23}$$

where

$$f(|c|^2) = \frac{|c|^2}{|c|^2 + \frac{\underset{\sim}{x}^{(\alpha a)\dagger}\,\underset{\sim}{\underset{\sim}{A}}\,\underset{\sim}{x}^{(\alpha a)}}{\underset{\sim}{x}^{(\alpha b)\dagger}\,\underset{\sim}{\underset{\sim}{A}}\,\underset{\sim}{x}^{(\alpha b)}}}. \tag{A-24}$$

In similar fashion we can derive the equation

$$\frac{1}{p_{s,\alpha c}} = \frac{1}{p_{s,\alpha a}} + \left[\frac{1}{p_{s,\alpha b}} - \frac{1}{p_{s,\alpha a}}\right] f(|c|^2) \tag{A-25}$$

from Eq. A-21.

Equations A-23 and A-25 give us expressions for the noise-to-signal ratio and the reciprocal of the exchangeable power at the output of the third imbedding network in terms of the corresponding quantities for the first two imbeddings and as a function of the parameter $|c|^2$. The function $f(|c|^2)$ in Eq. A-24 is a monotonically increasing function of $|c|^2$; it is zero at $|c| = 0$, and increases to the value 1 as $|c|$ approaches infinity.

If now we subtract α multiplied by Eq. A-25 from Eq. A-23, we find, with the help of Eq. A-16, that

$$\frac{1}{\sigma_{\alpha i}} = \frac{1}{s_{s,\alpha c}} - \frac{\alpha}{p_{s,\alpha c}}. \tag{A-26}$$

From Eq. A-26 we see that all of the points in the characteristic noise plane that can be obtained by varying the third lossless reduction network, in accordance with varying the parameter c in Eq. A-17, lie on the same straight line that contains the points determined by the first two lossless reductions. Equations A-23 and A-25 are the parametric equations of the segment of this line which we can achieve by such variations. As the parameter $|c|^2$ varies from zero to infinity, the point determined by this third reduction network moves monotonically along this straight line from the point whose coordinates are $1/p_{s,\alpha a}$ and $1/s_{s,\alpha a}$ to that whose coordinates are $1/p_{s,\alpha b}$ and $1/s_{s,\alpha b}$ (see Fig. 21). It follows directly that the source region outer boundary is semiconvex.

APPENDIX B

THE NATURE OF THE EIGENVALUES OF EQ. 101 WHEN THE SIGNAL-VOLTAGE MATRIX IS SEMIDEFINITE

We shall examine Eq. 101 for the case in which $\underset{\sim}{\overline{E_s E_s^\dagger}}$ is positive semidefinite of order m and rank r. If we define matrices $\underset{\sim}{A}$ and $\underset{\sim}{D}$ as

$$\underset{\sim}{A} = \underset{\sim}{\overline{E_s E_s^\dagger}} \tag{B-1}$$

$$\underset{\sim}{D} = \underset{\sim}{\overline{E_n E_n^\dagger}} - 2\mu\left(\underset{\sim}{Z_s}+\underset{\sim}{Z_s^\dagger}\right), \tag{B-2}$$

we may write Eq. 101

$$\underset{\sim}{A}\underset{\sim}{x} - \sigma\underset{\sim}{D}\underset{\sim}{x} = 0. \tag{B-3}$$

We wish to show that Eq. B-3 has r finite real eigenvalues and m-r solutions for $\sigma = 0$. We begin by changing variables. We define a new set of variables by the transformation

$$\underset{\sim}{Q}\underset{\sim}{y} = \underset{\sim}{x}. \tag{B-4}$$

By premultiplying Eq. B-3 by $\underset{\sim}{Q}$ and using Eq. B-4, we find that Eq. B-3 becomes

$$\underset{\sim}{A'}\underset{\sim}{y} - \sigma\underset{\sim}{D'}\underset{\sim}{y} = 0, \tag{B-5}$$

where

$$\underset{\sim}{A'} = \underset{\sim}{Q}^\dagger\underset{\sim}{A}\underset{\sim}{Q}$$

and

$$\underset{\sim}{D'} = \underset{\sim}{Q}^\dagger\underset{\sim}{D}\underset{\sim}{Q}.$$

We note that the matrices $\underset{\sim}{A'}$ and $\underset{\sim}{D'}$ are still Hermitian. We may pick the transformation matrix in such a way that $\underset{\sim}{A'}$ is a diagonal matrix with the last m-r elements on the diagonal zero.

For convenience, we partition the vector $\underset{\sim}{y}$ and the matrices $\underset{\sim}{A'}$ and $\underset{\sim}{D'}$:

$$\underset{\sim}{y} = \begin{bmatrix} \underset{\sim}{y_1} \\ \cdots \\ \underset{\sim}{y_2} \end{bmatrix}, \tag{B-6}$$

where $\underset{\sim}{y_1}$ is an r-dimensional vector, and $\underset{\sim}{y_2}$ is an (m-r)-dimensional vector.

$$\underset{\sim}{A'} = \begin{bmatrix} \underset{\sim}{A'_{11}} & \vdots & \underset{\sim}{0} \\ \cdots\cdots & \vdots & \cdots \\ \underset{\sim}{0} & \vdots & \underset{\sim}{0} \end{bmatrix} \tag{B-7}$$

and

$$\underset{\sim}{D}' = \begin{bmatrix} \underset{\sim}{D}'_{11} & \vdots & \underset{\sim}{D}'_{12} \\ \cdots\cdots & \vdots & \cdots\cdots \\ \underset{\sim}{D}'_{21} & \vdots & \underset{\sim}{D}'_{22} \end{bmatrix} = \begin{bmatrix} \underset{\sim}{D}'_{11} & \vdots & \underset{\sim}{D}'^{\dagger}_{21} \\ \cdots\cdots & \vdots & \cdots\cdots \\ \underset{\sim}{D}'_{21} & \vdots & \underset{\sim}{D}'_{22} \end{bmatrix} \tag{B-8}$$

in which $\underset{\sim}{A}'_{11}$ and $\underset{\sim}{D}'_{11}$ are square matrices of order r, $\underset{\sim}{D}'_{22}$ is a square matrix of order m-r, etc. Using (B-6)-(B-8) in (B-5), we obtain

$$\underset{\sim}{A}'_{11}\underset{\sim}{y}_1 - \sigma\left[\underset{\sim}{D}'_{11}\underset{\sim}{y}_1 + \underset{\sim}{D}'^{\dagger}_{21}\right]\underset{\sim}{y}_2 = 0 \tag{B-9}$$

and

$$\sigma[\underset{\sim}{D}'_{21}\underset{\sim}{y}_1 + \underset{\sim}{D}'_{22}\underset{\sim}{y}_2] = 0. \tag{B-10}$$

For $\sigma = 0$, we see that for $\underset{\sim}{y}_1$ also equal to zero any vector $\underset{\sim}{y}_2$ satisfies (B-9) and (B-10). Since $\underset{\sim}{y}_2$ is an (m-r)-dimensional vector, we can find m-r independent vectors that satisfy these equations (and hence satisfy Eq. B-5). This means that there is an m-r-fold degeneracy for the eigenvalue $\sigma = 0$.

If σ is not zero, Eq. B-10 is satisfied only if

$$\underset{\sim}{y}_2 = -\underset{\sim}{D}'^{-1}_{22}\,\underset{\sim}{D}'_{21}\underset{\sim}{y}_1. \tag{B-11}$$

In general, the matrix $\underset{\sim}{D}'_{22}$ will have an inverse. If it does not, we can change μ slightly (see Eq. B-2) to obtain a new $\underset{\sim}{D}'_{22}$ matrix that does have an inverse. It follows that $\underset{\sim}{D}'_{22}$ can only fail to have an inverse for a finite number of values of μ. These values correspond to degeneracies.

Using (B-11) in (B-9), we obtain

$$\underset{\sim}{A}'_{11}\underset{\sim}{y}_1 - \sigma\left[\underset{\sim}{D}'_{11} - \underset{\sim}{D}'^{\dagger}_{21}\underset{\sim}{D}'^{-1}_{22}\underset{\sim}{D}'_{21}\right]\underset{\sim}{y}_1 = 0. \tag{B-12}$$

We note that the matrix $\underset{\sim}{A}'_{11}$ is Hermitian and positive definite, and that the matrix $\underset{\sim}{D}'_{11} - \underset{\sim}{D}'^{\dagger}_{21}\underset{\sim}{D}'^{-1}_{22}\underset{\sim}{D}'_{21}$ is also Hermitian. This insures that Eq. B-12 has r real eigenvalues. These eigenvalues are also the eigenvalues of (B-5) and therefore of Eq. 101. We have shown, therefore, that in general Eq. 101 has r real finite eigenvalues and m-r eigenvalues that are zero for the case in which $\underset{\sim}{E}_s\underset{\sim}{E}_s^{\dagger}$ is positive semidefinite of order m and rank r.

APPENDIX C

PROOF OF EQUATION 111

We begin by picking a value for μ, say μ_1, and solving Eq. 101. Let us consider the j^{th} eigenvalue, σ_{1j}, of this equation. Corresponding to this eigenvalue is the eigenvector, $\underset{\sim}{x}^{(1j)}$, which when applied to the expressions of Eqs. 96 and 97 specifies a point on one of the source-region boundaries. In accordance with Eq. 104 the coordinates of this point are related through the equation

$$\frac{1}{\sigma_{1j}} = \frac{1}{s_{s,1j}} - \frac{\mu_1}{p_{s,1j}}. \tag{C-1}$$

We may also solve Eq. 101 for $\mu = \mu_2$, where μ_2 is only slightly larger than μ_1. That is,

$$\mu_2 = \mu_1 + \Delta\mu. \tag{C-2}$$

The j^{th} eigenvalue of Eq. 101 for $\mu = \mu_2$ is σ_{2j}, and the corresponding eigenvector is $\underset{\sim}{x}^{(2j)}$. This eigenvector specifies a second point in the noise-performance plane. The coordinates of this point are $1/p_{s,2j}$ and $1/s_{s,2j}$, and they are related by

$$\frac{1}{\sigma_{2j}} = \frac{1}{s_{s,2j}} - \frac{\mu_2}{p_{s,2j}}. \tag{C-3}$$

We have chosen the j^{th} eigenvalue for both of these cases, so presumably both of the determined points are on the same branch of the source region boundary. Consequently, first-order changes in μ about μ_1 produce first-order changes in the vector $\underset{\sim}{x}$ about $\underset{\sim}{x}^{(1j)}$, and as $\Delta\mu$ approaches zero $1/\sigma_{2j}$ approaches $1/\sigma_{1j}$, $1/s_{s,2j}$ approaches $1/s_{s,1j}$, $1/p_{s,2j}$ approaches $1/p_{s,1j}$, and $x^{(2j)}$ approaches $x^{(1j)}$.

We may express the change in $1/\sigma_{\mu j}$ with respect to small changes in μ about μ_1, using (C-1) and (C-3).

$$\frac{\frac{1}{\sigma_{2j}} - \frac{1}{\sigma_{1j}}}{\mu_2 - \mu_1} = \frac{\frac{1}{s_{s,2j}} - \frac{\mu_2}{p_{s,2j}} - \frac{1}{s_{s,1j}} + \frac{\mu_1}{p_{s,1j}}}{\mu_2 - \mu_1}. \tag{C-4}$$

We may also write (C-4)

$$\left[\frac{\Delta\frac{1}{\sigma_{\mu j}}}{\Delta\mu}\right]_{\mu=\mu_1} = \frac{\left[\frac{1}{s_{s,2j}} - \frac{\mu_1}{p_{s,2j}}\right] - \left[\frac{1}{s_{s,1j}} - \frac{\mu_1}{p_{s,1j}}\right] + (\mu_1 - \mu_2)\frac{1}{p_{s,2j}}}{\Delta\mu}. \tag{C-5}$$

In order to evaluate the derivative, we take the limit of Eq. C-5 as $\Delta\mu$ approaches

zero. We note that for small values of $\Delta\mu$ we have to first order

$$\left[\frac{1}{s_{s,2j}} - \frac{\mu_1}{p_{s,2j}}\right] - \left[\frac{1}{s_{s,1j}} - \frac{\mu_1}{p_{s,1j}}\right] = \delta\left[\frac{1}{\sigma_{1j}}\right] = 0. \tag{C-6}$$

Equation C-6 states that the difference in the two bracketed terms in (C-5) is just the variation of $1/\sigma_\mu$ (of Eq. 106) for $\mu = \mu_1$ about its j^{th} stationary value for small changes in $\underset{\sim}{x}$ about $\underset{\sim}{x}^{(1j)}$. It follows that the limit of Eq. C-5 as $\Delta\mu$ approaches zero is just

$$\left[\frac{\partial}{\partial\mu}\left(\frac{1}{\sigma_{\mu j}}\right)\right]_{\mu=\mu_1} = -\frac{1}{p_{s,2j}} = -\frac{1}{p_{s,1j}}. \tag{C-7}$$

Since Eq. C-7 is valid for any value of μ_1, we have shown that

$$\frac{\partial}{\partial\mu}\left(\frac{1}{\sigma_{\mu j}}\right) = -\frac{1}{p_{s,\mu j}}. \tag{C-8}$$

Acknowledgement

I wish to express my sincere thanks to Professor Hermann A. Haus for introducing me to the subject of this report and for his enthusiastic encouragement and guidance of my thesis research.

Thanks are also extended to Professor Paul L. Penfield, Jr. and Professor Richard B. Adler for their helpful suggestions and comments.

I would like to thank the Department of Electrical Engineering and the Research Laboratory of Electronics of the Massachusetts Institute of Technology for their support of my thesis work.

References

1. H. Heffner and G. Wade, "Gain, Bandwidth, and Noise Characteristics of the Variable-Parameter Amplifier," J. Appl. Phys. 29, 1321-1331 (1958).
2. J. M. Manley and H. E. Rowe,"Some General Properties of Nonlinear Elements — Part I: General Energy Relations," Proc. IRE 44, 904-913 (1956).
3. H. A. Haus and P. Penfield, Jr.,"On the Noise Performance of Parametric Amplifiers," Internal Memorandum No. 19, Energy Conversion Group, Department of Electrical Engineering, M.I.T., August 11, 1959 (unpublished).
4. P. Penfield,Jr., "Fundamental Limits of Varactor Parametric Amplifiers," Microwave Associates, Inc., Burlington, Massachusetts, August 15, 1960.
5. P. Penfield, Jr. and R. P. Rafuse, Varactor Applications (The M.I.T. Press, Cambridge, Mass., 1962).
6. D. G. Brennan, "Linear Diversity Combining Techniques," Proc. IRE 47, 1075-1102 (1959).
7. L. R. Kahn, "Ratio Squarer," Proc. IRE 42, 1704 (1954).
8. D. G. Brennan, "On the Maximum Signal-to-Noise Ratio Realizable from Several Noisy Signals," Proc. IRE 43, 1530 (1955).
9. J. Granlund, "Topics in the Design of Antennas for Scatter," Technical Report No.135, Lincoln Laboratory, M.I.T., November 23, 1956.
10. R. Q. Twiss, "Nyquist's and Thévenin's Theorems Generalized for Nonreciprocal Linear Networks," J. Appl. Phys. 26, 599-602 (1955).
11. H. T. Friis, "Noise Figure of Radio Receivers," Proc. IRE 32, 419-422 (1944).
12. K. Franz, "Messung der Empfangerempfindlichkeit bei kurzen elektrischen Wellen," Z. Elektr. Elektroakust. 59, 105 (1942).
13. H. A. Haus and R. B. Adler, "Invariants of Linear Networks," IRE Convention Record, Part 2, pp. 53-67, 1956.
14. H. A. Haus and R. B. Adler, "Limitations des performances de bruit des amplificateurs linéaires," Ond. Élec. 38, 777-790 (November 1958).
15. H. A. Haus and R. B. Adler, "Optimum Noise Performance of Linear Amplifiers," Proc. IRE 46, 1517-1533 (1958).
16. R. B. Adler and H. A. Haus, "Network Realization of Optimum Amplifier Noise Performance," IRE Trans. on Circuit Theory, Vol. CT-5, No. 3, pp. 156-161, September 1958.
17. H. A. Haus and R. B. Adler, "Canonical Form of Linear Noisy Networks," IRE Trans. on Circuit Theory, Vol. CT-5, No. 3, pp. 161-167, September 1958.
18. H. A. Haus and R. B. Adler, Circuit Theory of Linear Noisy Networks (The Technology Press of the Massachusetts Institute of Technology, Cambridge, Mass., and John Wiley and Sons, Inc., New York, 1959).
19. F. B. Hildebrand, Methods of Applied Mathematics (Prentice-Hall, Inc., Englewood Cliffs, N.J., 1952).
20. S. Perlis, Theory of Matrices (Addison-Wesley Publishing Company, Inc., Cambridge, Mass., 1952).
21. W. B. Davenport, Jr. and W. L. Root, An Introduction to the Theory of Random Signals and Noise (McGraw-Hill Book Company, New York, 1958).
22. H. A. Haus et al., "Representation of Noise in Linear Twoports," Proc. IRE 48, 69-74 (1960).
23. M. W. Muller, "Noise in a Molecular Amplifier," Phys. Rev. 106, 8-12 (1957).

24. J. C. Helmer and M. W. Muller, "Calculation and Measurement of the Noise Figure of a Maser Amplifier, IRE Trans. on Microwave Theory and Techniques, Vol. MTT-6, No. 2, pp. 210-214, April 1958.

25. W. D. Rummler, "Optimum Noise Performance of Multiterminal Amplifiers," Sc. D. Thesis, Department of Electrical Engineering, Massachusetts Institute of Technology, September 1963.

26. E. Goursat, A Course in Mathematical Analysis, Vol. I (Ginn and Company, Boston, Mass., 1904; reprint Dover Publications, Inc., New York, 1959).

27. "IRE Standards on Methods of Measuring Noise in Linear Twoports, 1959," 59 IRE 20.S1, Proc. IRE 48, 60-68 (1960); "IRE Standards on Electron Tubes: Methods of Testing, 1962," 62 IRE 7.S1, Proc. IRE 50, 135-142 (1962).

28. P. Penfield, Jr., Frequency-Power Formulas (The M.I.T. Press, Cambridge, Mass., and John Wiley and Sons, Inc., New York, 1960).